

UNCLASSIFIED

AD NUMBER

AD387034

CLASSIFICATION CHANGES

TO: unclassified

FROM: confidential

LIMITATION CHANGES

TO:

Approved for public release, distribution unlimited

FROM:

Distribution authorized to U.S. Gov't. agencies and their contractors; Administrative/Operational Use; Nov 1967. Other requests shall be referred to AFRPL [RPPR/STINFO], Edwards AFB, CA 93523.

AUTHORITY

AFRPL ltr dtd 15 Mar 1971; AFRPL ltr dtd 5 Feb 1986

THIS PAGE IS UNCLASSIFIED

CONFIDENTIAL

AFRPL-TR-67-278

19

(Unclassified Title)

ADVANCED CRYOGENIC ROCKET ENGINE PROGRAM
AEROSPIKE NOZZLE CONCEPT -- MATERIALS AND PROCESSES
RESEARCH AND DEVELOPMENT REPORT

AD 387034

Rocketdyne, A Division of
North American Rockwell Corporation
6633 Canoga Avenue
Canoga Park, California

Technical Report AFRPL-TR-67-278

November 1967

Group 4
Downgraded at 3-Year Intervals
Declassified After 12 Years

DDC
RECEIVED
FEB 12 1968
RECEIVED
D

THIS MATERIAL CONTAINS INFORMATION AFFECTING THE NATIONAL DEFENSE OF THE UNITED STATES WITHIN THE MEANING OF THE ESPIONAGE LAWS, TITLE 18 U.S.C., SECTIONS 793 AND 794, THE TRANSMISSION OR REVELATION OF WHICH IN ANY MANNER TO AN UNAUTHORIZED PERSON IS PROHIBITED BY LAW.

"In addition to security requirements which must be met, this document is subject to special export controls and each transmittal to foreign governments or foreign nationals may be made only with prior approval of AFRPL (RPPR/STINFO), Edwards, California, 93523."

Air Force Rocket Propulsion Laboratory
Edwards Air Force Base, California
Air Force Systems Command
United States Air Force

CONFIDENTIAL

CONFIDENTIAL

When U.S. Government drawings, specifications, or other data are used for any purpose other than a definitely related Government procurement operation, the Government thereby incurs no responsibility nor any obligation whatsoever, and the fact that the Government may have formulated, furnished, or in any way supplied the said drawings, specifications, or other data, is not to be regarded by implication or otherwise, or in any manner licensing the holder or any other person or corporation, conveying any rights or permission to manufacture, use, or sell any patented invention that may in any way be related thereto.

In addition to security requirements which must be met, this document is subject to special export controls and each transmittal to foreign governments or foreign nationals may be made only with prior approval of AFRPL (RPPR/STINFO), Edwards, California 93523.

This material contains information affecting the national defense of the United States within the meaning of the espionage laws, Title 18 U.S.C., Sections 793 and 794, the transmission or revelation of which in any manner to an unauthorized person is prohibited by law.

CONFIDENTIAL

(This page is Unclassified)

ERRATA

1. Page 87, photograph (Confidential)
2. Page 88, photograph (Confidential)

D-387034

CONFIDENTIAL

AFRPL-TR-67-278

(Unclassified Title)

ADVANCED CRYOGENIC ROCKET ENGINE PROGRAM
AEROSPIKE NOZZLE CONCEPT -- MATERIALS AND PROCESSES

RESEARCH AND DEVELOPMENT REPORT

Rocketdyne, A Division of
North American Rockwell Corporation
6633 Canoga Avenue
Canoga Park, California

Technical Report AFRPL-TR-67-278

November 1967

Group 4
Downgraded at 3-Year Intervals
Declassified After 12 Years

Prepared by
F. B. Lary

This material contains information affecting the national defense of the United States within the meaning of the espionage laws, title 18 U.S.C., sections 793 and 794, the transmission or revelation of which in any manner to an unauthorized person is prohibited by law.

"In addition to security requirements which must be met, this document is subject to special export controls and each transmittal to foreign governments or foreign nationals may be made only with prior approval of AFRPL (RPPR/STINFO), Edwards, California, 93523."

Air Force Rocket Propulsion Laboratory
Edwards Air Force Base, California
Air Force Systems Command
United States Air Force

CONFIDENTIAL

CONFIDENTIAL

FOREWORD

This report has been prepared under G.O. 08779 in compliance with report requirements of Air Force Cryogenic Aerospike Engine Program, Contract AF04(611)-11399.

This report has been assigned Rocketdyne report number R-7251.

This technical report has been reviewed and is approved.

Vernon L. Mahugh
Capt, USAF
Project Engineer
Air Force Rocket Propulsion Laboratory

Ernie D. Braunschweig
Capt, USAF
Program Manger
Air Force Rocket Propulsion Laboratory

ii
CONFIDENTIAL

(This page is Unclassified)

ABSTRACT

Reported herein are the results of Materials and Processes effort related to development and fabrication of experimental Aerospike thrust chamber hardware.

This report includes information relative to the selection of materials and information concerning the fabrication of the 250K combustor bodies and injectors, the development of the small tapered thrust chamber tubes, and the development of tooling and successful brazing of the small tubes to backup structure, and the injectors. Fabrication details of the 2.5 and 20K segment hardware is also included.

Highlighted are:

1. Data for prediction of tube life, based on elevated temperature cyclic strain tests, analytical calculations, and life cycle tests.
2. The development of small-diameter, tapered, variable wall thickness, formed tubes with an internal surface roughness requirement.
3. The brazing of the small tapered tubes to the backup structure utilizing the pressure bag concept.
4. The thermographic method of braze bond inspection.

CONFIDENTIAL

CONTENTS

Introduction and Summary	1
Cyclic Strain Tests of Thrust Chamber Tube Materials	1
Tube Material Life Analysis and Experimental Verification	2
Thrust Chamber Tube Tester	3
Tube Tapering	4
Furnace Braze Tooling	6
Nondestructive Testing of Tube-to-Body Braze Joints	8
Tube Material Selection Program	11
Program Plan	11
Selection of Candidate Materials	11
Literature Survey	11
Oxidation-Erosion and Surface Protection Studies	14
Mechanical Property Tests	16
Brazing Feasibility Studies	16
Mechanical Strain, Elevated Temperature	
Fatigue Studies	18
Tube Tapering and Forming Feasibility Study	19
Material Selection	19
Nickel Tube-Wall Thrust Chamber Cycling Tests	22
Nickel Tube-Wall Thrust Chamber Fatigue Results Analysis	23
Fabrication of 250K Combustors	33
General Description	33
Thrust Chamber Tube Processing	35
Brazing of Tubes to Combustor Bodies	46
250K Solid-Wall Chamber, Copper Throat Weld Overlay	94
Fabrication of 250K Injectors	97
Injector Strips, Deburring Baffles	97
Brazing of Injectors	101
Fabrication of 2.5K Segments	109
Nickel 200 Tube-Wall Fabrication	109
OFHC Copper Tube-Wall Fabrication	123

CONFIDENTIAL

Fabrication of 20K Segments	129
Nickel 200 Tube-Wall Fabrication	129
Injector Fabrication	168

CONFIDENTIAL

ILLUSTRATIONS

1. Material Selection Program	12
2. 250K Thrust Chamber Assembly	34
3. Typical Longitudinal Splits Found on Inner and Outer Tubes Subsequent to High-Pressure Die Forming	39
4. Longitudinal Split Which Penetrated Through the Tube Wall Causing Tube Not to Form to Final Shape	40
5. Location of Cross Sections Removed From High-Pressure Die-Formed Outer Tubes After Flow Check	42
6. Photos of Attack Produced on ID of Tubes by Walnut Shells in Laboratory Test	45
7. Three Pressure Bag Configurations Tested in the Laboratory for Pressure Response and Efficiency	48
8. Internal Pressure vs External Force for a 1-21/32 x 6-3/4 Flat Pressure Bag	49
9. Full-Length Inner and Outer Tube and Body Test Segments Ready for Brazing	52
10. Lower End Tube-to-Body Joint Scaled After the First Brazing Cycle.	54
11. Typical Exit End Tube-to-Body Joint	55
12. Outer Wall Segment, Injector End	56
13. Typical 317 Stainless-Steel Test Specimens	58
14. View of an Outer Wall Assembly During First Cycle Preparation.	62
15. Location of Nickel Filler Metal and 90Ag-10Pd Braze Alloy Application For the First Braze Cycle	64
16. Outer Body Assembly on Retort Base With Pressure Bag Tooling Installed	65
17. The 270 cu ft Aerospike Vacuum Retort	67
18. Time-Temperature Curve for the First Braze Cycle, Outer Wall Unit No. 1	69
19. Outer Wall Pressure Bag Tooling	70

CONFIDENTIAL

20. Braze Test Specimen	72
21. Location of Nickel Filler Metal and 90Ag-10Pd Braze Alloy Application for the First Braze Cycle	75
22. Pressure Bag Pressure Requirements During Brazing Cycle, Inner Wall Units No. 1 and 2	76
23. Location of Pressure Bags and Purge Lines for the First Braze Cycle on the Inner Wall Assembly	77
24. Inner Wall Assembly in Brazing Position on Retort Base	79
25. Time-Temperature Curve for the First Braze Cycle, Inner Wall No. 1	81
26. View of Inner Wall Unit No. 2 in the Exit End Down P Position Following the Second Braze Cycle	87
27. Closeup View of Inner Wall Unit No. 2	88
28. Silver-Palladium Brazed Tube Crown Repair on Type 347 Stainless-Steel Tube (50X)	90
29. Repair of Tube-to-Tube Leakage by Stylus Plating With Silver	90
30. Thermographic Test Results on Laboratory Development Sample	92
31. Thermographic Inspection Results Showing Areas of Disbonds	93
32. Completed and Sectioned Baffle Assemblies	99
33. Section Through Braze Fixture and Two Baffles Showing Gas Purge System	100
34. Broached Strip and Baffle Seat on Injector Segment	102
35. Passage From Strip and Baffle Seat to Manifold by the EDM Method	102
36. Braze Alloy Placement Between Strips	104
37. Braze Alloy and Nickel Through Placement	105
38. Partial Thermocouple Attachment	106
39. Furnace Retort for Brazing 250K Injector	107
40. Location of Metallographic Specimens Removed from Nickel 200 Tubes (RL000044X)	113

CONFIDENTIAL

41.	Typical Conditions Observed on Book Die Formed Nickel 200, 2.5K Segment Tube.	115
42.	2.5K Nickel Tubular Thrust Chamber Segment During Assembly	116
43.	2.5K Nickel Tubular Thrust Chamber Segment Before Addition of Backup Structure	118
44.	Repair of 2.5K Nickel Tubular Thrust Chamber Segment . . .	119
45.	Braze Alloys Dots Applied to the ID Tube Crowns of the 2.5K Nickel Tubular Thrust Chamber Segment	120
46.	Location of Metallographic Specimens Removed From OFHC Copper Tubes (RL000060X)	126
47.	Typical Conditions Observed on Book Die Formed OFHC Copper Tubes for 2.5K Segment	127
48.	Wall Thickness Profile of Tapered RL000109X Nickel 200 Tube	130
49.	Location of Metallographic Specimens Removed From Straight Tapered Tubes During "In-Process" Control Evaluations (RL000109X)	134
50.	Location of Metallographic Specimens Removed From Preformed and Finish Formed Tubes (RL000109X)	140
51.	Typical Conditions Observed on Book-Die-Formed, Nickel 200, 20K Segment Tubes	141
52.	Baffle Seat Assembly RL000113X After Furnace Brazing and Final Machining	144
53.	View of Brazed Baffle Seat Assembly Showing Outer Tube Deformation	146
54.	Typical Components of RL000107X End Plate Assembly Before Assembly for Brazing	148
55.	Tube-Wall Assembly RL000108X on Furnace Brazing Fixture	149
56.	Tube-Wall Assembly RL000108X Following Assembly on the Brazing Fixture Cold Side Up	152
57.	Hot-Gas Side of RL000108X Tube Wall Assembly	153

CONFIDENTIAL

58. Cross-Sectional Views of Tube Wall and Braze Fixture Taken at Throat Area	154
59. Cross-Sectional Views of Tube Wall and Braze Fixture Taken at Throat Area	155
60. Unit No. 1 RL000110X Chamber Braze Assembly After Furnace Brazing	159
61. View of Area of Thrust Chamber	162
62. Uncured Strips of Verifilm 643 Applied to the Tube Bundle Prior to Trial Assembly	166
63. Uncured Adhesive Film Pattern Applied to a Titanium Backup Structure Prior to Assembly	167
64. Baffle Assembly RL000104X Showing Components Before and After Assembly	170
65. Thermocouple Location, Purge Line Position, and Position in Furnace	172

CONFIDENTIAL

TABLES

1. Candidate Materials for Thrust Chamber Usage	13
2. Summary of Results, Material Property Literature Survey	15
3. Cyclic Strain Test Results	17
4. Factors Affecting Selection of 2CK-Segment Tube Material	20
5. Factors Affecting Selection of Long-Range Tube Materials	21
6. Summary of 2.5K Segment Cycle Tests	24
7. Thermal Fatigue Tube Tester Results on Nickel 200	32
8. Brazed Lap Patch Test Data	59
9. Outer Wall Furnace Braze Data	68
10. Inner Wall Furnace Braze Data	80
11. Results of Metallurgical Evaluations Conducted on Tapered Nickel 200 Tubes (RL000044X)	111
12. Results of Metallurgical Evaluation Conducted on Finish Formed Nickel 200 Tubes	114
13. Results of Metallurgical Evaluations Conducted on Tapered OFHC Copper Tubes (RL000060X)	125
14. Results of Metallurgical Evaluations Conducted on Tapered Nickel 200 Tubes (RL000109X) During Tapering Parameter Development	132
15. Metallurgical Sample Requirements Established for In-Process Control and Final Acceptance of Nickel 200 Tubes (RL000109X)	133
16. Results of Metallurgical Evaluations Performed on Straight Tapered Nickel 200 Tubes In-Process Control Checks of Production Runs	135
17. Metallurgical Evaluation Conducted on Preformed Nickel 200 Tubes (RL000109X) From Manufacturing Lot 8062	137

18.	Results of Metallurgical Evaluation Conducted on Preformed Nickel 200 Tubes (RL000109X) Subsequent to Annealing	138
19.	Results of Metallurgical Evaluation Conducted on Finish Formed Nickel 200 Tubes (RL000109X)	139
20.	Baffle Seat Assembly (RL000113X) Fabrication History , .	145
21.	Tube-Wall Assembly (RL000108X) Leakage and Repair History .	150
22.	Chamber Braze RL000110X Furnace Brazing History	158
23.	Chamber Braze Assembly RL000110X Post-Torch Braze Leakage and Repairs	161
24.	Baffle Assembly RL000104X Fabrication History	169

CONFIDENTIAL

INTRODUCTION AND SUMMARY

(U) Fabrication of toroidal configuration thrust chambers and injectors and various thrust chamber segments was made possible only after the development of specialized fabrication methods and tooling to accommodate the advanced design of the hardware. The requirement for fabricating two tubular thrust chamber assemblies with no allowance for spares demanded rigorous planning and development. This required that techniques hazardous to the assemblies were avoided, and that safe, reliable techniques were to be used at all times.

(U) Joining of component parts was accomplished by standard welding and brazing practices and with adhesive bonding and bolting during the final stages of segmented-hardware assembly.

(U) Highly specialized repair techniques were developed to repair damaged tubes. Unique methods were used to remove dents, seal holes, and to remove restrictions in the small-diameter tubes.

CYCLIC STRAIN TESTS OF THRUST CHAMBER TUBE MATERIALS

(U) To provide data for prediction of tube life, elevated temperature cyclic strain tests were conducted for the candidate tube materials. Three types of tests were considered: (1) thermal cycling of restrained tubular specimen; (2) thermal cycling of tubular specimens with sufficient cyclic mechanical strain added to simulate strain levels calculated for the thrust chamber regenerative cooling tubes; (3) mechanical strain cycling of bar specimens at constant temperature. The third test method was chosen because of the immediate availability of cyclic mechanical strain test equipment and the inherent simplicity of this type of testing.

1
CONFIDENTIAL
(This page is Unclassified)

CONFIDENTIAL

(C) The materials selected for testing were OFHC copper, nickel 200, nickel 270, type 347 stainless steel, and beryllium copper #10.

(U) Test specimen configuration consisted simply of a cylindrical tensile specimen with a 3/8-inch long, 1/4-inch diameter reduced section. Attachment points of the extensometer were located in the V-grooves on either side of the reduced section. Mechanical strain, representing the equivalent thermal strain calculated for the thrust chamber tubes, was applied by an Instron mechanical test machine controlled by extensometer feedback. The specimen was heated during test by a modified tube furnace which was capable of maintaining ± 10 F in the test section.

(C) The test temperatures were selected to include the tube crown temperatures predicted for each candidate material during firing of the demonstration thrust chamber. The higher annealing temperatures represented anticipated brazing temperatures. The lower temperatures were standard anneals which do not produce appreciable grain growth. All tests with the exception of one were stopped at 400 cycles if complete separation had not occurred.

(C) The data obtained from these tests together with general design considerations, analytical calculations and life cycle tests on the 2.5K Ni segment, resulted in the selection of Ni 200 as the tube material for the demonstrator design.

TUBE MATERIAL LIFE ANALYSIS AND EXPERIMENTAL VERIFICATION

(U) An analytical approach to the prediction of tube life was formulated. A "strength-of-materials" approach to the approximate solution of the multi-axial, cyclic, plastic strains was used in conjunction with low-cycle fatigue relationships to enable a prediction of the tube fatigue life. Comparisons between the predicted and experimentally determined thermal fatigue lives were then made by hot-firing tests of a full-scale thrust chamber segment.

(C) A 2.5K nickel tube wall segment was tested by cycling chamber pressure, and thus, tube wall temperature, in a series of cyclic test groups. During each test group, the fuel flow through the injector and tube banks remained unchecked, while the LO_2 flow was intermittently stopped. Ignition was obtained with TEAB hypergol, and maintained during the idle phases of each test group by a small gaseous oxygen flow.

(C) Thermal fatigue tube cracks began to appear at about test 200, and steadily increased in number to include 80 percent of the tubes at test 314, with the thrust chamber still in operable condition. It was noted that the predicted thermal fatigue life of the 2.5K segment was about mid-way between test 200 and 314.

THRUST CHAMBER TUBE TESTER

(U) A unique experimental tool for simulation of the complex thermal strain conditions of thrust chamber tubes was used during the program. This thermal fatigue tester employed an electrically heated, hydrogen-cooled tubular specimen. Heat generated by electrical resistance was applied to the tube specimen, which was in turn continuously cooled internally. A near steady-state heat transfer condition was thereby established resulting in the simulation of the thrust chamber tube-wall temperature drop. The electrical power was varied to simulate changes in thrust chamber operating conditions.

(C) This tube tester was used to conduct thermal-fatigue evaluations on the selected Nickel-200 tube material. Some engine start-stop sequence simulation tests were initially completed. The segment cycling tests later largely superseded the results of this effort. Of special interest, however, was a unique test designed to simulate a complex fatigue-creep condition, which could be more critical to thrust chamber life than the start-stop sequential life.

(C) A severe "steady-state" tube gas-wall cycling condition of 1365 to 1435 F at a frequency of about 1 cps, in combination with a pressure stress of 4500 psi, was applied to the specimen. The calculated nominal temperature drop through the specimen tube crown was 520 F. This test represented conditions more severe than any predicted for the aerospike nozzle. Testing continued for 7 hours, accumulating 22,500 thermal cycles without fracture or leaks.

(U) It was difficult to compare the experimental results of this test against analytical predictions, since a large extrapolation of the thermal-fatigue curve used to predict the start-stop sequential life was required, with a resultant loss in confidence. The test did demonstrate, however, the adequacy of the selected material in a complex fatigue-creep operating condition.

TUBE TAPERING

(U) The development of small-diameter tapered and formed tubes which were brazed together to form toroidal and segmented assemblies was a major step in the successful fabrication of hardware. Although some experience had previously been gained in the tapering of small 347 tubes during previous segment test programs, the techniques of tapering cross section and wall thickness on small tubes were advanced.

(U) Engineering drawing requirements which specified a wall thickness of 0.007 to 0.009 inch in the area of maximum taper, with an inside diameter longitudinal surface roughness of rms 50-100 represented a significant challenge to the tapering process. This fact coupled with the requirement for a 0.010 to 0.012 inch wall thickness at the portions of the tube away from the throat and taper transition areas required considerable development work.

(U) In order to impose the maximum of control upon a complex process and still ensure a reasonably inexpensive tube of high quality, a processing specification was issued which was unique in that it required a test for ensuring the tapered tubes would be capable of being plastically deformed by internal pressure to withstand high-pressure die forming. In addition, requirements for cleaning and annealing of preformed tubes were specified along with final acceptance criteria for a lot of tubes which used the actual high-pressure die forming of a representative sample from each lot as the basis for acceptance of the lot.

(U) Metallurgical evaluation of experimental and preproduction runs of tapered outer tubes revealed that the tube could be successfully made in one pass. The outside diameters, on both tube configurations, in areas which were not tapered, were on the minimum side of the acceptable tolerance range, and the wall thickness in the area of maximum taper was on the maximum side of the acceptable tolerance range.

(U) Tapering tubes with a tapered wall and an ID surface roughness with specific values in the area of maximum reduction (where the wall is also at the smallest dimension) was achieved. Values between 43 and 75 rms were obtained on the outer tubes and 47 to 72 rms on the inner tubes.

(U) The expansion capability requirement specified that a percentage of tapered and annealed tubes of each configuration be expanded 6 percent diametrically in a high-pressure die in order to show formability of the represented lot of tubes. No problems were experienced on the outer tubes during this test. During initial expansion tests on inner, tapered and annealed tubes the tubes burst at pressures considerably below the pressure required to expand the tubes 6 percent.

(U) Results of the extensive analysis performed on the mechanics of the test itself revealed that the tubes failed because of unbalanced axial

pressure loads which occurred during tube pressurization. These loads cause the tube to shift longitudinally in the die cavity before expansion could occur. The axial loads created axial compressive stresses of sufficient magnitude in the area of maximum reduction on the tube to first yield the material in compression, then buckle the entire cross section into a tight kink when the tube translated into the divergent section of the die. Subsequent increasing pressurization brought on hoop failure at the buckled location.

(U) The situation was resolved by swaging both ends of the inner tubes, and modification of the tube pressurization fixture. These changes reduced the unbalanced axial load in the tube diameter to a negligible value and the data obtained gave high assurance that the inner tubes would form properly. Since there was a considerable time span between tapering and high-pressure die forming, these tests protected the schedule by demonstrating assurance early that the tubes were of adequate quality for the severe deformation encountered during high-pressure die forming. Very few rejections were subsequently encountered in high-pressure die forming (the ultimate check on the tube tapering operation) on the 12,000 outer and 10,000 inner tubes produced.

(U) A numerical traceability system was maintained on all 250K thrust chamber tubes so that metallurgical and dimensional inspection could be controlled and related to specific tubes.

FURNACE BRAZE TOOLING

(U) Considerable experience has been accumulated in the use of internal pressure bags to hold regenerative cooling tubes in place during

the brazing of large bell shaped chambers. However, the brazing of the inner and outer walls for a 100-inch-diameter, toroidal shaped chamber was an advancement in the following areas:

1. Brazing small tubes to a massive backup structure
2. Maintaining precise throat gap requirements by constant and uniform pressure
3. Controlling differential thermal expansion through the use of pressure bag tooling. A temperature differential of only 1 F would produce a differential expansion over the 100-inch diameter of about 0.001 inch.
4. Maintaining tube-to-body fit with the provision for physical inspection of the tubes after installation of the pressure bag tooling.

(U) The pressure bag concept allowed the forces on the tubing to be varied with temperature in such a way that proper tubing location was maintained without crushing the tubes at elevated temperature. Proper use of the bags required knowledge of the relationship between internal pressure and external forces through the ambient to 2000 F temperature range. Knowledge of the elevated temperature strength of the type 347 stainless steel tubing under transverse compressive loads was also necessary. To satisfy these requirements laboratory tests were conducted on pressure bag force relationships and tube crushing strengths.

(U) Pressure bags with diagonal expansion grooves had been used previously in large tube bell chamber applications to allow for expansion and contraction of the bag while minimizing stretching and uncontrolled wrinkling. A flat, pillow type bag was also selected for test to reduce the stiffness characteristics of the grooved bags and to reduce the risk of losing tube-to-body contact at groove locations on the small tube Aerospike configuration. Testing of the three bag configurations demonstrated the superior performance of the flat type.

(U) Tube crushing experiments were run at both ambient and elevated temperatures by applying loads through a steel block to a simulated tube assembly. The forces required to hold the tubes in place at 2000 F were much less than 50 psi, indicating a satisfactory margin of safety at all temperatures.

(U) The above design considerations and test data resulted in the construction of flat, pillow-type inflatable pressure bags attached to equally spaced rigid backing rings, four rings on the outer wall and seven rings on the inner wall. The rings were approximately 4 sq in. cross sectional area, with 2-inch separation between the rings. Sufficient tube area was covered by the pressure bags, backed by the rings, to prevent tube movement; yet, sufficient space remained open between pressure bag rings to allow physical verification (by moving tubes) of tube-to-body fit. The space between rings also provided free circulation of the furnace atmosphere for cleanliness and temperature uniformity during brazing.

(U) The experimental data on the pressure bags and tube strengths were utilized in the subsequent line pressure-temperature requirements used in the furnace brazing operation. This tooling proved very satisfactory in obtaining tube-to-backup structure bond as revealed by the thermochromistic inspection.

NONDESTRUCTIVE TESTING OF TUBE-TO-BODY BRAZE JOINTS

(U) Post braze inspection of the tube-to-backup braze bond was necessary to: (1) prove the tooling and brazing procedures, and improve the quality of subsequent bodies by tooling modification, if necessary (2) provide a measure of disbond that determines the maximum pressure which could be tolerated between the tubes and the bodies which might result from leakage, and (3) indicate whether repair or a rebraze cycle was necessary, in the case of gross disbond.

(U) The determination of tube-to-body braze joint bond or disbond was not feasible by normal inspection methods, i.e., ultrasonic or X-ray. The use of thermochromistic pigments appeared to be simple, inexpensive, and practical.

(U) The thermographic method is the application of a temperature-sensitive paint upon the hardware to be inspected, and the application of heat at a rapid rate from the same side in which the paint was applied. Changes in the conductivity, due to the presence or absence of a heat sink, of the sub-surface material are detected by color changes of the surface paint. The absence of a heat sink (disbond) causes the area of the tube over the void to increase in temperature at a faster rate than bonded adjacent areas. A temperature of 140 F will cause the thermochromistic paint to change color from a light pink to a vivid blue. The change in color is reversible with higher humidities, which is beneficial in that this permits "erasing" the blue color, but humidity must be controlled so that sufficient time is provided for recording results. Initially a sample group of tubes was brazed to a backup panel with various sizes of slots in the panel to deliberately create disbonds in the brazed assembly. The resulting thermochromistic scan clearly showed the lack of bond in the slot areas, as well as tubes that lifted from the backup panel during brazing.

(U) In addition to many other test specimens, the test proved its practicality on 0.008 to 0.011 inch wall thickness 347 stainless steel tubes brazed to a massive stainless steel backup structure.

(U) To ensure repeatability, it was necessary to establish the effects of temperature and relative humidity on the rate of color recession. The time available to record the location and size of the void as manifested by the initial color change could then be ascertained for a given temperature and humidity.

(U) The test results indicated that a relative humidity of 60 percent was the maximum humidity at and below which ample time would exist to make the necessary recordings.

(U) Other extensive tests were necessary to establish the distance of the heat source from the hardware being tested, and the rate of travel of the heat source around the circumference of the combustor bodies.

(U) The development effort permitted the highly successful inspection of the outer combustor bodies in 35 minutes each and the inner bodies in 90 minutes. The time difference for inspection was not because of significant differences in area of the bodies, but was due to repositioning the camera used for recording any indications around the circumference of the inner body compared to its pivot position at the center of a circle for the outer body.

(U) The thermo detection method of testing was very simple, reliable and inexpensive. It made possible, what is extremely difficult, expensive, or impracticable by other inspection methods. The test method proved the adequacy of the braze tooling, techniques, and procedures on the first body brazed, and revealed no gross areas of disbond which could have interfered with operating parameters, or necessitated rework.

CONFIDENTIAL

TUBE MATERIAL SELECTION PROGRAM

PROGRAM PLAN

(U) A materials evaluation and selection effort was planned to provide the critical data needed to select a long-life, high-performance, fabricable tube material. The logic flow diagram for the material selection program is shown in Fig. 1.

SELECTION OF CANDIDATE MATERIALS

(U) In the selection of the candidate tube materials for thrust chamber usage, an effort was made to utilize basic analysis as a means of screening a broad range of materials. A plastic strain analysis, in conjunction with an analysis of high-temperature ductility and fatigue data, was used to select the candidates. In general, a candidate material was evaluated by comparing the predicted cyclic plastic strain against its fatigue properties over a range of temperatures. Other considerations, such as ease of fabrication, mechanical properties, and estimated cost and availability, influenced the selection (Table 1).

(U) The candidate materials thus selected were then the subject of preliminary studies in processing, availability, and cost. As a result of these preliminary studies, a further screening of the original candidates was made. The original candidate materials which survived the preliminary screening are also shown in Table 1.

LITERATURE SURVEY

(U) A survey was made of all available data on the physical and mechanical properties of the candidate materials. All existing valid data were compiled using, wherever possible, the properties of the material in the

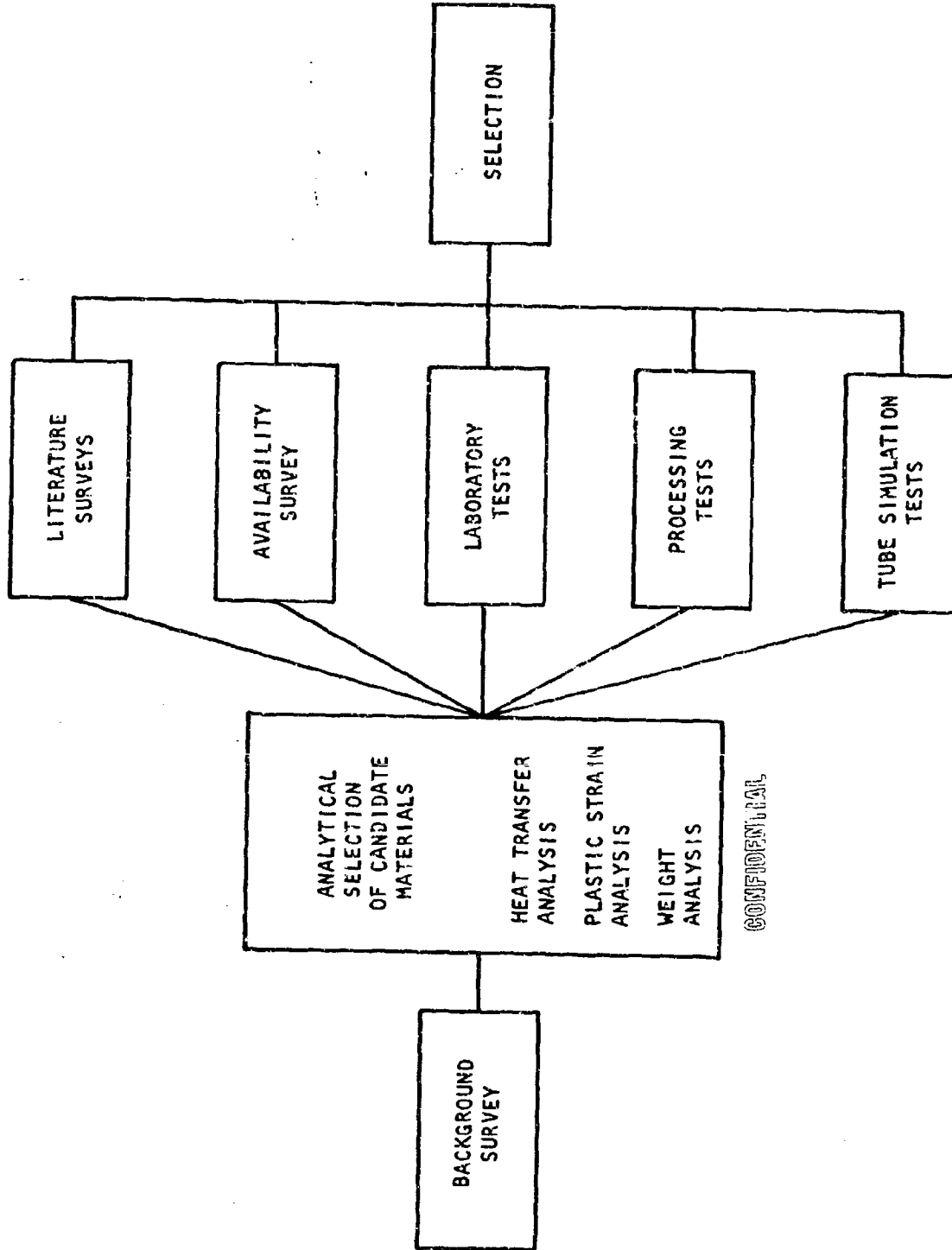


Figure 1. Material Selection Program

TABLE 1

CANDIDATE MATERIALS FOR THRUST CHAMBER USAGE

Original Candidates, Selected by Analysis	
Nickel	200 270 TD
Copper	OFHC Boron Deoxidized Beryllium Alloy 10 Zirconium Alloy Chromium Alloy
Stainless Steel	347
Screened Candidates, Evaluated by Tests	
Nickel	200 270
Copper	OFHC
Additional Candidates for Long-Range Application, Evaluated by Tests	
Copper	Boron Deoxidized Beryllium Alloy 10

as-furnace-brazed condition. The results of the literature survey are shown in Table 2. In some instances, the required data were not available. Testing was therefore scheduled to obtain these data on the remaining candidate materials, as indicated by the shaded boxes. As stated earlier in this section, four of the candidate materials were eliminated. Chrome copper and zirconium copper were eliminated because of difficulties in furnace brazing. TD-nickel and Hastelloy-X were eliminated because of the shortage of supply in tube stock and long lead time to procure samples and stock. Also, TD-nickel cost was excessive when procured in bar stock as necessary for this effort.

OXIDATION-EROSION AND SURFACE PROTECTION STUDIES

(U) The oxidation-erosion studies revealed that from strictly thermodynamic considerations, copper and nickel should not oxidize in a water vapor environment. With excess hydrogen in the water vapor, copper and possibly nickel should not oxidize, even under the flow conditions characteristics of the thrust chambers. It seems probable, then, that the oxidation-erosion problem, if it appears, centers around such practical considerations as nonuniform mixture ratio distribution and adverse perturbations in tube temperature. These effects can only be determined by tests, and are characteristic of injector design, start sequence, throttling range, and other system-controlled effects.

(U) The diffusion layers and coating studies were intended to reveal those state-of-the-art processes which might be applied to nickel or copper tubes to enhance their oxidation-erosion resistance. Two different approaches were explored. Studies indicated that braze alloy wetting may increase the oxidation resistance of nickel and copper since these alloys are essentially composed of noble metals. A concurrent literature review revealed the existence of several state-of-the-art intermetallic diffusion processes which would be applicable to nickel and possibly copper. Diffusions of aluminum appear particularly attractive because such diffusions

(C) TABLE 2

SUMMARY OF RESULTS, MATERIAL PROPERTY LITERATURE SURVEY

Alloy	Thermal Conductivity	Total Thermal Expansion and Contraction	Modulus of Elasticity	Poisson's Ratio	Tensile Data Before Braze (Annealed)	Tensile Data After Braze	Stress-Strain Curves to 0.5 Percent	Percent R.A. Data Braze Condition	Creep Tubing or Sheet
Ni 200	Have data	Need data, have mean linear only	Have data	R.T. Elastic only, need data	Have data	Have data	Have data	Need data	Need data
Ni 270	Have data	Need data, have mean linear only	P.T. only, need data	Need data	Need data	Need data	Need data	Need data	Need data
TD Ni	Have data	Need data	Have data	R.T. only, need data	Have data	Have data to 0.5 percent	Have data to 0.5 percent	Need data	Need data
Hastelloy-X	Have data	Need data, have mean linear only	Have data	-108 F and R.T. only, need data	Have data	Have data	Have data	Need data	Need data
347 SS	Have data	Have data	Have data	Have data, elastic only	Have data	Need new data	Have data	Need data	Need data
OFHC Cu and Boron Deoxidized Cu	Have data	Have data	Have data	Have data, elastic only	Have data	Have data	Have data to 0.5 percent	Have some data, need data	Need data
Be-Cu	Have some data, need data	Need data, have mean linear only	Need data	Need data	Need data	Need data	Need data	Need data	Need data
Zr-Cu	Have data	Need data, have mean linear only	Need data	Need data	Need data	Need data	Need data	Need data	Need data

CONFIDENTIAL

reputedly have ductilities close to that of the base metal. Other diffusion systems in current use employ chromium and aluminum-chromium combinations. All diffusion coatings would adversely affect thermal conductivity to some degree. The significance of this degradation could only be determined by heat transfer tests and analyses.

(U) As a result of the oxidation-erosion and diffusion layers and coatings studies, a decision was made to eliminate the surface protection screening tests until a firm requirement was established by hot-firing tests.

MECHANICAL PROPERTY TESTS

(C) The mechanical property and ductility tests were simple tensile tests on rod and tube specimens, both in the annealed condition, and were also processed in a way similar to a furnace-brazed tube. Tests were conducted at room temperature in air and also at elevated temperature in an argon environment. The results of these tests are shown in Table 3. Some significant findings from these tests were the excessively low yield stress of Nickel 270 and the effects of grain size on the tube materials apparent tensile properties.

BRAZING FEASIBILITY STUDIES

(C) The braze process and contamination studies and tests were intended to define initially proposed furnace step braze cycles for each candidate tube material. These initially proposed braze cycles were then applied to test specimens to determine the alloy wetting and flow characteristics, and to determine any tendencies for the braze alloys to induce tube alloying or intergranular penetration. The results of these tests indicate that while Nickel 200 and 270 apparently may be successfully furnace brazed with current technology, brazing of bare OFHC and beryllium copper is limited by tendencies of the common braze alloys to dissolve part of the base metal.

(c) TABLE 3

CYCLIC STRAIN TEST RESULTS

Material	Annealing Temperature, F	Specification No.	Test Temperature, F	Cycles To Crack	Total Cycles	Condition of Specimen After
Strain 0.0134*						
OFHC Cu	900	1	500	230	322	90 percent crack
OFHC Cu	900	2	500	104	400	Separation
OFHC Cu	900	7	750	-	400	No crack
OFHC Cu	900	8	750	-	400	No crack
OFHC Cu	1900	13	500	135	308	Separation
OFHC Cu	1900	14	750	50	400	Separation
OFHC Cu	1900	9A	750	490	511	20 percent crack**
OFHC Cu	1900	3	500	-	400	No crack
Strain 0.0257*						
Ni 200	1350	4	1100	100	168	Separation
Ni 200	1350	3	1100	50	283	Separation
Ni 200	1350	6	1400	100	355	Separation
Ni 200	1350	5	1400	20	390	Separation
Ni 200	1975	22	1100	74	327	Separation
Ni 200	1975	21	1400	20	400	Separation
Strain 0.0257*						
Ni 270	1975	16	1100	180	400	50 percent crack
Ni 270	1975	15	1100	180	400	20 percent crack
Ni 270	1975	18	1400	170	529	Separation
Ni 270	1975	17	1400	230	400	90 percent crack
Strain 0.0360*						
347 Stainless	1975	20	1200	70	315	Separation
347 Stainless	1975	19	1650	50	105	Separation
Strain 0.0098*						
Be Cu #10	1650 + 1100	11	500	-	400	No crack
Be Cu #10	1650 + 1160	12	500	-	400	No Crack
Be Cu #10	1650 + 1100	10	750	-	251	Separation
Be Cu #10	1975	24	500	-	400	No crack
Be Cu #10	1975	23	750	-	400	No crack

*Total strain range

**Separated through 20 percent of reduced section

CONFIDENTIAL

MECHANICAL STRAIN, ELEVATED TEMPERATURE FATIGUE STUDIES

(U) The mechanical strain at elevated-temperature fatigue tests were designed to simulate the strain cycle experienced by a thrust chamber during the start and shutdown sequence. These tests were run at constant elevated temperatures, and utilized rod specimens which were axially strained. Materials in the annealed and furnace-brazed condition were tested. Plastic strain analysis was used to predict the equivalent axial strains which each material would experience as a thrust chamber throat tube. The tests were run at temperatures which represented the maximum predicted tube gas-wall temperature for each material. Tests were also run at a reduced temperature known to represent a condition of minimum ductility for each material. All tests were run in an argon environment.

(U) A record of each load-strain cycle was continuously printed out by automatic equipment. An unsymmetrical curve was developed after a large number of cycles which represented the load-deflection behavior of the progressing fatigue crack alternately stressed in tension and compression. As the crack grew, the tensile load-carrying ability decreased as strain remained constant, thus providing a convenient technique for recording crack progression.

(U) While it is customary in tests of this nature to report the number of cycles to complete fracture, a more meaningful technique was used which gave a measure of the development of internal fatigue damage, as well as the conventional cyclic life. This was obtained by plotting the ratio of maximum cyclic tension (compression loads in the specimen vs the number of test cycles). These load values were obtained from the load-strain hysteresis loops. Groups of curves for each common material and process condition were then drawn for each specimen run at various test temperatures.

TUBE TAPERING AND FORMING FEASIBILITY STUDY

(C) A related tube-tapering feasibility program was also completed, and the results were made available for the material selection program. The materials evaluated in this program were type 347 stainless steel, Nickel 200, Nickel 270, and OFHC copper. These materials were experimentally tapered to tube dimensions and tolerances. Inspection of the finished tubes yielded an initial estimate of tube-tapering confidence with regard to process time, tolerance control, lubricant contamination, and the effect of inclusions in the material.

MATERIAL SELECTION

(U) To select a tube material for the demonstrator segment thrust chamber, a criteria list was developed as an aid. The criteria were taken from life, performance, and fabrication considerations. Each tube material was then evaluated by these criteria, as determined from the results of the Materials Selection Program, from previous experience, from published literature, and from the results of the hot-firing tests.

(C) A comparison of the demonstrator segment thrust chamber tube materials, as determined by these criteria, is given in Table 4. It was concluded that Nickel 200 offered the best combination of necessary features for this application. This material was therefore selected, in combination with a process cycle which produced the best obtainable properties.

(U) A similar comparison was made of the long-range candidate materials (Table 5). It was seen that the beryllium copper alloy No. 10 material offered a large increase in thermal fatigue life and uprating capability. Its practical thrust chamber use, however, awaits the development of suitable manufacturing processes.

CONFIDENTIAL

TABLE 4

FACTORS AFFECTING SELECTION OF 20K-SEGMENT TUBE MATERIAL

(Based on State-of-the-Art Fabrication Technology

(C)

and Chamber Operating Conditions)

Material Criterion	Type 317 Stainless Steel	Nickel 200	Nickel 270	OFHC Copper
Strength to Withstand Hydraulic Stress	Good	Good	Poor	Good
Thermal Stress Fatigue Resistance	Poor	Good	Poor	Fair
Metallurgical Stability	Excellent	Good	Poor	Poor
Oxidation-Erosion Resistance	Good	Good	Good	Good
System Compatibility	Excellent	Good	Good	Fair
Comparative Coolant Pressure Drop	1.0	0.85	0.75	0.95
Comparative Weight	1.0	1.05	1.05	1.20
Up-rating Capability	Poor	Fair	Fair	Good
Drawing, Tapering, and Forming Confidence	Good	Excellent	Excellent	Good
Brazing Confidence	Excellent	Good	Good	Poor
Availability	Good	Good	Good	Good
Total Cost	Low	Low	Low	Low

CONFIDENTIAL

CONFIDENTIAL

(c) TABLE 5

FACTORS AFFECTING SELECTION OF LONG-RANGE TUBE MATERIALS
(Based on Current Knowledge and Chamber Operating Conditions)

Material Criterion	Boron Deoxidized Copper	Beryllium Copper Partial Heat Treat	Beryllium Copper Full Heat Treat
Strength to Withstand Hydraulic Stress	Good	Excellent	Excellent
Thermal Stress Fatigue Resistance	Good	Excellent	Unlimited
Metallurgical Stability	Good	Excellent	Excellent
Oxidation-Erosion Resistance	Fair	Good	Excellent
System Compatibility	Fair	Good	Good
Comparative Coolant Pressure Drop	0.95	0.95	0.95
Comparative Weight	1.20	1.05	1.05
Up-rating Capability	Good	Excellent	Excellent
Drawing, Tapering, and Forming Confidence	Good	Unknown	Unknown
Brazing Confidence	Poor	Poor	Poor
Availability	Fair	Good	Good
Total Cost	Low	Moderate	Moderate

CONFIDENTIAL

CONFIDENTIAL

NICKEL TUBE-WALL THRUST CHAMBER CYCLING TESTS

Test Conditions

(C) An experimental determination of the thermal fatigue life of a 2.5K segment thrust chamber was completed. The goal of this 2.5K tube-wall segment cycling program was to demonstrate by actual hot-firing tests the life expectancy of the Nickel 200 tube material selected for the Demonstrator tubes. A further benefit derived from this tests series was an experimental verification of the analytical tube life predictions.

(U) To achieve these goals, it was necessary to reproduce operating conditions which simulated the critical fatigue life parameters of the Demonstrator at rated operation in a segment thrust chamber having an identical tube material.

(C) The second nickel tube-wall 2.5K thrust chamber was made available from a related program and used for these cycling tests. This segment was fabricated of Nickel 200 tubes which were drawn, tapered, and pressure formed following a process planning which closely resembled that described for the Demonstrator Module. The segment thrust chamber experienced two-step furnace braze cycles, using the braze alloy systems selected during the tube material selection program. The total furnace time at high temperature was adequate to ensure that tube material grain growth effects were simulated.

(C) Ignition was obtained by the use of TEA-TEB hypergol. The current plan for the Demonstrator Module ignition makes use of O_2/H_2 1800 F hot gas. No appreciable differences in environmental effects were predicted as a result of the substitution of the hypergolic ignition fluid. During the test series, no deposits resulting from the combustion of TEA-TEB were found in the thrust chamber except in very minute quantities.

CONFIDENTIAL

(C) It is thus reasonable to conclude that the effects of chemical and temperature environment on the metallurgy of the Demonstrator Nickel 200 tube material were simulated in the 2.5K segment.

Testing Procedure

(C) The 2.5K segment was tested by cycling chamber pressure, and thus tube wall temperature, in a series of cyclic test groups. During each test group, the fuel flow through the injector and tube banks remained unchecked, while the LO_2 flow was intermittently stopped. Ignition was obtained at the start of each test group with TEA-TEB hypergol, and was maintained during the idle phases of each test group by a small, continuous, gaseous oxygen flow. During these cyclic idle phases, the heat flux to the walls was very low, and by analysis, a tube-wall and adjacent-structure average temperature which approached -230 F was realized. The upper cyclic tube-wall temperatures were near those predicted for the Demonstrator throat. A summary of the operational, tube cooling, and life parameters for each test group is given in Table 6.

(C) The chamber segment was still in a satisfactory operating condition at the conclusion of the 315 hot-firing tests. However, since the program goal of demonstrating the feasibility of obtaining 300 hot-fire cycles with the Nickel 200 tube material selected for the Demonstrator Module chamber had been exceeded, the hardware was removed from the test facility in favor of a detailed metallurgical analysis of the chamber and injector.

NICKEL TUBE WALL THRUST CHAMBER FATIGUE RESULTS ANALYSIS

Analysis of Test Conditions

(C) The most severe limitation to the extended usage of well-designed, regeneratively cooled thrust chamber is imposed by the fatigue of the coolant tubes. The fatigue phenomenon ordinarily manifests itself in

CONFIDENTIAL

TABLE 6
SUMMARY OF 2.5K SEGMENT CYCLE TESTS

Test No.	Operational Parameters				Tube Cooling and Life Parameters at Throat				
	Cycle No.	Chamber Pressure, psia	Injector Mixture Ratio*	Coolant Mass Velocity	Tube Gas Wall Temperature, * F	Tube Mean Wall Temperature, * F	Tube Hydraulic Stress, * psi	Approximate Life Simulation* Ratio	
1		Ignition Only							
2	1	610	6.05	12.55	810	524	3836	3.091	
3	2	930	5.30	11.28	1195	828	3375	1.522	
4	3-17	956	5.06	12.45	1140	758	3355	1.595	
5	18	1320	5.04	11.50	1550	1108	2814	0.944	
6	19-35	1322	5.31	12.13	1525	1058	2810	0.971	
7	36-51	1303	5.22	12.13	1505	1062	2940	0.983	
8	52-67	1230	5.07	11.28	1490	1064	2945	1.020	
9	68-84	1071	5.42	10.68	1360	964	3175	1.213	
10	85	1210	4.47	10.63	1510	1090	2971	1.011	
11	86-116	1309	4.96	12.03	1520	1075	2900	0.968	
12	117-147	1330	5.00	12.03	1535	1087	2795	0.948	
13	148-178	1230	5.14	10.40	1545	1123	2950	0.975	
14	179-209	1260	4.94	10.85	1545	1117	2640	0.967	
15	210-242	1310	5.31	10.96	1585	1144	2830	0.942	
16	243-277	1330	5.00	10.53	1620	1178	2800	0.890	
17	278-314	1270	4.45	10.64	1560	1129	2890	0.954	

* Average values

CONFIDENTIAL

the form of tiny transverse cracks which nucleate and grow through the hot wall of the tube. The primary cause may be described as the gradual destruction of the material's internal bonding due to plastic strain or slip.

(U) Thermally induced plastic strains in the Demonstrator tubes occur during the engine start and shutdown sequence, especially near the throat plane. Here a transient gas-wall temperature ranging from near the coolant bulk temperature to the nominal operating value occurs with the rapid heat flux buildup which follows ignition.

(U) An approximate technique for calculating the "equivalent uniaxial" strain resulting from these tube-wall, multiaxial strains was developed. The uniaxial strain referred to here is the plastic strain in a low-cycle fatigue test measured along the axis of applied cyclic mechanical strain. An analytical relationship between the tube wall plastic strains and the plastic strain of a laboratory fatigue test is thus established. A tube life prediction based on laboratory test data is then possible.

(U) Since the test objective was the accurate modeling of the Demonstrator thrust chamber thermal fatigue, the most important criterion of test design was that the maximum value of the gas-wall cyclic plastic strain be reproduced in the test segment. Other important test design criteria were the simulation of the cyclic temperature range which the Demonstrator tube gas wall experiences, and the simulation of the tube-wall environmental conditions. These environmental conditions included those experienced during fabrication as well as those during operation. A high tube-wall pressure stress in combination with cyclic thermal strain can also be critical, causing the axial crack fatigue failure mode to predominate over the transverse crack failure mode. This complex fatigue-creep failure mode was effectively simulated on the tube tester, described later. In the selection of the 2.5K segment cycling test conditions, consideration was given to all of the above criteria so that these life parameters for the Demonstrator Module were simultaneously matched as closely as possible in the 2.5K segment.

CONFIDENTIAL

(U) The throat tubes of the Demonstrator Module outer body were selected as the reference base for test design because the operating conditions of the outer body tubes afford a more basic limitation to the thermal fatigue life of the Demonstrator.

(C) The 2.5K segment test conditions were selected to simulate the Demonstrator gas-wall thermal cycle in combination with the pressure stress. It was again found that a good correlation was realized when chamber pressure was 1250 to 1350 psia at a mixture ratio of 4.5 to 6.0 with a coolant flow-rate of about 1.0 to 1.2 lb/sec. The mean tube-wall temperature, and thus the tube wall yield strength, was also found to be comparable at these operating conditions.

Life Prediction

(U) By use of a thermal fatigue diagram with the computered cyclic plastic strain, a tube-wall life in thermal cycles was predicted. This predicted life was consistent with the Demonstrator Module restart requirements.

(U) Table 6 includes a calculated life simulation ratio for each test. This number is defined as the ratio of the predicted life of the segment thrust chamber cycling from -240 F to the peak heat transfer conditions of that case to the predicted life of the Demonstrator outer body. Life simulation ratios less than one indicate test conditions were more severe than those expected on the Demonstrator Module design. The predicted lives used to compute this ratio were in all cases obtained by identical use of the plastic strain equations and fatigue diagram. Because the computed values of these ratios are less than unity for most cases, it was seen that the segment operated under conditions which were, for the most part, more severe from a thermal fatigue standpoint than the Demonstrator outer body. (Some of the earlier tests in the series were less severe.)

CONFIDENTIAL

Experimental Life

(U) By observing the chamber throughout the test series, a record of the fatigue progression was obtained. The general appearance of the overall tube was generally excellent and well-progressed fatigue symptoms were only noted in a narrow band near the throat. On some tubes, initial evidence of fatigue was also visible on sections near the injector. At the conclusion of the testing (see Table 6 Testing) fatigue symptoms (microcracks) were evident on the majority of tubes. Operation of thrust chamber tubes containing microcracks generally has no notable effect on chamber flows, cooling, or performance. This trait was again verified during this test series. Comparison of the appearance of microcracks to the analytical predictions showed good correlation. Analytical data had predicted that 50 percent of the tubes would have microcracks after 26 $\frac{1}{2}$ cycles.

(U) There was a divergence in the appearance of the two sides of the chamber. The fatigue indications on Side A followed an ordinary progression with microcracks appearing as would be expected from the usual scatter experienced in thermal fatigue data. On Side B, it appeared that there was an unbalance in throat tube-wall temperature such that a portion of the tubes were undergoing higher than nominal temperature conditions, while the remainder of this side was operating at temperatures less severe than the nominal. Midway through the tests, axial microcracks appeared on a small percentage of the tubes on Side B. These gradually developed into sources of leakage as testing continued. All of these tubes appeared to the left of the centerline of Side B, while the tubes to the right of the centerline on Side B generally indicated less fatigue than any other portion of the chamber. The reason for this temperature unbalance has not been accurately determined.

Metallurgical Examination

(U) A detailed metallurgical examination of the segment thrust chamber was conducted after test 315. The chamber was cut in half by sawing

27
CONFIDENTIAL
(This page is Unclassified)

CONFIDENTIAL

through the center of the copper side plates. Following photography of the two chamber halves, additional saw cuts were made to expose the throat area tube hot and cold side to stereobinocular examination. This examination showed that no gross melting or erosion of the tube crowns in the throat had occurred. All but five tubes in the A side appeared to have microcracks in the throat area. The appearance of the tubes was remarkably uniform on the A side. Unlike the A side, there was considerably more tube crown damage in the left side of the throat of the B side than in the right side. Extensive, highly localized metal movement had occurred in the hot-gas surface of the tubes in the A and B side throat area, which is characteristic of low-cycle thermal fatigue. The four tubes brazed to the copper side plates suffered axial cracks near the throat apparently caused by additional restraint imposed by the side plates. On side B, these axial cracks developed into major leaks during the latter tests.

(U) A metallographic examination was made of sections across the throat. The hot-gas crowns showed an alternate increase and decrease of thickness which is typical of metal movement caused by thermal cycling. Typical variations were between 0.010 and 0.015 inch compared to the original 0.012 inch. Examination at high magnification confirmed the lack of sulfur contamination or braze alloy penetration. There was some erosion damage to a few tubes which protruded about 0.020 inch into the combustion zone. This erosion is normal where direct flame impingement occurs.

(U) A microhardness survey was made at regular intervals along the section of a tube at the throat. The observed variations in hardness are attributable to strain cycling under variable conditions of temperature and restraint around the tube crown.

(C) A thin black film had formed on the tube surfaces in the convergent and throat areas. A spectrographic analysis of this film indicated that this deposit contained no major component (over 10 percent); it contained minor quantities of chromium, nickel, iron, copper, aluminum, gold, boron, and other trace elements. No nickel corrosion products formed from the TEA/TEB hypergol were found. The spectrographic analysis also confirmed that the tubes were originally unalloyed nickel, with no alloy additions.

CONFIDENTIAL

CONFIDENTIAL

(U) There was general evidence of thermal fatigue, with a few tubes split by hoop stresses. There were no failures from erosion and/or melting of tube crowns in the throat.

(C) The choice of braze alloy and the brazing operation appear correct. Tube wetting was good, and yet the penetration of braze alloy into the nickel was almost nil. No differences in tube materials, fabrication, or service-produced metallurgical changes could be detected in the throat area. The nickel tube segment was judged to have been well made and assembled, and to have good life performance in the test program.

Thrust Chamber Tube Tester

(C) The objective of the tube tester experiments was to evaluate the thermal fatigue life and hydraulic stress adequacy of the nickel material under simulated chamber operating conditions. Some of the tests were representative of operating conditions more severe in temperature than those anticipated on the Demonstrator Module and thus were conducted as material limit tests.

(C) The electrically heated, hydrogen-cooled, thermal fatigue tube tester was the experimental tool used for these tests. Five thermal fatigue temperature cycle ranges were employed either individually or in combination to evaluate six tubular specimens. The temperature cycle ranges were selected to demonstrate the life capability of Nickel 200 under various cyclic chamber pressure operating conditions.

(C) The first four tests were designed to verify the thermal fatigue life of the throat tubes when subjected to a continuous series of engine start-stop sequences. Two of these tests utilized cyclic gas-wall temperatures of 100 to 1400 F, and thus approached the predicted gas-wall temperature range of the Demonstrator Module throat tubes. One specimen was in the "as received," small-grained condition, while the other was furnace processed with the resulting enlarged grain size. Penetrating crack

CONFIDENTIAL

CONFIDENTIAL

failures occurred at 315 cycles in the "as-received" specimen, while the furnace-processed specimen was run a total of 320 cycles without failure. Fatigue cracks were initiated, however, and further testing was deemed unnecessary. These tests were run at temperature conditions somewhat less severe than the Demonstrator Module throat tubes ($T_{wg} = 1400$ vs 1520 F, $T_B = 100$ vs -230 F, also a reduced heat flux); consequently, the induced cyclic plastic strains were less.

(C) The other two engine start-stop sequence tests employed 0.012-inch wall tubes in the furnace-processed condition with cyclic gas-wall temperatures of about 100 to 1800 F. Such a temperature range on the Demonstrator Module tubes would be representative of an ambient to over 2000 psi chamber pressure start cycle. The fatigue failures occurred at 142 and 143 cycles.

Intermediate Throttling Fatigue Tests.

(C) Two other tests on a related program were intended to explore the limits of the Nickel 200 tube material under more complex operating conditions. Two cyclic temperature ranges were employed on the first specimen. A cyclic temperature range of 620 to 1140 F was initially applied to the specimen a total of 800 times with no evidence of failure. The same specimen was then additionally cycled 195 times between 100 to 900 F. Although the heated tube crown still showed no visible evidence of fatigue cracks, testing was stopped because of a breakdown of the specimen in another area.

Steady-State Creep and Fatigue Tests.

(C) The last test employed an 0.028-inch wall specimen which was designed for high heat flux continuous testing. The objective was to verify the limits of Nickel 200 in combined thermal fatigue and hydraulic stress

CONFIDENTIAL

induced creep. A severe steady-state gas wall temperature cycling condition of 1365 to 1435 F at a frequency of about 1 cps, in combination with a heat flux of 50 Btu/in.²/sec and a hydraulic stress of 4500 psi, was applied to the specimen. Testing continued for 7 hours, accumulating 22,500 thermal cycles without fracture or leaks. Routine inspection revealed that microcracks were initiated, however, and further testing was stopped. Table 7 summarizes the results of these thermal fatigue tests.

- (U) A tube tester data reduction computer program was developed on separate funding. This program gave an accurate measure of the specimen wall temperature drop. Included in the wall drop numerical solution were the variables of thermal and electrical conductivity with temperature, and variable current distribution in the bimetallic bus bars.
- (U) A computation of the plastic strains was also included in the program, based on the plastic strain analysis; the measured test gas wall cyclic temperature; and the program computed wall drop. These values are given in Table 7 which also includes a computed equivalent fatigue life for the demonstrator throat tubes. This computed life is based on an extrapolation of the tube tester data, using the relationship $N_F^k \Delta \epsilon_p = C$, where k was assumed to have a value of 1/2.
- (U) It is seen that the technique gave a lower life (about 1/3) for the Demonstrator tubes than was realized in the 2.5K segment start-stop cycling tests. This difference was attributed to non-uniform specimen tube crown cyclic heating in the tangential strain concentrations at the tube crown, and perhaps other effects unresolved at this time. The "steady state" creep and fatigue test results, however, were thought to reasonably represent the Demonstrator tube life, if such "steady state" temperature fluctuations were actually realized in service.

31
CONFIDENTIAL
(This page is Unclassified)

CONFIDENTIAL

(C) TABLE 7
 THERMAL FATIGUE TUBE TESTER RESULTS ON VICKEL 200

Type of Test	Tubular Specimen Metallurgical Condition	Cyclic Gas Wall Temperature, F	Wall Temperature Drop, F	Hydraulic Stress in Heated Tube Crown, psi	No. of Thermal Cycles	Final Appearance of Heated Tube Crown	Equivalent Cycles at Demonstrator Conditions
Demo Module Start Simulation	As received	100 to 1400	74	1000	315	Intergranular and transgranular cracks, rupture	86
Demo Module Start Simulation	Furnace Processed	100 to 1400	65	1000	320	Intergranular and transgranular cracks, no rupture	94
Overtemperature Limit Test	Furnace Processed	100 to 1800	87	1000	142	Intergranular cracks, rupture	80
Overtemperature Limit Test	Furnace Processed	100 to 1800	92	1000	143	Intergranular cracks, rupture	86
Exploratory Limit Test	Furnace Processed	620 to 1140 100 to 900	200	3300 3300	800 293	No visible cracks, no leaks or rupture	Not Applicable
Steady State Limit Test	Furnace Processed	1365 to 1435	520	4500	22,500 over 7 hours	Cracks Initiated, no leaks or rupture	22,500

CONFIDENTIAL

CONFIDENTIAL

FABRICATION OF 250K COMBUSTORS

GENERAL DESCRIPTION

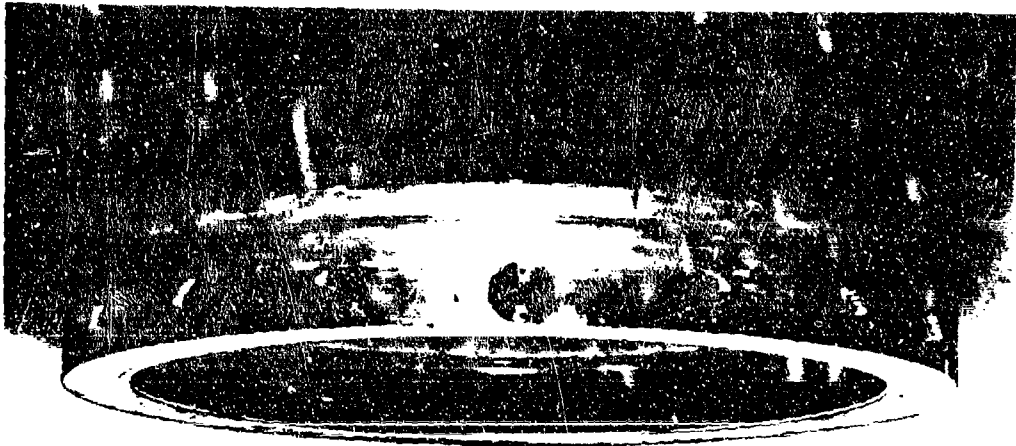
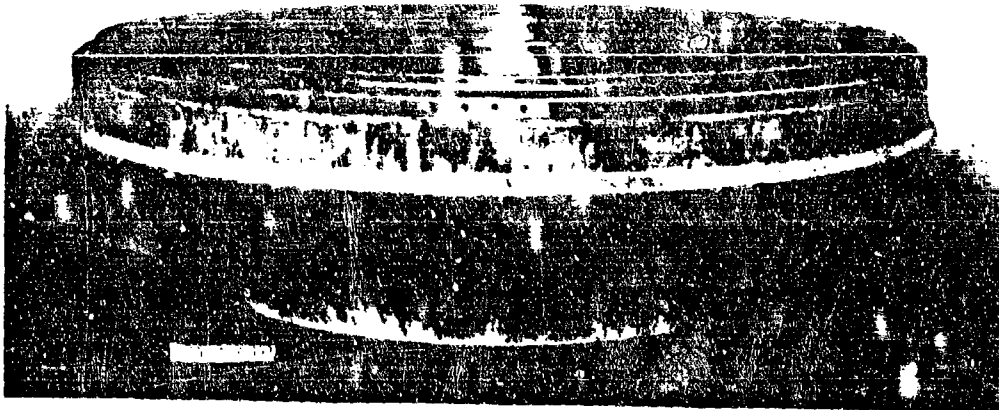
(C) The 250K thrust chamber assembly (Fig. 2) consists of concentric, regeneratively cooled, inner and outer combustor assemblies forming an annular chamber leading to a converging throat (0.271 throat gap at a mean diameter of 93.00 inches), a shrouded outer tubular wall, and an inner tubular nozzle wall extending to a nozzle length equivalent to 11.3 per cent the length of a 15-degree, half-angle cone of the same area ratio. Each of the combustor assemblies is fabricated of 347 stainless steel tubing brazed to a 304L stainless steel structural backwall. The nozzle exit of the inner combustor contains a two-inlet distribution manifold through which fuel enters the coolant tubes. A collection manifold at the injector end is formed by the inner combustor and injector. A similar coolant circuit exists on the outer combustor to the discharge manifold where 20 outlets distribute fuel to the injector assembly.

(U) The combustion chamber geometry is 2 inches wide at the injector and has a 6-inch length from the injector face to the throat. The chamber walls are parallel down to a point approximately 4.5 inches downstream of the injector face, and then converge at a 40-degree angle.

(U) Radial and axial positioning of the inner combustor with the outer combustor is obtained by attachment to the injector through the use of axial studs. Relative location is facilitated by shear lips at the combustor/injector interface.

(U) Provision is made to attach an eight-point thrust mount support assembly to the inside surface of the inner combustor, also a solid-wall nozzle extension at the exit plane of the inner nozzle representing a 25 per cent nozzle length. The perforated base closure for secondary flow attaches at the exit plane of the nozzle extension.

CONFIDENTIAL



0-250K-111

Figure 2. 250K Thrust Chamber

CONFIDENTIAL

THRUST CHAMBER TUBE PROCESSING

(U) Properties which had to be controlled in the thrust chamber tubing were formability (strength and ductility), wall thickness, surface defects, cross-section geometry, and grain structure (grain size, intergranular attack). It was also necessary to maintain traceability on tubing so that all inspection for these items can be related to specific tubes.

(U) Control of the necessary fabrication parameters involved development in several areas, primarily because of the thin wall and small diameters (0.080 inch) of the tubing. Development work was performed on tapering methods to ensure defect-free tubing with correct surface finishes in the small sizes. Improved cleaning methods were established to reach the minute small tube ID surfaces.

The basic process steps and major inspection points established were:

1. Raw material procurement
2. Raw material inspection--metallography and physical test
3. Tapering
4. Solvent cleaning
5. Annealing
6. Metallographic sampling and expansion testing
7. Solvent cleaning
8. Preforming
9. Solvent cleaning
10. Annealing
11. Metallographic sampling
12. High-pressure die forming
13. Solvent cleaning
14. Final inspection, dimensional-metallographic
15. Flow testing

(U) Raw Material. Welded and drawn type 347 stainless-steel tubing manufactured from air melted strip was specified for use as coolant passage tubes on the inner wall and outer wall combustor bodies.

(U) The raw tubing for the combustor tubes was procured by the tapering vendor. (La Fuelle Manufacturing Co.) Tubing with a 0.122-inch diameter by 0.011-inch wall and 20 inches long was received for fabrication of the outer combustor body tubes. Tubing with a 0.152-inch OD by 0.011-inch wall thickness, and 40-inch length was used for the inner combustor body tubes. Identification by lot number was maintained on individual tubes throughout the complete fabrication process. Subsequently, a taper log number was added to this identification number. A fluorescent penetrant inspection was performed on 100 percent of the raw tube by the tapering vendor. Less than 10 percent of the tubing was rejected because of indications.

(U) Tapering. Although some experience had been gained in the tapering of type 347 stainless-steel aerospike configuration tubes during previous segment test programs, no experience in the fabrication of tapered wall tubes of an overall length comparable to the inner combustor tubes was available. Very little experience was available in producing tubes to the required configuration with a tapered wall. With these facts in mind, close surveillance was maintained during experimental tapering and preproduction runs of 500 tubes of each configuration.

(U) To impose maximum control upon a process that is proprietary with the tapering source and still ensure a reasonably inexpensive tubing of high quality, a processing specification was issued which required a test for plastic deformation by high-pressure die forming. Final acceptance criteria were based upon the actual high-pressure die forming of a representative sample from each lot of tapered tubes after receipt.

CONFIDENTIAL

(U) Metallurgical evaluation of experimental and preproduction runs of tapered outer tubes indicated that the tube could be successfully made in one pass without rejectable defects. However, the OD's on both tube configurations were undersize as much as 0.001 inch in areas which were not tapered. It was determined that the undersize condition was caused by the high axial loads imposed upon the tube during one-pass tapering to achieve a tapered wall within equipment limits (standard tapering equipment is too large). The OD variations were accepted.

(C) This local diameter reduction had a marked effect upon the wall thickness at the area of maximum taper. Although a nominal wall thickness of 0.008 inch was the objective of the tapering vendor, the dimension was extremely difficult to achieve. The wall thickness, as determined by metallographic examination on tubes of both configurations during pilot and preproduction runs, was between 0.0085 and 0.0092 inch.

(U) Tapering a tube with a tapered wall and also requiring an ID surface roughness with specific values in the area of maximum diameter reduction (the wall is also at smallest diameter here) was a unique task. By the nature of the process itself, tapering the tube wall tends to reduce ID surface gathering and thus reduces surface roughness. Results of measurements made on tubes from the pilot and preproduction runs revealed that values between 43 and 75 rms could be obtained on the outer tubes and 47 to 72 rms on the inner tubes. These values were subsequently accepted for the production run of tubes.

(U) Preforming. Preforming of the tapered and annealed inner and outer tubes was performed at the tapering vendor's facility. Subsequent to preforming and inspection for contour and station location, the tubes were cleaned and final annealed. The final anneal after the preform operation was necessary because inconsistent final tube dimensions were obtained after the initial high-pressure die forming of both tube configurations.

CONFIDENTIAL

(U) Subsequent to the annealing of the preformed tubes, five tubes from each manufacturing lot were examined metallurgically for compliance with thickness, defect level, and microstructure requirements.

(U) High-Pressure Die Forming. High-pressure die forming of the tubes to final form was considered a major advance by Rocketdyne. Although Rocketdyne has had comprehensive experience in high-pressure die forming of conventional rocket nozzle coolant tubes, no experience in the high-pressure die forming of aerospace-size tubes was available at the inception of the program.

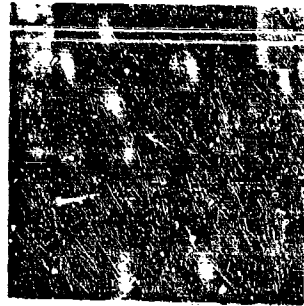
Each inner and outer tube, by engineering requirement, was subjected to a flow check with close tolerances between minimum and maximum flow values from tube-to-tube. Also the large number of tubes (3700) in a combustor body, with attendant tolerance accumulations, demanded forming accuracy. Preproduction lots of 500 tubes of each configuration were used to develop the forming techniques.

(U) To assist in expediting the die-forming operation, an epoxy potting compound was injected into the closed die set. The tube facsimile produced was then subjected to metallographic examination by removing cross sections at critical station locations. Photoacographs of the cross-section configuration were made and used to assist in finishing the die cavities to final shape.

(U) Initial high-pressure die forming of the outer and inner tube preproduction lots produced many tube failures. A substantial number of tubes split longitudinally during the forming operation and an investigation was conducted to determine the cause. Metallurgical evaluation indicated that the splits resulted from the propagation of OD raw tube defects (Fig. 3 and 4). Investigation of the processing history at the tapering vendor showed that a substantial quantity of raw tubing in the first few lots re-

38
CONFIDENTIAL

(This page is Unclassified)



a. Typical longitudinal split (arrow) which was found on hot gas crown at throat section of tubes. Split was not through tube wall

Mag: 10X



b. Typical longitudinal splits (arrows) found on hot gas and body side crowns of tubes in combustion zone and exit ends of tubes. These splits were in areas where no tapering was done on tubes.

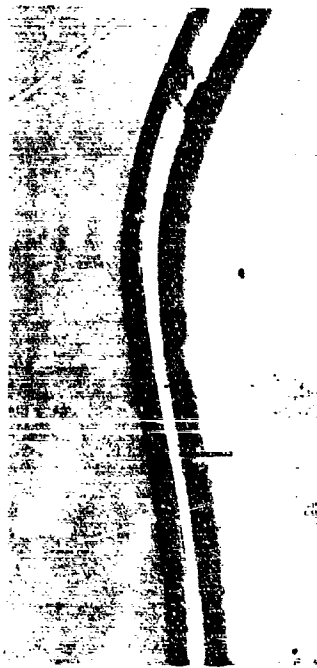
Mag: 10X



c. Photomicrograph of fracture surface of longitudinal split through tube wall shown in Fig. 3a. Fracture surface is Zone A. Zone B is portion of wall which did not fail in forming.

Mag: 40X

Figure 3. Typical Longitudinal Splits Found on Inner and Outer Tubes Subsequent to High-Pressure Die Forming



a. Location of longitudinal split on side of tube (90° from die cavity parting line) in area of maximum taper (arrow) which penetrated through tube wall. Mag: 4X



b. Photomicrograph of a cross section specimen taken through split shown in Fig. 4a. Macro-examination of fracture disclosed portion between A and B was raw tube defect which was in tube prior to forming. Note that defect is 2/3 of way through tube wall. Specimen unetched. Mag: 200X

Figure 4. Longitudinal Split Which Penetrated Through the Tube Wall Causing Tube Not to Form to Final Shape

CONFIDENTIAL

ceived had not been flash pickled prior to penetrant inspection. Flash pickling was added to raw tube inspection requirements for production runs when it was determined that belt polishing on the OD of the tubes at the mill had smeared the surfaces so that fluorescent penetrant inspection was invalid.

(U) The fact that tubes split in the die demonstrated the necessity of using the high-pressure die-forming operation as a final acceptance criterion for tapered and preformed tubes. Otherwise, a large number of defective tubes could have been purchased before the problem was discovered.

(U) To establish a relationship between wall thickness and flow values, a number of high-pressure, die-formed tubes of each configuration were flow tested, and then measured metallographically at critical stations (Fig. 4) for wall thickness and ID. Photomicrographs of the controlling cross section from each tube were made at exact magnifications. These photographs were used to determine the flow areas. Although care was exercised to produce a die cavity which would form tubes with a correct cross-section configuration, tubes of both inner and outer shapes did not completely meet the final shape. The area of nonconformance was limited, however, to the circular cross section in the throat area (area of maximum reduction). A perfect semicircular cavity is difficult to sink in a die with a shallow cavity 0.059 inch deep in each die half.

(U) Final Cleaning of Finished Tubes. In preparation for the furnace brazing of the tubes into combustor body assemblies, requirements were established for cleaning and handling of the tubes subsequent to fabrication and final inspection and immediately prior to shipment to the white room.

(U) Because of the unique configuration of the tubes and the extremely small ID's, specialized processing facilities and procedures were necessary. Combination vapor degreasing and flushing fixtures specifically developed for the finish-formed tubes were used to remove shop soil and ECM dielectric fluid from the tubes. To accomplish this cleaning operation, the tubes were

41
CONFIDENTIAL
(This page is Unclassified)

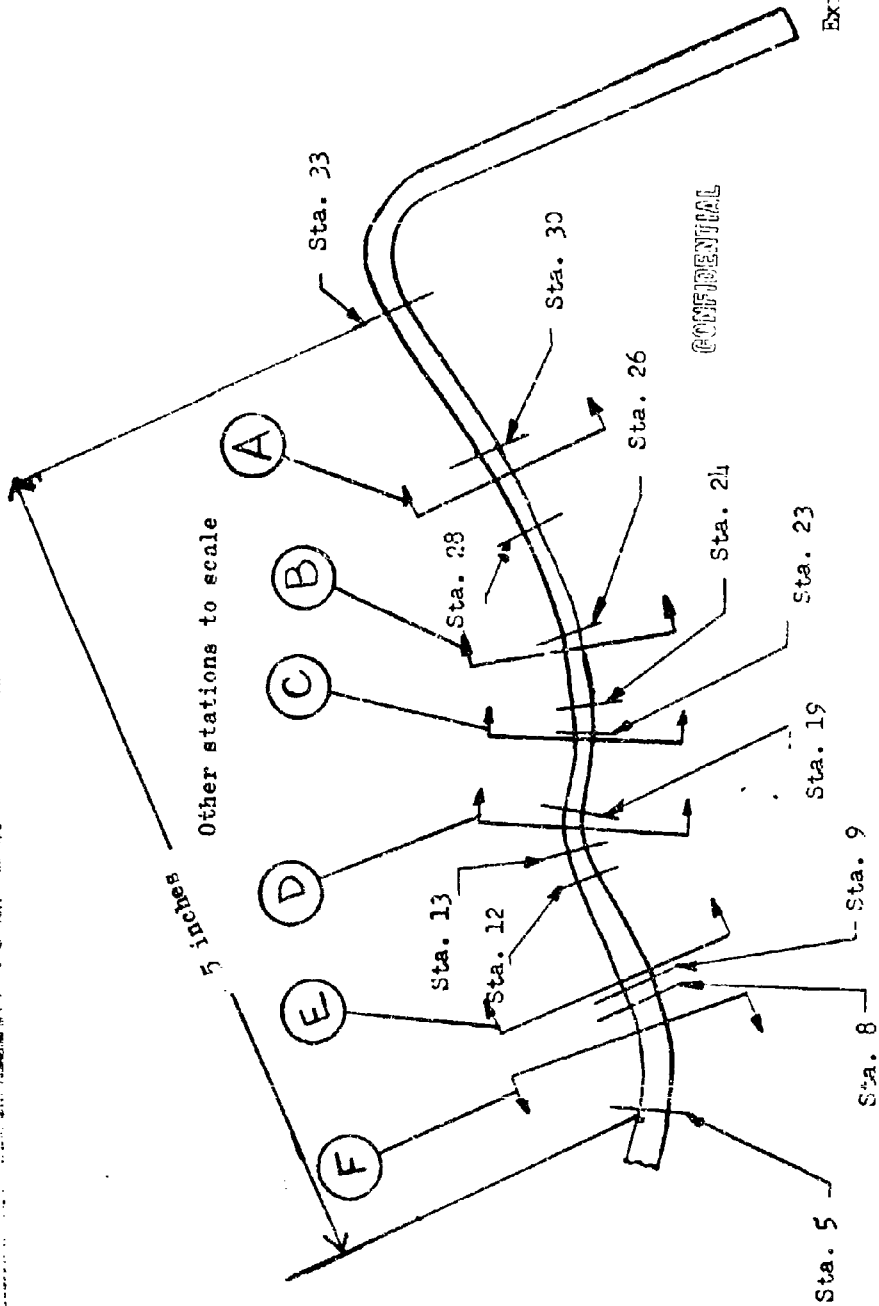


Figure 5. Location of Cross Sections Removed From High-Pressure, Die-Formed Outer Tubes After Flow Check

vapor-spray-vapor degreased in trichloroethylene for a minimum of 10 minutes. Trichloroethylene was also flushed through the tubes at a minimum of 200 milliliters per tube. Periodic checks of the fluid were made to ensure that nonvolatile residues, as detected by infrared analysis, were kept below a specified maximum level.

(U) Final surface preparation was effected by means of an acid descale. The solution used in this operation consisted of the following constituents:

4 to 6 percent hydrofluoric acid (50 degrees Baume)
20 to 25 percent nitric acid (42 degrees Baume) per O-N-350
Balance, deionized water (50,000 ohm-cm min)

(U) A specialized facility for accomplishing the descale was constructed; it consisted of a set of specialized holding racks and tanks. The descale operation was followed by rinsing in tap water, deionized water, then an oven bake to dry.

Problems Encountered During Fabrication of the Tubes

(U) Pickle Attack and Carburization. The final surface preparation operations (acid descale, prebraze pickle) performed on finished outer tubes were brought to an immediate stop when it was discovered that one tube in a rack of 96 pickled tubes had one end dissolved off by the acid. At the time the stop order was issued, approximately 2300 outer tubes had been through the pickle operation and were on racks in the white room.

(U) Metallurgical evaluation of a number of these tubes revealed severe intergranular attack, intergranular carbide precipitation in grain boundaries, and carbon contents of 0.4 percent carbon in the areas of failure (normal

carbon content for type 347 stainless steel is 0.08 maximum). It was evident from the data obtained that the tubes were carburized and were susceptible to the severe pickle attack because of this condition.

(U) A complete evaluation of all prior processing of the tubes, including a rigorous survey of all vendor operations, was conducted. During this portion of the investigation, it was found that pre-anneal cleaning of the preformed tubes was not adequate and not in complete accordance with specification requirements. The tubes were cleaned in bundles, rather than individually, which prevented complete removal of the lubricants from the tapering operation. Subsequent annealing and prebrazing pickling resulted in the "frosty" or smutty appearance caused by carburization (Fig. 6, 7, and 8). In addition, it was discovered that the "Agra-Shell" exit seal, used on the hydrogen furnace at the tapering vendor to anneal straight tapered tubes, was harmful. The shell particle seal is a standard device on most continuous hydrogen tube annealing furnaces. The seal which consists of very small crushed particles of walnut shells must be penetrated by the tubes as they leave the furnace cooling jacket. Shell particles were introduced into the ID of the tubes during this operation. Laboratory tests revealed that annealing tubes with walnut shells caused carburization and that subsequent prebrazing pickling produced intergranular pickle attack, as shown in Fig. 5.

(U) To prevent recurrence of this problem, major revisions were made to the tapered and preformed tube processing specification. These revisions required the reverse flushing of the ID of straight tapered tubes subsequent to each anneal in a continuous furnace. Pre-anneal cleaning of preformed tubes was revised so that a vapor-spray-vapor degrease with concurrent ID flushing using fixtures to accomplish the flush was required in a manner similar to that specified for final cleaning of finish-formed tubes.

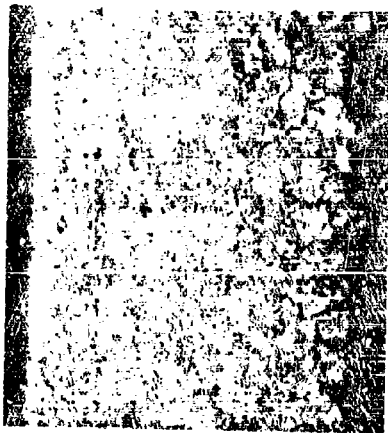
(U) It became apparent through a series of brazing tests that successful brazing of tubes could be accomplished without the benefit of preparing the tubes by pickling. Since 2500 outer tubes or approximately 60 percent of one combustor body's complement of tubes had already been exposed to the



a. Photomicrograph showing typical size and configuration of walnut shells used in exit end seal of tapering vendors continuous annealing furnaces
Mag: 15X



b. Photomicrograph showing I.D. of outer tube after anneal with walnut shells trapped inside. Tube was subjected to prebraze pickle subsequent to anneal. A = "Frosty" area, B = Residual walnut shell, C = "Frosty" area
Mag: 16X



c. Photomicrograph showing intergranular pickle attack on I.D. surface and continuous intergranular carbide network. Iron corrosion was observed in area A (Fig. 5b). Specimen etched electrolytically with oxalic acid.
Mag: 200X

Figure 6. Photos of Attack Produced on ID of Tubes by Walnut Shells in Laboratory Test

pickle, it was also necessary to determine whether or not any of these tubes could be used. Visual examination had disclosed only a small percentage with visual indications of pickle attack.

(U) An ultrasonic inspection method was developed which was capable of detecting pickle attack more than 0.0007 inch in depth.

(U) With the knowledge that a considerable number of tubes which had not been exposed to prebraze pickle were carburized and that these tubes would be used in fabrication of the combustor bodies, cryogenic tensile testing was conducted on carburized tubes. These data were essential in establishing the effects of carburization on the performance of the coolant tubes during hot-firing tests. Because adequate data were available concerning room and elevated temperature tensile properties of carburized type 317 stainless steel, only cryogenic testing was performed.

(U) The results of the cryogenic tests conducted at -200 and -320 F disclosed that no significant changes in mechanical properties between uncarburized and carburized tubes were evident when carburized tubes were exposed to furnace brazing cycles (specimens actually accompanied an inner body through braze cycle) prior to test.

BRAZING OF TUBES TO COMBUSTOR BODIES

Braze Tooling

(U) The thrust chamber braze assembly tooling employed inflatable stainless-steel pressure bags to hold the thrust chamber tubing in place during brazing. The bags were attached to rigid backing rings, four rings on the outer wall and seven rings on the inner wall. Sufficient tube area was covered by the pressure bags, backed by the rings, to prevent tube movement; yet, sufficient space remained open between pressure bag rings to allow physical verification (by moving tubes) of tube-to-body fit. The space between rings also provides free circulation of the furnace atmosphere for cleanliness and

temperature uniformity during brazing. A single, large pressure bag covering the entire tube surface, as used on conventional bell-shaped chambers, would have limited access for both inspection of fits and atmosphere circulation.

(U) The pressure bag concept allows the forces on the tubing to be varied with temperature in such a way that proper tubing location is maintained without crushing the tubes at elevated temperature. Proper use of the bags required knowledge of the relationship between internal pressure and external forces through the ambient to 2000 F temperature range. Knowledge of the elevated temperature strength of the type 317 stainless-steel tubing under transverse compressive loads was also necessary.

(U) A series of laboratory tests was conducted on both pressure bag force relationships and tube crushing strengths. The three pressure bag types and the effective pressure areas are shown in Fig. 7. The pressure bags are shown in Fig. 7, and typical data from the test series are shown in Fig. 8. The families of curves show the required internal bag pressure to obtain specific forces on the tubing at 2000 F and at several intermediate temperatures.

(U) Tube-crushing experiments were run at both ambient and elevated temperatures. At ambient temperature, it was found that the pressure bags would deform grossly without tube damage as ring-to-tube clearances decreased and forces increased. At a temperature of 2000 F, the tubing, formed to thrust chamber shapes and sizes, proved capable of supporting 50 psi (projected surface area of the tube crowns) without significant deformation. The forces required to hold the tubes in place at 2000 F are much less than 50 psi, indicating a satisfactory margin of safety at all temperatures.

(U) The experimental data on the pressure bags and tube strengths were utilized in the subsequent line pressure-temperature requirements used in the furnace brazing operation.

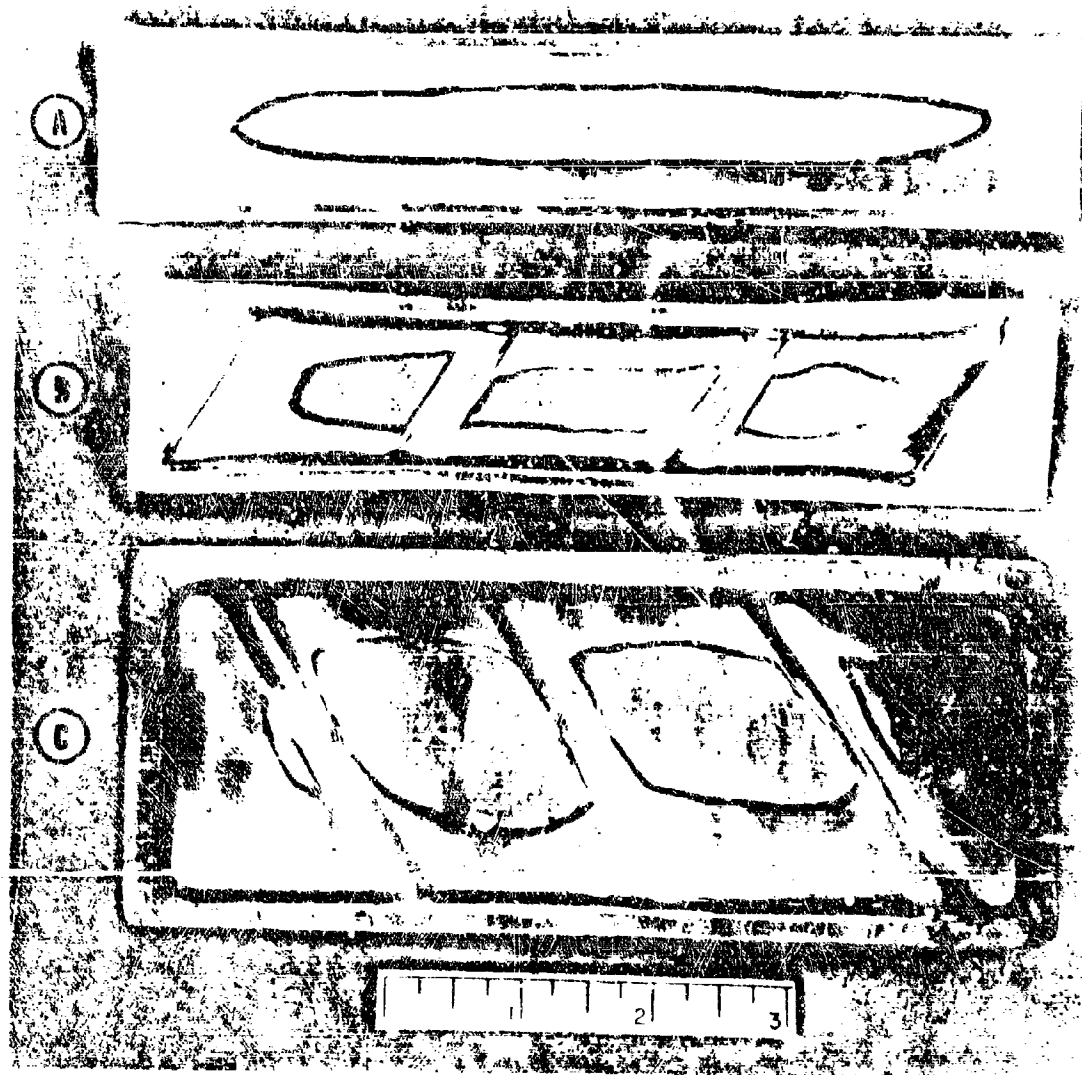


Figure 7. Three Pressure Bag Configurations Tested in the Laboratory for Pressure Response and Efficiency. Areas Encircled on Bags Represent Bag-to-Tube Contact Area When Pressurized Under Simulated Brazing Conditions. Pillow-Type Bag "A", Above, was the Design Selected for Production Tooling Because of Less Rigidity and a Continuous Tube Contact Area as Opposed to Designs With Diagonal Expansion Grooves as Shown in "B" and "C"

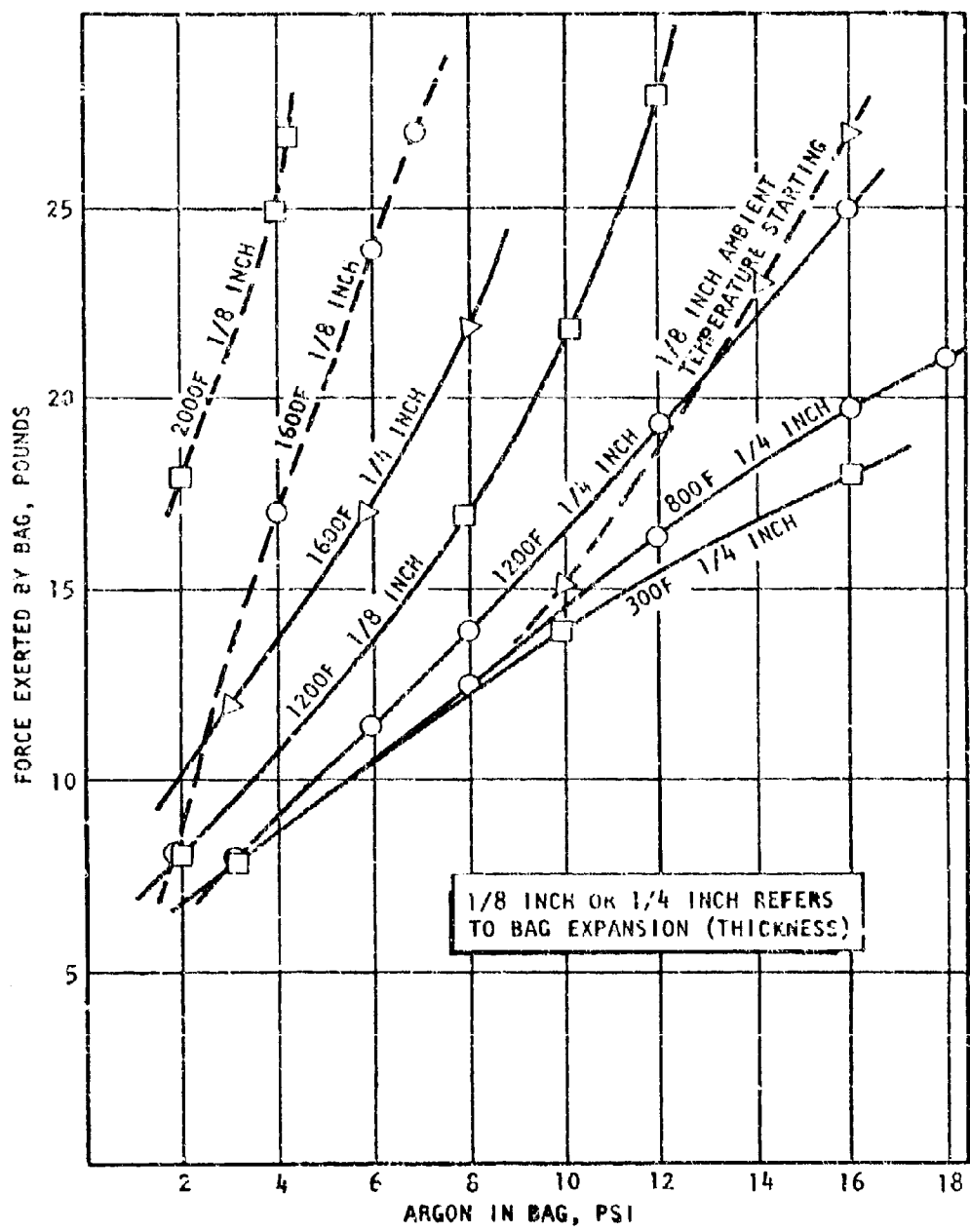


Figure 8. Internal Pressure vs External Force for a 1-21, 32 x 6-3, 4 Flat Pressure Bag

Braze Process, Initial Review and Selections

(U) The requirement of fabricating two tubular thrust chamber assemblies was studied initially with one apparent factor in mind--the program called for fabrication of two complete assemblies with no allowance for spares. This meant that rigorous planning and preproduction development were required, techniques hazardous to the assemblies had to be avoided, and safe and reliable techniques were to be used at all times.

(U) A detailed braze process development program was performed to maximize the processing reliability and minimize the occurrence of problems during fabrication.

(U) The 90Ag-10Pd braze alloy was selected for use as a primary braze alloy for the type 347 stainless-steel tube combustors. This was based on its generally good brazing characteristics and its negligible "aggressiveness" to the tube materials over long high-temperature braze operations. It is in current use on the J-2 production thrust chamber and was successfully used on the 40K toroidal thrust chamber.

(U) The 82Au-18Ni braze alloy was selected for use as the secondary braze alloy for the type 347 stainless-steel tube combustors, based also on extensive Rocketdyne background with this alloy and minimal reaction with type 347 stainless tubing.

Braze Process Development, Initial Test Program

(U) Thrust chamber brazing tests were prepared utilizing two full-length, 2-inch wide outer and inner tube and body segments. Type 347 stainless-steel tubes were used during the test program. Major test objectives were to:

1. Determine the correct amount of alloy to be preplaced on the assemblies

CONFIDENTIAL

2. Evaluate tube-to-body and tube-to-end ring sealing capabilities
3. Evaluate methods to prevent braze alloy tube plugging

(U) The test segments were assembled and alloyed, duplicating the procedures planned for the full-size assemblies. RB0170-002 (90Ag-10Pd) braze alloy wire was inserted in alloy grooves machined in the nickel-plated bodies, and 0.002-inch-thick braze sheet was spot welded to the tube contact surfaces for first-cycle brazing.

(U) Green stop-off was painted inside the tubes prior to assembly. Two sets (outer and inner wall configurations comprising a set) of body segments were assembled with type 317 stainless-steel tubes. Simulated injector and exit ring segments were not assembled until the second-cycle preparation.

(U) Triangular nickel fillers were utilized to fill most of the space occurring between tubes and flat surfaces of bodies and rings. Various lengths and attachment positions were evaluated as well as capabilities of the fillers for sealing with and without nickel powder washed around them.

(U) Fixturing of tubes to the body was performed by strapping tubes to the body at pressure bag locations. Figure 9 shows the first set of test segments ready for first-cycle brazing. The two sets were fixtured for both brazing cycles in the injector end down position.

(U) Test Results. The alloy wire preplaced in body grooves on the first set of segments appeared to give sufficient alloy for bonding except for the exit end of the inner-body segment. An additional alloy groove was added to the second segment and subsequent results were satisfactory. A drawing change was made to add the groove to both inner and outer bodies on production hardware. No alloy paste was added to tube-to-tube joints on any of the test segments.

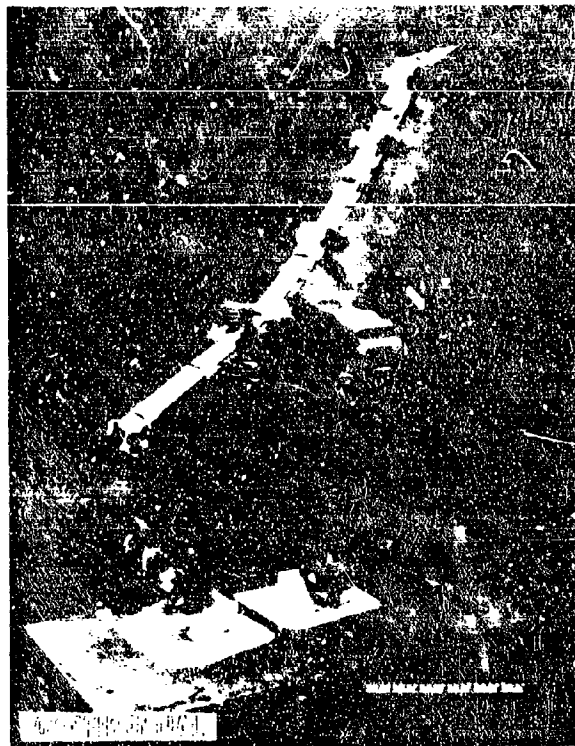


Figure 9. Full-Length Inner and Outer Tube and Body Test Segments Ready for Brazing. Three Sets of Segments, Such as the One Above, Were Brazed During Development.

(U) Utilization of triangular nickel fillers proved to be effective as a sealing plug between tubes and flat body and ring surfaces. Fillers at the lower end (as-brazed) of vertical joints would usually seal during the first braze cycle. However, if the joint was on top, capillary forces usually were not sufficient to maintain braze alloy around the fillers to seal the joint during the first cycle. Figure 9 shows an injector end tube-to-body joint completely sealed in one cycle. Figure 10 shows a typical exit end tube-to-body joint that required two cycles to seal. The use of nickel powder around fillers on first cycle joints was avoided so that additional alloy could feed unrestrictedly into the joints during the second braze cycle. Nickel powder paste was required to obtain a seal on second-cycle joints. Fillers were attached by both spot-welding and by hooking one end to retain them in a joint. Both methods were effective.

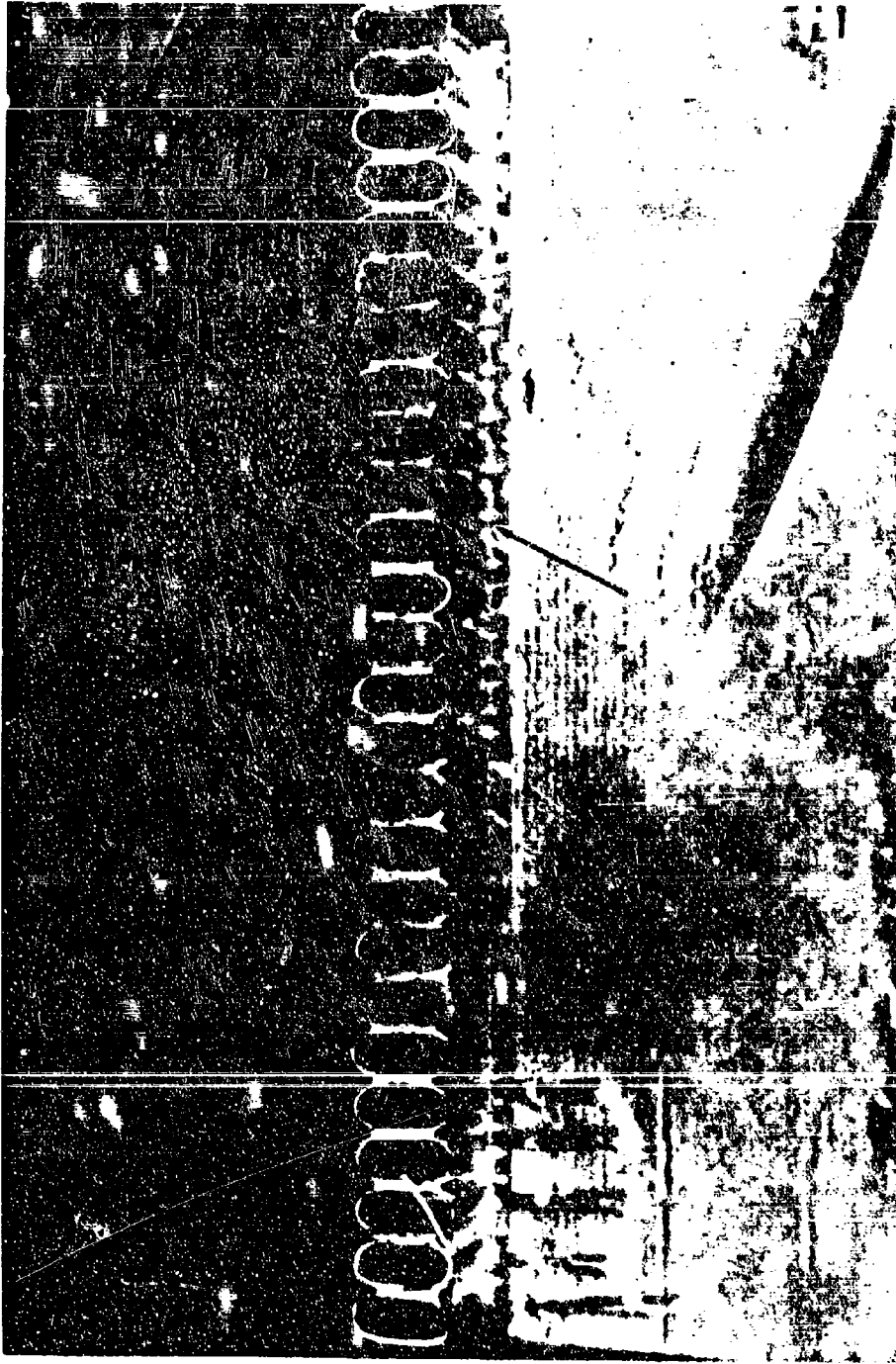
(U) On the current series of development tests, green stop-off was successfully used to restrict braze alloy flow into the tubes. Previous experience has shown it to be effective in limiting alloy flow. It was also noted that the possibility of alloy runoff entering the tubes at the lower end of the assemblies was very probably averted by the triangular nickel fillers which directed the flow of alloy away from the tube ends and down the body. Figure 11 shows the direction of braze runoff flow. More work has been done to prevent tube plugging and is reported in the section on In-Process Development Tests.

In-Process Development Tests

(U) Various brazing tests were performed during hardware fabrication to improve processes or overcome problems as they were encountered. Some of the tests were lengthy but are described briefly in the following sections.

1. Repair of Holes in Tubes caused by arc burns, accidental blows by sharp tools, etc.

Test Procedure: Simulated holes in tubes were furnace braze repaired utilizing nickel sheet lap patches of 0.002-, 0.004-, and

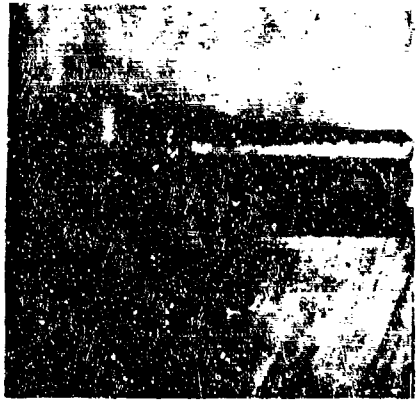


MAG: 4X

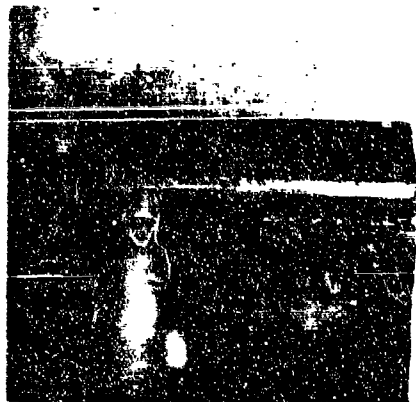
Figure 10. Lower End Tube-to-Body Joint Sealed After the First Braze Cycle. Arrow Locates a Triangular Nickel Filler at Joint



Upper End Tube-to-
Body Joint was Un-
sealed After the
First Cycle. Fillers
Were Installed By
Both Hecking and Spot
Welding Prior to Brazing



Specimen Shown Above
was Prepared for
Second-Cycle Brazing
by Preplacing Nickel
Powder Paste Around
Fillers. Joint was
Capped With Fillet
of Second-Cycle Alloy
Paste as Shown at Left



Tube-to-Body Joint
is Shown Completely
Sealed After Second-
Cycle Brazing

Figure 11. Typical Exit End Tube-to-Body Joint



MAG: 3X

Figure 12. Outer Wall Segment, Injector End. Arrows Show Direction of Excess Alloy Run-Off Flow Away From Tube Ends and Down the Body By Following Paths Created By the Nickel Fillers

0.006-inch thickness, pressure test cyclic loaded, and pressurized to destruction.

Results: Braze appearance was satisfactory. No restrictions in tubes. All samples ruptured in parent tube material. Figure 13 shows typical brazed tube specimens that were evaluated. Table 8 lists brazed lap patch test data. The lap patch repair method was accepted for use on damaged tubes.

2. Improved Nickel Powder Binder

Reason for Test. Nickel powder in R-2 Binder paste vehicle (a polybutene base braze alloy binder) was not easily worked into joints.

Test Procedure: Carbopol vehicle (a water soluble suspending agent) used in the past was reviewed for the present application. Nickel paste was mixed with Carbopol and washed into test joints with a water-wet brush and capped with braze alloy paste. Samples were brazed and checked for effect on tube material and nickel powder placement.

Results: Nickel powder in Carbopol binder was sufficiently workable to produce desired nickel fillets. Binder was changed from R-2 to Carbopol as nickel powder vehicle on all inner and outer combustor assemblies.

3. Wide-Gap Brazing Material

Reason for Test: Wide gaps under exit rings after the first braze cycle require filler powder addition around shims. Use of nickel powder could result in porous, leaking joints.

Test Procedure: Combine braze alloy powder with other filler powders in various amounts and note braze results including braze bond and porosity level.

Results: Combination of 66 percent braze alloy (second cycle 82Au-18Ni alloy), 17 percent 90Ag-10Pd, and 17 percent pure nickel in powder form resulted in an effective wide-gap brazing material. Some minor porosity was noted. The material was used as a filler in gaps under exit end rings on units No. 1 and 2 inner and outer assemblies.

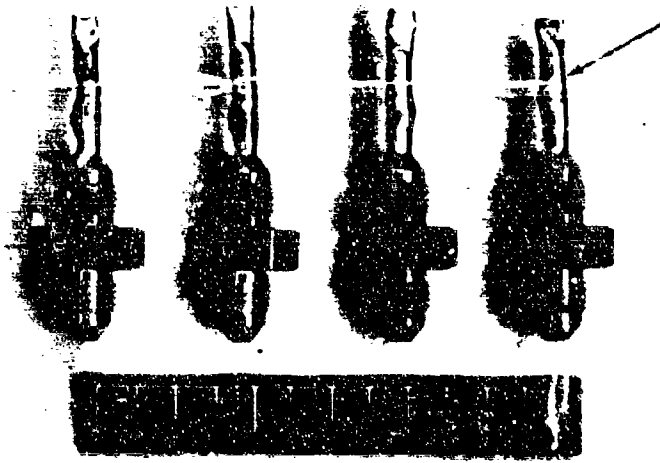


Figure 13. Typical 317 Stainless-Steel Test Specimens With 0.002-Inch Nickel Sheet Patch (Arrow) Brazed Over 0.050-Inch Hole in Tube. Hydrostatic Pressure Test Failure Occurred in Adjacent 0.011-Inch Tube-Wall Material

TABLE 8

BRAZED LAP PATCH TEST DATA

Sample No.	Patch* Thickness, inch	Hydrostatic Pressure, psi	Five-Minute Hold	Number of Cycles	Hydrostatic Pressure, psi	Number of Cycles	Burst Pressure, psi
1	0.002	5000	No leaks	50 cycles (no leaks)	800	50 cycles (no leaks)	14,600
2	0.002			50 cycles (no leaks)		25 cycles (no leaks)	15,600
3	0.002			50 cycles (no leaks)		25 cycles (no leaks)	14,400
4	0.004			50 cycles (no leaks)		25 cycles (no leaks)	13,600 (pinhole leak)
5	0.004			50 cycles (no leaks)		50 cycles (no leaks)	15,800
6	0.004			50 cycles (no leaks)		25 cycles (no leaks)	15,400
7	0.006			50 cycles (no leaks)		25 cycles (no leaks)	14,400
8	0.006			50 cycles (no leaks)		50 cycles (no leaks)	15,000

*Patches were made from pure nickel shim material of various thicknesses. Each patch was spot welded over a 0.037-inch-diameter hole in a tube and furnace brazed with 90Ag-10Pd alloy prior to pressure testing.

4. Silver-Palladium Shims

Reason for Test: Sporadic tube-to-tube gaps in throat region after the first braze cycle required shimming. A better heat transfer material than nickel was desired.

Test Procedure: 90Ag-10Pd braze alloy wire was flattened to form shim inserts. Braze tests were performed to note braze quality. Powder filler material around shims was also evaluated.

Results: 90Ag-10Pd shims and powder brazed successfully and were used on assemblies 2 inches forward and aft of the throat in tube-to-tube gaps. 90Ag-10Pd powder was used around shims on inner and outer units No. 1. Nickel powder was used around shims on both No. 2 units.

5. Tube Plugging

Reason for Test: Tube plugging from second-cycle alloy was experienced. An effective stop-off was needed.

Test Procedure: Thrust chamber tube ends were coated or plugged with various inhibitors and oxidizing media. Tube ends were enveloped in braze alloy paste and were brazed duplicating time and temperature above braze solidus temperature used on production hardware.

Results: CaO powder added to R-1 Binder was found to be effective and was used on inner and outer units No. 1 and 2.

6. First Cycle Alloy Remelt Tests

Reason for Test: Determine remelt temperature of 90Ag-10Pd first-cycle braze alloy as affected by: (1) brazing with 82Au-18Ni alloy, and (2) an expected increase in silver composition as the alloy flows, resulting in a corresponding drop in melting point.

Test Procedure: Apply second-cycle alloys over prebrazed first-cycle alloy. Braze at increasingly higher temperatures until remelt is noted. Determine analysis of alloy runoff on first production assembly and related remelt temperature.

CONFIDENTIAL

Results: Tests with the second-cycle alloy over 90Ag-10Pd braze deposits showed no remelt below 1835 F. Melting temperatures of alloy samples were:

<u>Sample</u>	<u>Solidus Temperature, F</u>	<u>Liquidus Temperature, F</u>	<u>Percent Pd</u>
New 90Ag-10Pd Alloy	1882	1909	9.98
Run-off Sample	1837	1857	8.50

Alloy remelt temperature was determined to be above brazing temperature range for the second-cycle alloy.

Brazing, Outer Wall Assembly Unit No. 1

(U) Assembly Preparation. Assembly preparation began with the application of green stop-off to threaded holes and other surfaces on the body where braze alloy flow was prohibited. The attachment of braze alloy wire in machined grooves on the body followed, and braze alloy sheet was spot-welded to the body tube contact surface. Green stop-off was applied to the OD of all tube ends. The tubes were stacked to the body in the exit end down position with a base fixture holding the tubes upright during stacking. A total of 3700 tubes were ultimately used in the assembly to obtain a tight tube-to-tube and tube-to-body fit.

(U) Braze alloy wire was installed in alloy grooves on both injector and exit rings and was followed by spot-welding 0.002-inch-thick braze alloy sheet the brazing surface of the rings. Both rings were assembled and secured in place. Figure 14 shows an outer wall assembly during first-cycle preparation.

(U) Triangular nickel fillers were used as sealing plugs between tubes and flat body and ring surfaces. During spot-welding of fillers to the injector ring, two tubes were damaged by arcing; one tube had surface

61
CONFIDENTIAL
(This page is Unclassified)

CONFIDENTIAL

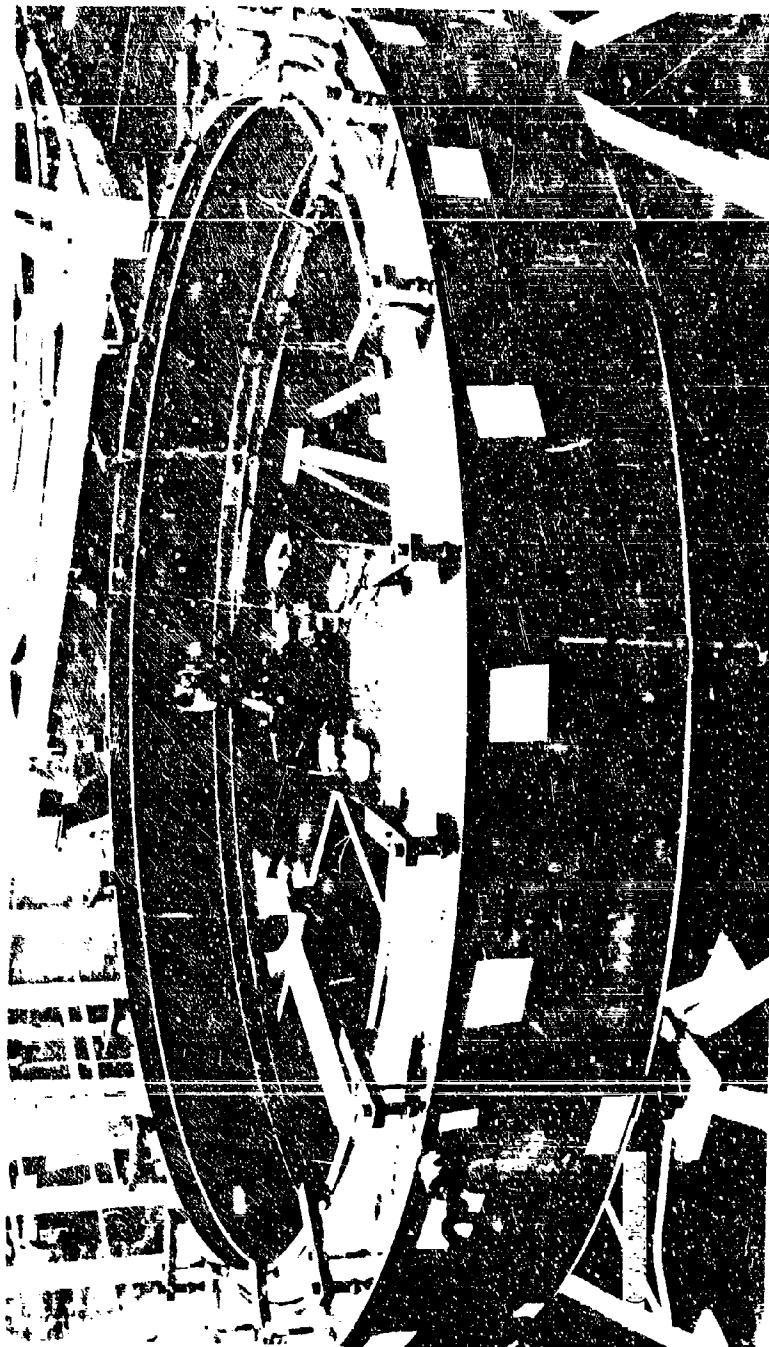


Figure 14. View of an Outer Wall Assembly During First Cycle Preparation. Arrows (A) and (B) Locate Temporary Tooling Used to Hold End Rings Firmly Against Tubes During Assembly and Alloying

CONFIDENTIAL

melting, the other had an arc burned hole approximately 0.035 inch wide. It was considered impossible to replace the two discrepant tubes without tearing down the complete tube stack including the spot-welded fillers. A local repair method was selected; it consisted of a 0.002-inch nickel sheet formed and spot-welded over the discrepant tubes. The patch would be brazed in place during the first furnace braze cycle. This process was previously described, In-Process Development Tests.

(U) Corrective action to prevent arc burns was undertaken by alerting all shop personnel concerned of the problem and instructing them to ground spot-welder leads to the same part being spot-welded. Caution notes and special instructions were added to brazing procedures and Assembly and Operation Records.

(U) Nickel filler installation was completed and was followed by placing nickel powder, braze alloy paste, and nickel drip tabs in locations indicated on the sketch in Fig. 15.

(U) After completion of alloying, the assembly was placed over the pressure bag tooling. The correct elevation for the tooling was obtained by adjusting wedges on the bottom of the fixture. The bag rings were adjusted to be concentric with the body and spaced from 0.103 to 0.133 inch between the surface of the thrust chamber tubes and the surface of the Refrasil on the pressure bags. Each pressure bag was pressurized to 60 psi in the assembly white room to size the bag against the tubes. It was noted that at 20 psi, the pillow-type bags expanded enough to make initial contact with the tubes, which coincided with room temperature data from pressure bag tests.

(U) Thermocouples were attached to the assembly, tooling, and retort in accordance with the written brazing procedure to monitor the brazing cycle. The retort base was placed on the furnace hearth which had previously been leveled to within ± 0.010 inch. Figure 16 shows the pressure bag tooling (less the manifold lines) assembled to an outer body and positioned on the retort base.

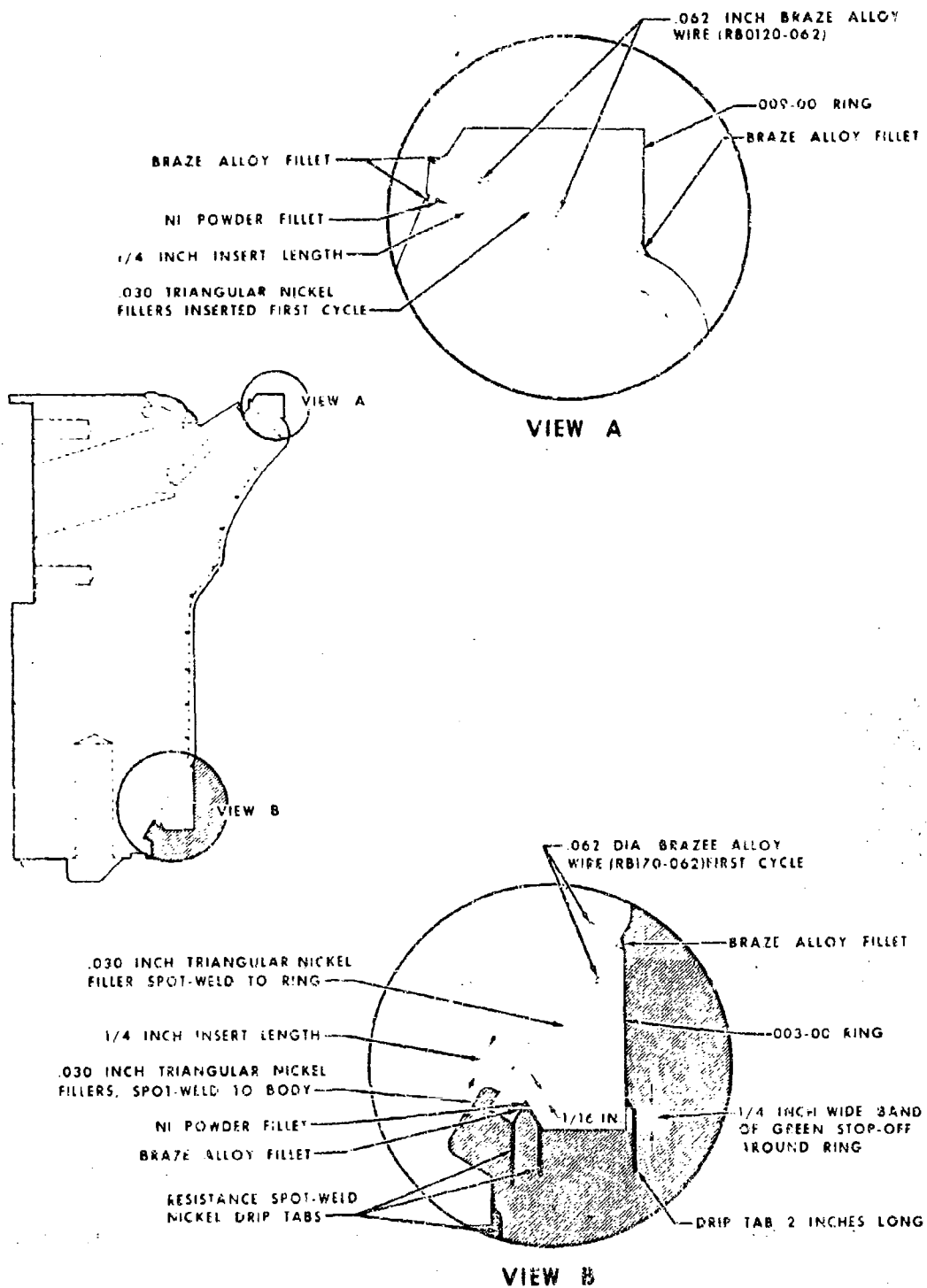


Figure 15. Location of Nickel Filler Metal and 90Ag-10Pd Braze Alloy Application For the First Braze Cycle. Also, Tube-to-Tube Joints Were Alloyed Full Length of the Assembly. Braze Position was as Shown Above. Braze Wire was Installed in All Body Alloy Grooves

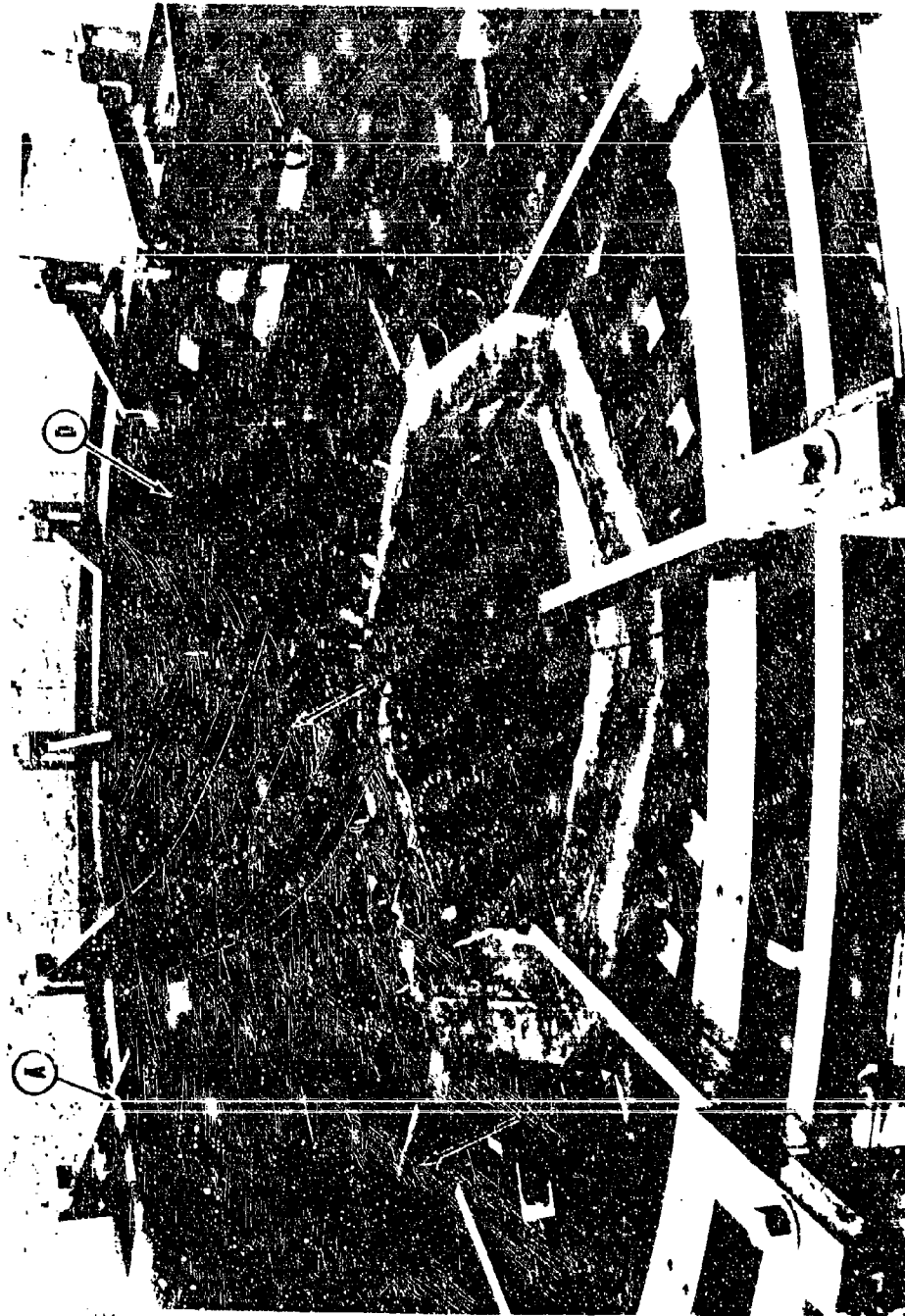


Figure 16. Outer Body Assembly on Retort Base with Pressure Bag Tooling Installed. The ID View With Purge Manifold Lines Removed Shows (A) Exit End Ring Counterweights, (B) Injector End Ring Counterweights, (C) Adjustable Wedges Which Establish Correct Elevation of Pressure Bag Tooling, (D) Typical Pressure Bag Inlet Line, (E) Typical Shims Used to Hold Bag Rings Concentric With Body

(U) The retort was designed to permit a partial vacuum of 300 microns of mercury up to 750 l. It was to be sealed well enough so that when evacuating at room temperature to 500 microns and the pumpdown was held, the time required for pressure to increase from 500 to 590 microns would not be less than 2 minutes. After the first vacuum cycle that met the acceptable leak rate was obtained, one additional 300-micron evacuation was required at room temperature and one at 700 F, each followed by backfilling with argon. Figure 17 shows the weld-sealed retort on the furnace hearth.

(U) First Braze Cycle. Furnace braze data are listed in Table 9. Figure 18 shows the time-temperature curve resulting from the first braze cycle. Time-temperature data from all thermocouples on the assembly were entered on FORTRAN data sheets and plotted by the computer for analysis of the braze cycle.

(U) Following the braze cycle, pressure bag tooling was carefully removed from the chamber according to steps outlined in the brazing procedure. Figure 19 shows the pressure bag which functioned successfully during the braze cycle. Postbraze examination of the braze assembly revealed the following:

1. About 95 percent of the tube-to-tube joints at the lower half of the chamber were filleted with braze alloy. About 75 percent of the tube-to-tube joints at the upper half were filleted. Some tube-to-tube gaps were noted that would require shimming; the largest were about 0.015 inch wide.
2. Braze fillets at the injector ring-to-tube joints appeared satisfactory. Some small voids were noted that could be remedied during the second braze cycle. Exit end ring-to-tube and tube-to-body joints were only intermittently filleted.
3. There were light brown oxidation spots on the tubes that coincided with 0.014 inch pressure bag bleed holes. A slight amount of oxidation could distinguish itself through pressure bag holes and not through the main retort inlet since a small stream of gas from the pressure bags would impinge directly on the tubes first before

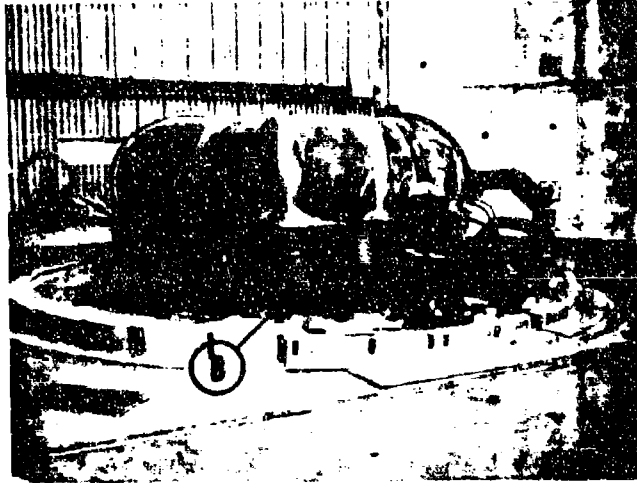


Figure 17. The 270 cu ft Aerospike Vacuum Retort is Shown on the Furnace Hearth. Edges of the Retort Seal Flange, Arrow (A), and Plumbing Lines and Ducts are Weld Sealed Prior to the Brazing Cycle. Hearth Posts, Arrow (B), are Levelled to ± 0.010 Inch Prior to Placing the Retort Base on the Hearth Before Each Run

TABLE 9

OUTER WALL FURNACE BRAZE DATA

Data	Outer Wall Assembly, First Braze Cycle
Time In, Date	6:30 AM, 17 February 1967
Time Out, Date	9:20 AM, 19 February 1967
Total Time	62 hours, 50 minutes
Assembly Levelness, in	0.180 inch from level*
Assembly Levelness, out	0.060 inch from level
Room Temperature Evacuation 500 to 500 Microns, time	2 minutes, 30 seconds
Braze Position	Injector end down
Pressure Bag Pressures	40 psi at ambient; gradual reduction to 100-inch water column at 1800 F
Temperature Differentials	See Fig. 20
Atmosphere Requirement: Argon, Minimum Flowrate Hydrogen, Minimum Flowrate Helium, Flowrate	1400 CFH heating and cooling cycle 1600 CFH above 1400 F Helium not used
Auxiliary Purge Line, Four Places	25 to 30 CFH
Braze Alloy	RB0170-062 (90Ag-10Pd)
Braze Temperature	2010 F ⁺³⁵ ₋₀ F, 20-minute hold

*The retort base has movable plates which causes the initial levelness measurement to be more out of level than after brazing.

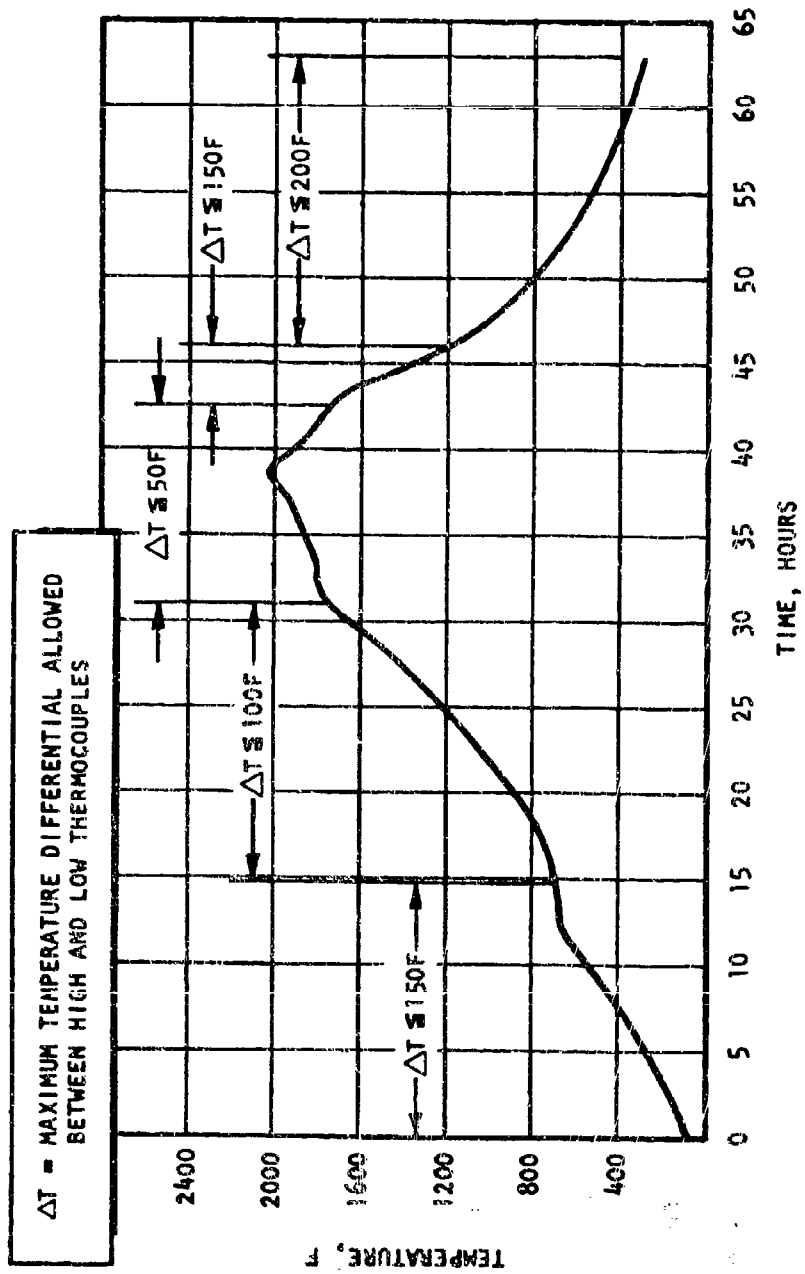


Figure 18. Time-Temperature Curve for the First Braze Cycle, Outer Wall Unit No. 1



Figure 19. Outer Wall Pressure Bag Tooling Shown With Refrasil Removed From Bag Skins Following the First Braze Cycle

mixing with the large volume of atmosphere in the retort. Leak checking of the pressure bag line system was performed, but no specific leaks were found.

4. The lap patch over the arc-burned tubes showed satisfactory braze appearance.
5. Alcohol flow check of the individual tubes indicated no tube restrictions.

(U) Second Cycle Preparation. Shimming of all tube-to-tube gaps over 0.003 inch wide was performed by using single-thickness nickel shims. Shims were fitted into gaps by tapering the ends with a hammer on a solid block prior to inserting them into place. Nickel shims were used in all tube-to-tube gaps except from 1 inch forward to 1 inch aft of the throat, where 90Ag-10Pd braze alloy shims (braze alloy wire rolled flat) were used. The 90Ag-10Pd shims had 90Ag-10Pd braze alloy powder washed in around the shims while nickel powder was used around the nickel shims to form a complete seal at each gap.

(U) Nickel powder paste was washed into visible ring joint voids wherever they were found. Voids at the exit end tube-to-body joint required considerable time and effort in obtaining a nickel powder seal, especially in the space above triangular fillers. Figure 20 shows the described joint on a laboratory test segment. Nickel powder/Carbopol binder was extruded into the joint with a hypodermic syringe and No. 18 needle. A small brush dampened in deionized water was used to wash the nickel paste into the openings until they were sealed. A fillet of braze alloy paste over the preplaced nickel completed the exit end tube-to-body joint preparation.

(U) Gaps under the exit ring were first shimmed with solid nickel shims, followed by adding a special wide-gap brazing filler material until all void areas were filled. The wide-gap brazing material was prepared by combining 66 percent 82Au-18Ni, 17 percent 90Ag-10Pd, and 17 percent pure nickel and was used in dry powder form.

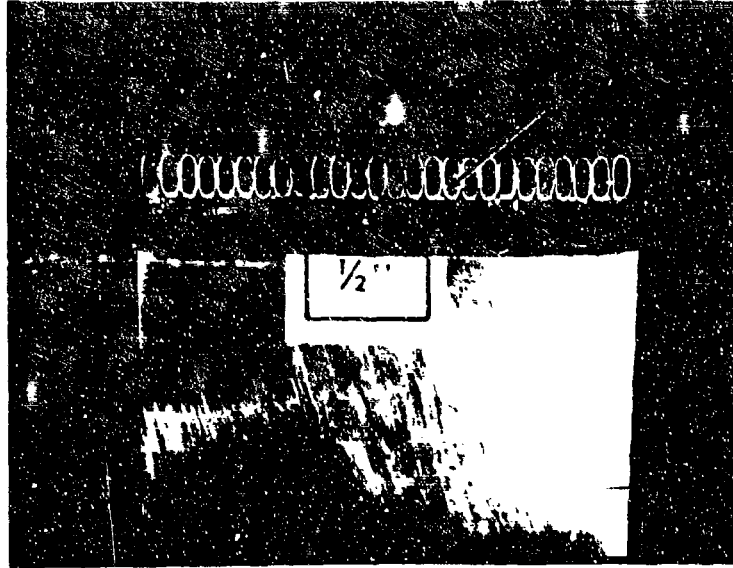


Figure 20. Braze Test Specimen. Arrow Locates Space Above Triangular Filler That Must Be Filled With Nickel Powder If a Braze Seal is Expected

(U) All joints partially or completely brazed during the first cycle were realloyed with second-cycle alloy whether they appeared sealed or not to preclude the possibility of leaving small pinhole voids unrepaired. Tube-to-tube joints were alloyed from the injector end ring to the exit end ring to complete the alloy preparation for the second braze cycle.

(U) A special stop-off mixture consisting of CaO powder mixed into R-1 Binder was extruded into the exit end of each tube using a hypodermic syringe in an effort to prevent braze plugging of tubes.

(U) Tooling rings, wedges, and clamps were installed on the assembly. Pressure bags were not required for the second braze cycle. Nickel foil drip tabs were attached to the lower parts of the assembly in accordance with the written brazing procedure to prevent excess alloy from collecting and plugging tubes. Thermocouples were attached, and the assembly was positioned on the retort base with the exit end down for brazing.

(U) Second Braze Cycle. Postbrazing examination revealed that:

1. Two small tube-to-tube joints were unbonded about 1/2 inch in length. In general, tube-to-tube joints appeared satisfactory.
2. The exit ring-to-tube joint appeared sealed except for an 18-inch-long area where there appeared to have been ring movement that disturbed the braze joint fillets. Local hand brazing would be required to repair the joint.
3. The injector end ring joint was sound.

(U) Braze discrepancies remaining in joints were considered repairable by manual processes, thus completing furnace braze requirements on the above assembly.

Brazing, Inner Wall Assembly Unit No. 1

(U) Assembly Preparation. Tube-to-body fit was evaluated after final machining of the body contour by holding finish formed tubes against the

body and observing the fit. Tube-to-body spacing was satisfactory except for the last 1 inch of the exit end on the straight section of the body where a 0.010-inch gap was evident between the body and tubes. Corrective measures were taken by building up the discrepant area with 0.010-inch-thick nickel plating.

(U) Assembly preparation began with the application of stop-off to threaded holes and other surfaces on the body where braze alloy flow was prohibited. The attachment of braze alloy wire and sheet to the body was performed and was followed by stacking of tubes to obtain a tight tube-to-tube and tube-to-body fit. After replacing tubes which were too short, bent, etc., 3642 tubes were ultimately counted in the assembly stack.

(U) The injector and exit end rings were prepared by attaching alloy wire and foil to alloy grooves and braze surfaces, respectively. The rings were assembled to the tubes and secured in place. No problems were encountered during alloy preparation. Installation of triangular nickel fillers and the application of nickel powder paste, braze alloy paste, and nickel drip tabs were performed as indicated on the sketch in Fig. 21.

(U) When alloying was complete, the lower pressure bag tooling was installed and adjusted for concentricity and elevation. The No. 2 bag was set and pressurized and determined as satisfactory. The upper bag tooling was lowered onto the assembly and bolted to the lower bag assembly. The upper bag rings were spaced concentrically with the assembly and from 0.130 to 0.160 inch between the surface of the Refrasil on the bags and the tubes.

(U) Pressure bag No. 2 was deemed a key bag in maintaining tube-to-body fit and was designed to operate from a separate purge line that was independent of the other bags. To ensure that enough pressure would be exerted by No. 2 bag, its pressure requirement was increased over the other bags for the heating and part of the cooling cycle. Figure 22 shows the pressurizing sequence and pressure requirements for the brazing cycle. Figure 23 shows the location of the bags and purge lines for the first braze cycle.

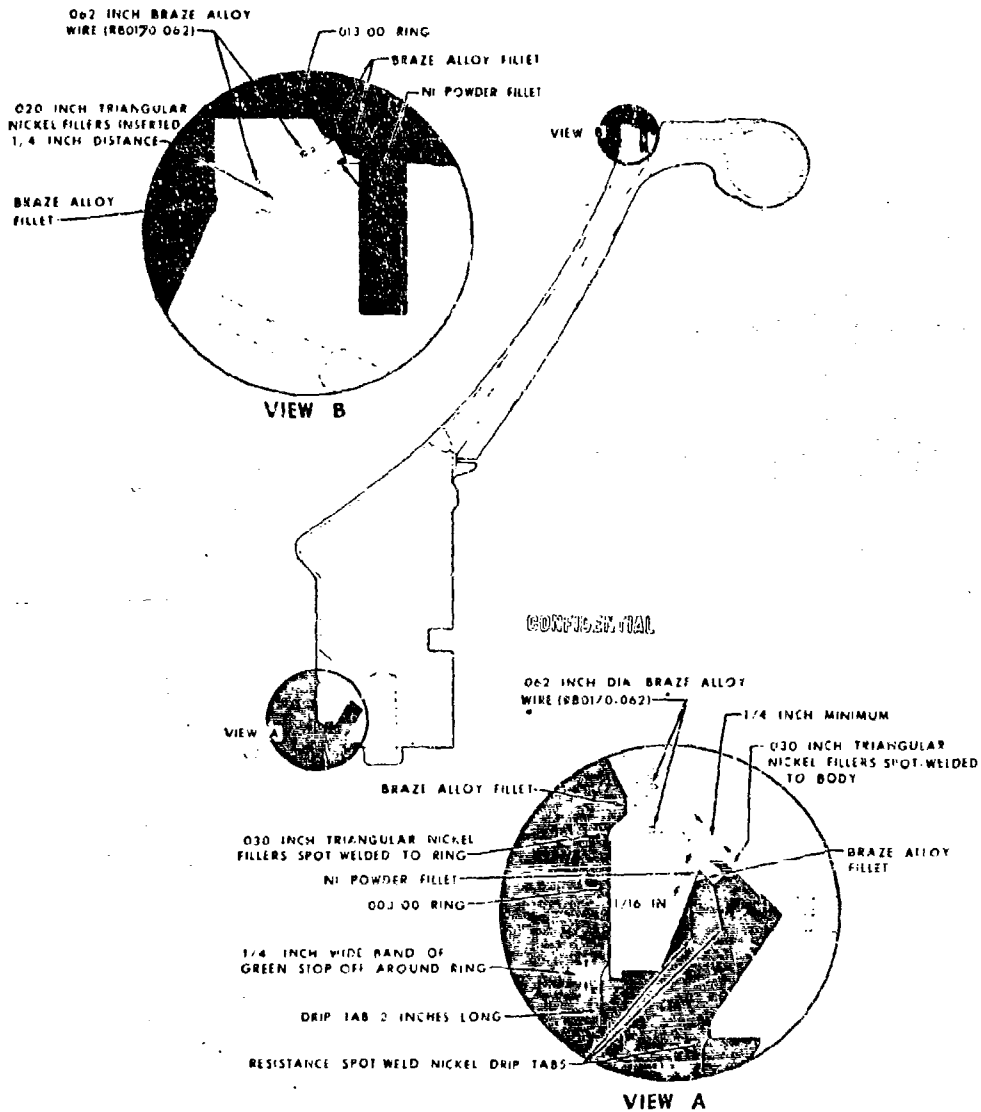


Figure 21. Location of Nickel Filler Metal and 90Ag-10Pd Braze Alloy Application for the First Braze Cycle. Also, Tube-to-Tube Joints were Alloyed Full Length of the Assembly. Braze Position was as Shown Above. Braze Wire was Installed in All Body Alloy Grooves

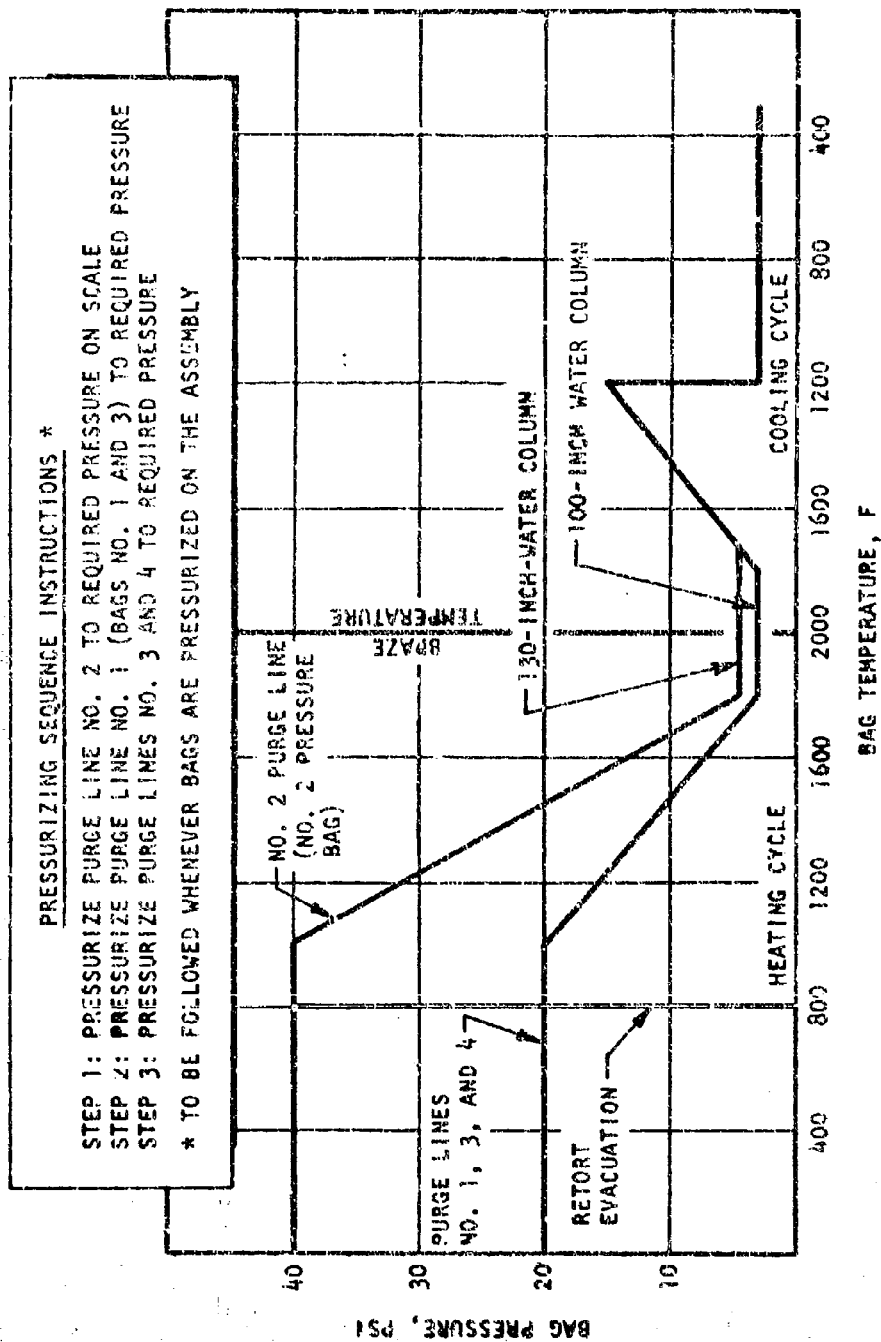


Figure 22. Pressure Bag Pressure Requirements During Brazing Cycle, Inner Wall Units No. 1 and 2

CONFIDENTIAL

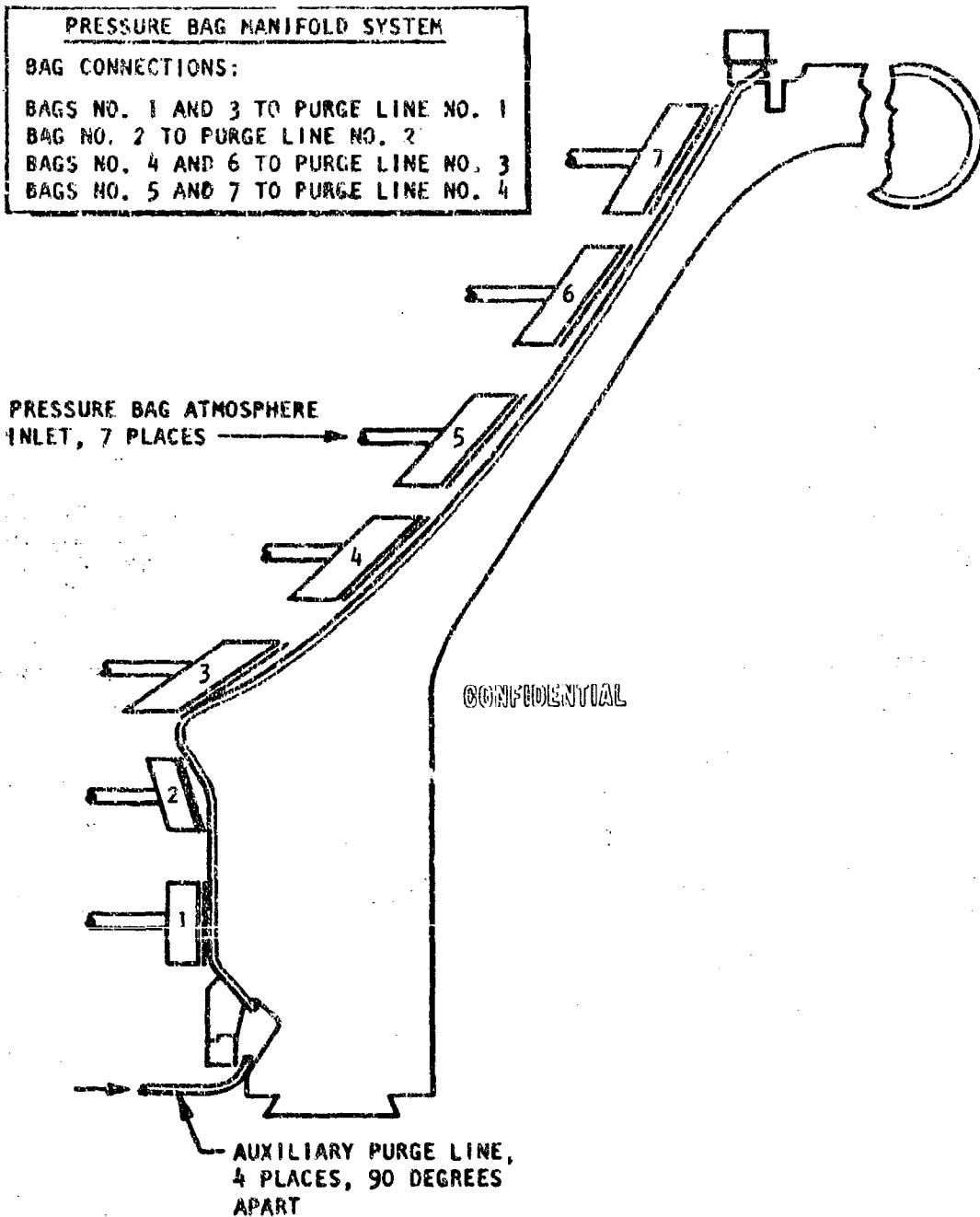


Figure 23. Location of Pressure Bags and Purge Lines for the First Braze Cycle on the Inner Wall Assembly

CONFIDENTIAL

CONFIDENTIAL

(U) Thermocouples were attached to the assembly and tooling and the part was lowered onto the retort base. The pressure bag tooling was bolted to the base with insulating brackets connecting the bolts to the retort base to prevent excessive thermal expansion of the bolts from base burner heat and resultant increase of pressure bag-to-tube spacing. Counterweight tooling and pressure bag lines were installed and all bags were pressurized to determine:

1. If the bags were holding the tubes against the body
2. If there were any leaks in the bag system

(U) Figure 24 shows the inner wall assembly in brazing position on the retort base.

(U) The retort, plumbing lines, and ducts were weld sealed and verified by evacuating the retort as described previously for the outer wall assembly.

(U) First Braze Cycle. Furnace braze data are listed in Table 10. Figure 25 shows the time-temperature curve resulting from the first braze cycle. Time-temperature data from all assembly thermocouples were entered on FORTRAN sheets and plotted by the computer for analysis of the braze cycle. Helium gas was used as the retort atmosphere during the cooling cycle on this run to take advantage of an increased cooling rate expected with the low-density gas.

(U) Postbraze examination of the braze assembly revealed the following:

1. Light brown oxidation spots were noted on the tubes from some of the pressure bag bleed holes, as had been noticed on the first outer wall assembly.
2. Approximately 80 percent of the tube-to-tube joints appeared to be filleted with braze alloy; most of the unfilleted joints were on the exit end.



Figure 24. Inner Wall Assembly in Brazing Position on Retort Base

- Arrows: A - Exit End Ring Counterweights
B - Typical Shims Which Hold Adjustable Bag Rings in Secure Position During Brazing
C - Bolts Connecting Upper Bag Assembly to the Base Insulation Brackets

TABLE 10

INNER WALL FURNACE BRAZE DATA

Data	Inner Wall Unit No. 1, First Braze Cycle
Time In/Date	2:35 AM/23 February 1967
Time Out/Date	7:45 PM/26 February 1967
Total Time	89 hours, 10 minutes
Assembly Levelness, in	0.120 inch from level*
Assembly Levelness, out	0.075 inch from level
Room Temperature Evacuation 300 to 500 Microns, time	4 minutes, 10 seconds
Braze Position	Injector end down
Pressure Bag Pressure Requirements	See Fig. 22
Temperature Differential Requirements	See Fig. 25
Atmosphere Requirement:	
Argon, Minimum Flowrate	1400 CFH heating cycle
Hydrogen, Minimum Flowrate	1600 CFH above 1400 F
Helium, Flowrate	540 to 1400 CFH during cooling from 1800 F
Auxiliary Purge Line, Four Places	25 to 30 CFH
Braze Alloy	RB0170-C62 (90Ag-10Pd)
Braze Temperature	2010 F ⁺³⁵ ₋₀ F, 20-minute hold

*The retort base has movable plates which causes the initial levelness measurement to be more out-of-level than after brazing.

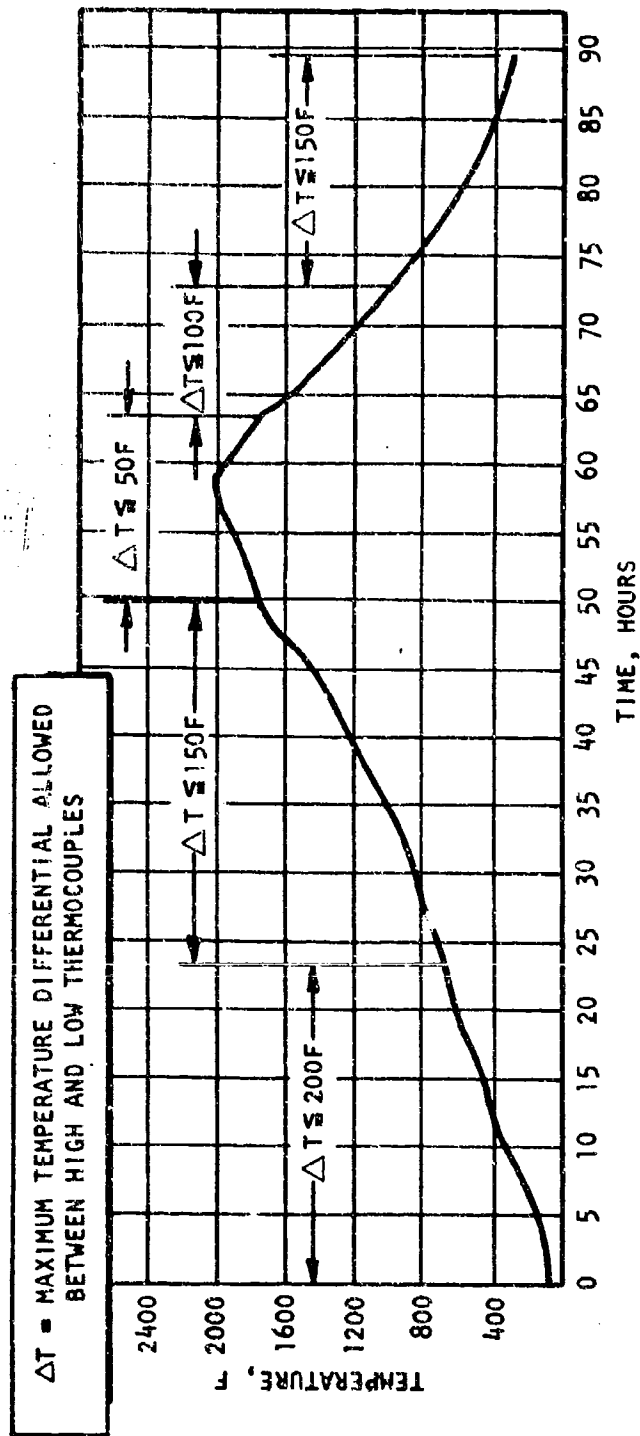


Figure 25. Time-Temperature Curve for the First Braze Cycle, Inner Wall No. 1

3. The injector ring joint had continuous fillets at each side of the ring and appeared to be sealed.
4. Tube-to-ring and tube-to-body joints at the exit end were unsealed.

(U) Second-Cycle Preparation. Shimming of tube-to-tube gaps was performed in the same manner as for the outer wall No. 1 assembly except that 90Ag-10Pd braze alloy shims were used for 2 inches forward to 2 inches aft of the throat.

(U) Nickel powder paste was washed into visible voids wherever they were found. The tube-to-body joint at the exit end had a continuous nickel fillet applied around the joint. Gaps under the exit ring were shimmed with nickel shims; this was followed by addition of the special wide-gap brazing filler material previously mentioned on outer wall No. 1.

(U) All joints were alloyed with second-cycle alloy paste regardless of whether they appeared sealed or not. Tube-to-tube joints were alloyed from the exit end ring to the injector end ring. The CaO and R-1 Binder stop-off material was inserted into the exit end of all tubes as a deterrent against braze alloy tube plugging.

(U) The assembly was thermocoupled and placed on the retort base exit end down for brazing. Pressure bag tooling was not required for the second braze cycle. Counterweights were used on the exit ring to overcome tension on the ring joint from the weight of the ring.

(U) Second Braze Cycle. Postbraze examination of the assembly revealed the following:

1. A bluish-gray discoloration was noted on one side of the assembly adjacent to the thermocouple inlet tunnel, indicating atmospheric contamination.
2. All braze joint fillets showed acceptable alloy flow and appearance including those in the area of the discoloration.

(U) Discussion of Results. Examination of the retort after the braze cycle failed to show any rupture or cracks which would cause the discoloration on the assembly. It is known that a small amount of air enters the retort through the thermocouple inlet tunnel, but this had not been a problem in the past. During the brazing cycle, the flow of argon and helium atmosphere into the retort was reduced to a minimum of 350 cu ft/hr for about one-half the run time to reduce overall gas usage during the cycle. The reduced flow was believed responsible for allowing minimal leakage from the thermocouple tunnel to contaminate the side wall of the assembly. Increased atmosphere flowrates prior to and subsequent to the present cycle have not shown a poor atmosphere condition.

(U) A 5-psi helium leak check disclosed some small pinhole-type leaks that could be repaired locally, thus completing furnace brazing on this unit.

Brazing, Outer Wall Unit No. 2

(U) Assembly Preparation. Assembly description for the most part will be of those things that differed from outer wall unit No. 1. An additional alloy groove was added to the body $1/4$ inch in from the exit end tube contact surface. After installing wire in the body alloy grooves, the grooves were filled with braze alloy paste to provide additional alloy to the tube and body joints. Stacking of tubes was performed to form a tight stack and good body contact with 3640 tubes ultimately assembled to the body.

(U) The assembly of end rings, triangular nickel fillers, and nickel powder and alloy was performed as in unit No. 1. Only one problem was encountered during assembly. Straps holding down the injector ring were somehow loosened after alloying was nearly complete, and the ring was raised about 0.100 inch above the tubes in one location. Considerable effort was spent in repositioning the ring (and nickel fillers) before it was acceptable.

(U) After alloying was complete the pressure bag tooling was installed in position. The bags were functionally tested and considered satisfactory.

Thermocoupling and furnace installation followed and the retort top was set over the part and weld sealed to the base. Before the run started, the bags were pressurized at 40 psi. All functioned except the No. 2 bag which didn't show any pressure from the return line. The system outside the retort was rechecked and nothing was found to be wrong, so the retort was cut open and the top removed for examination. It was discovered that the line leading to the No. 2 bag was pinched by the retort top when it was lowered onto the base. The problem was corrected and the furnace cycle was started and completed without further incident.

(U) First Braze Cycle. Postbraze examination of the assembly revealed that:

1. Tube-to-tube joints were satisfactory. Some gaps were noted aft of the throat. Two gaps were measured at 0.010 inch wide and were the largest seen in the assembly. About 10 percent of the joints were unbonded aft of the throat. Less than 1 percent were unbonded forward of the throat.
2. Appearance of the chamber showed good atmosphere.
3. Pressure bag function appeared to be satisfactory.
4. Injector end ring and body fillets were sound.
5. Exit end ring and body fillets were incomplete.

(U) Second Cycle Preparation. All gaps were shimmed with pure nickel and 90Ag-10Pd braze alloy shims as performed on outer wall No. 1 except that nickel powder was used around 90Ag-10Pd alloy shims instead of 90Ag-10Pd powder. The wide gap brazing material was used where possible under the exit ring. Nickel powder paste was used at exit ring and body fillets and wherever visible voids were found. All braze joints were alloyed with second-cycle alloy paste even though most of them appeared to be sealed after the first cycle. The CaO and R-1 Binder stop-off material were inserted into the exit end of all tubes, and the chamber was ready for brazing in the exit end down position.

(U) Second Braze Cycle. Postbraze examination of the assembly revealed excellent-appearing braze joints, and no voids were visible.

Brazing, Inner Wall Unit No. 2

(U) Assembly Preparation. A 0.010-inch discrepancy existed on the exit end of the body (as occurred on unit No. 1) and had to be built up with nickel plating.

(U) Braze wire and alloy paste were applied to all body alloy grooves before braze foil was attached. A total of 3637 tubes were counted in the assembly after stacking was complete.

(U) Injector and exit end rings were installed and triangular nickel fillers, nickel powder, and braze alloy paste were applied to the assembly as indicated for unit No. 1.

(U) Lower and upper pressure bag tooling was installed and positioned. There was one small bag leak, but it was considered too small to affect pressure bag operation. Thermocouple and furnace installation was performed as for inner wall unit No. 1.

(U) First Braze Cycle. Postbraze examination of the braze assembly revealed that:

1. There were fewer tube-to-tube gaps than on the previous inner wall unit.
2. Injector end ring and body joints appeared to be satisfactory. Exit end joints lacked complete fillets.
3. Overall brazing atmosphere appeared to be good except for the usual brown spots coinciding with pressure bag bleed holes.

(U) Second-Cycle Preparation. Shimming of tube-to-tube gaps was performed in the same manner as for inner wall unit No. 1 except that nickel powder was used around 90Ag-10Pd shims instead of 90Ag-10Pd alloy powder. Nickel powder was washed into visible voids at ring and body joints. The wide-gap brazing material was inserted where possible under the exit ring. Braze alloy paste was applied to all joints regardless of their previous braze bond appearance. Tube stop-off material was inserted into all exit end tubes, and the unit was ready for brazing.

(U) Second Braze Cycle. Examination of the assembly revealed several tube-to-tube voids that would be hand braze repaired. General overall braze quality showed an acceptable braze operation. Figures 26 and 27 show the assembly on the furnace braze following the second braze cycle.

Tubular Combustor Repairs

(U) Because of the complexity and fragility of the tubes on the thrust chamber assemblies, a small amount of damage occurred during processing. With the magnitude of sealing required between tube-to-tube joints and tube-to-manifold joints, a certain amount of manual repairing was required after the furnace brazing operation. Also, a sporadic problem of the small-diameter tubing being restricted by braze alloy was encountered. Most of the repairs were highly specialized, requiring unique techniques and highly skilled personnel. The repairs required and performed are listed briefly in the following paragraphs.

(U) Cutter Combustor No. 1.

(U) Tube Crown Repairs. Two tube crown pin holes $3/4$ inch downstream from the throat were inadvertently made by arcing with an electroplating stylus. Repair was made using a plasma-arc torch with 90Ag-10Pd braze alloy. Figure 28 shows a typical plasma-arc repair on a tube crown.



Figure 26. View of Inner Wall Unit No. 2 in the Exit End Down Position Following the Second Braze Cycle. Some Dark Spots are Seen on the Tubes that were Oxidized from the First Cycle Pressure Bleed Holes. Several Tube-to-Tube Gap Remained After the Second Cycle that were Repaired by Manual Torch Brazing



Figure 27. Closeup View of Inner Wall Unit No. 2 Showing the Exit End Ring with Four Counterweights (Arrow) in Position. A Total of 24 Counterweights Were Used Throughout the Circumference of the Ring

(U) Tube-To-Tube Repairs. Stylus electroplating was utilized on 19 leaks, applying a nickel flash first and followed by silver plating and burnishing. Figure 29 shows typical plating repair areas on a combustor.

(U) Tube-To-Exit Ring. An 8-inch-long leaking area on the hot gas wall side of the ring was sealed by torch brazing with 50Au-25Ag-22Cu-3Zn alloy.

(U) Inner Combustor No. 1.

(U) Tube-To-Tube Repairs. Approximately 150 leaks were repaired by stylus silver plating the narrow leaks (approximately 0.007 or less) and torch brazing those that were wider using 82Au-18Ni in the throat area and 50Au-25Ag-22Cu-3Zn in the remainder of the contour.

(U) Tube Crown Hole Near Throat. A small hole made by arcing with the plating stylus was sealed by TIG brazing with 82Au-18Ni.

(U) Outer Combustor No. 2.

(U) Tube-To-Tube Repairs. Approximately 12 leaks on the hot-gas wall were stylus silver plated. Tube-to-tube leaks under the exit ring at the extreme end of the tubes occurred intermittently throughout the circumference of the combustor and were repaired by TIG brazing with 50Au-25Ag-22Cu-3Zn alloy.

(U) Inner Combustor No. 2.

(U) Tube-To-Tube Repairs. Three leaks under the exit ring at the extreme end of the tubes were TIG braze repaired with 50Au-25Ag-22Cu-3Zn alloy. There were no leaks on the hot-gas wall contour.

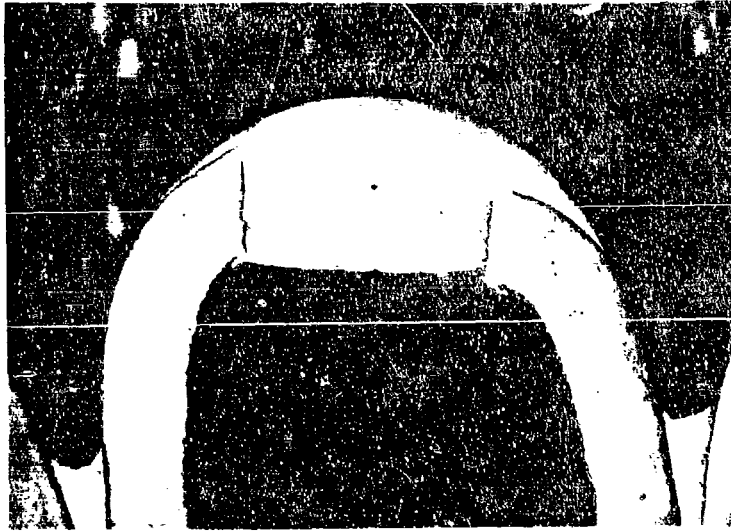


Figure 28. Silver-Palladium Brazed Tube Crown Repair
on Type 317 Stainless-Steel Tube (50X)

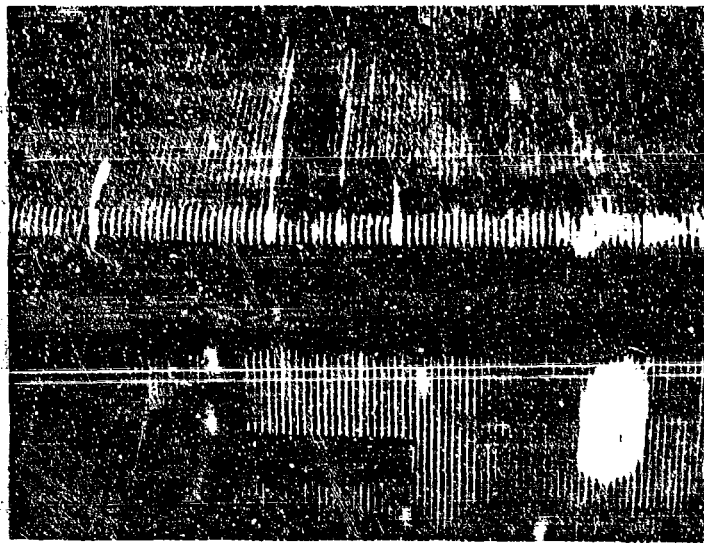


Figure 29. Repair of Tube-to-Tube Leakage by Stylus
Plating With Silver

Nondestructive Testing of Tube-to-Body Braze Joints

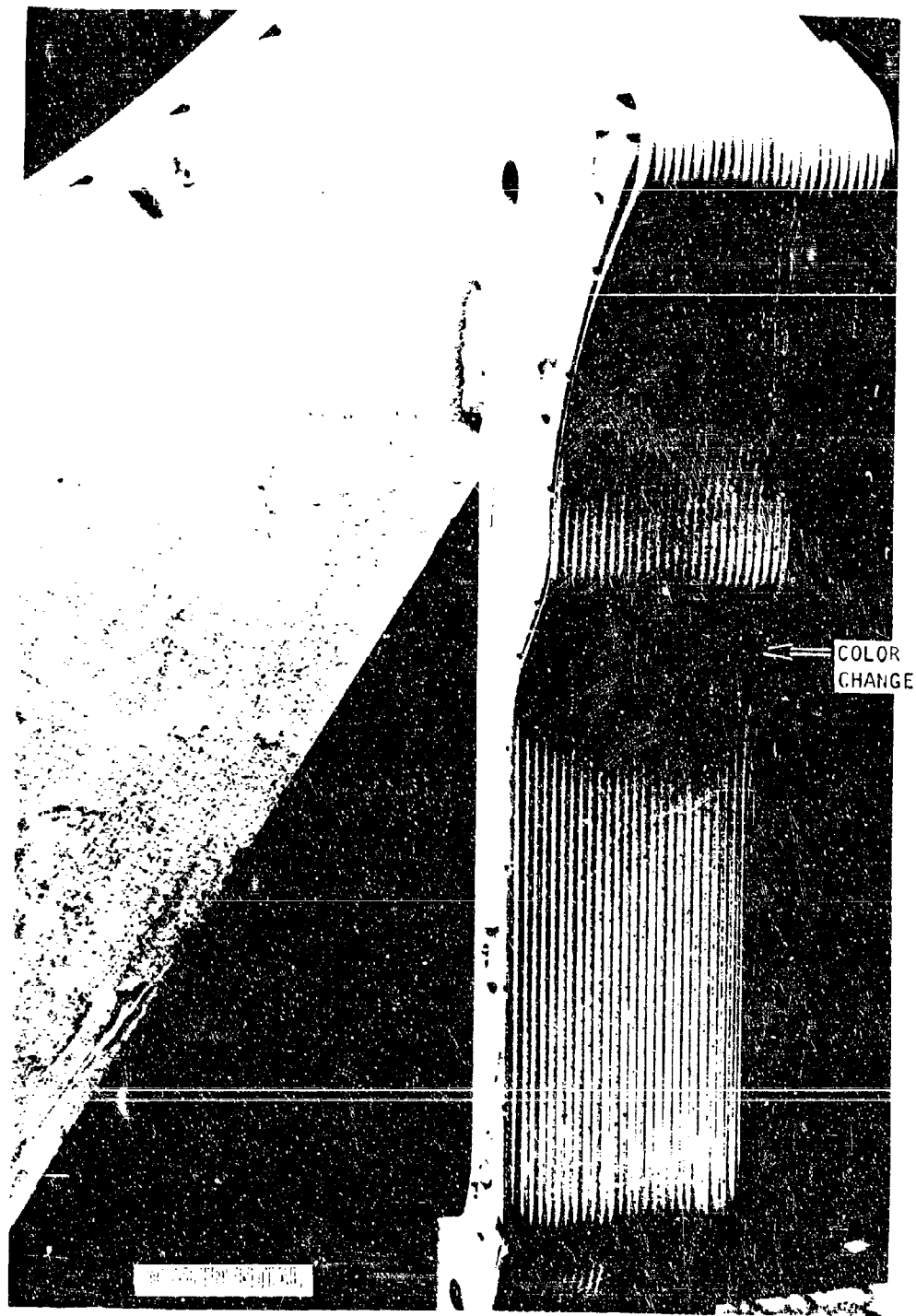
(U) An investigation to evaluate and determine whether thermochromistic pigments could be utilized as a thermographic nondestructive test technique for tube-to-backup structure braze bond integrity was performed. The procedure utilizes a product called "Detecto-Temp," a temperature-indicating paint.

(U) The principal approach used was to spray the pigment on the tube crowns, then to apply static heating with quartz radiant heat lamps for a specified time. When the radiant heat was introduced upon the tube crowns, the thermal transfer characteristics were observed the the thermochromistic pigment color change.

(U) The initial investigations were performed on various pieces of test samples which duplicated actual chamber configurations. These samples consisted of small-diameter type 347 stainless-steel tubes with nominal wall thicknesses between 0.008 and 0.011 inch brazed to a massive stainless-steel backup structure. Figure 30 illustrates the results achieved in the detection of braze disbands after the application of the pigment and testing with the radiant heat lamps. Based upon the results of metallurgical examinations of the void areas to determine the validity of the findings by thermographic technique, a detailed procedure was written for inspection purposes.

(U) Since the procedure has been in use for inspection, all components tested were found to be acceptable in that no disbond areas exceeded the dimensional limitations specified on the drawings.

(U) An example of the test results can be seen in Fig. 31 which shows the changes that occur when testing an actual piece of hardware.



1XE52-11/21/66-G1C

Figure 30. Thermographic Test Results on Laboratory Development Sample

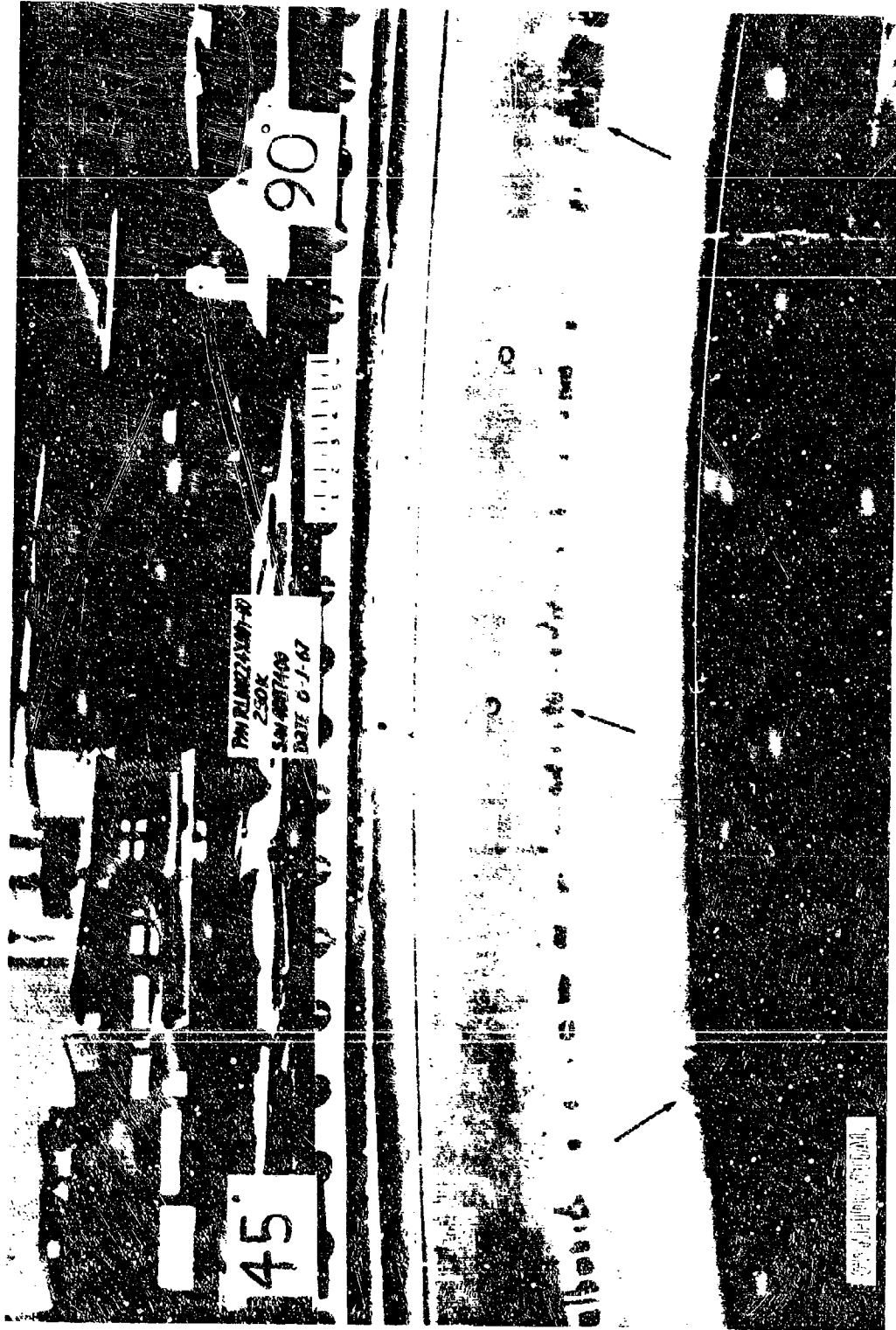


Figure 31. Thermographic Inspection Results Showing Areas of Disbonds Indicated by Dark Areas (Arrows) on Outer Combustor Unit No. 2

CONFIDENTIAL

250K SOLID-WALL CHAMBER, COPPER THROAT WELD OVERLAY

(U) It was initially determined that the throat of the solid-wall inner and outer bodies would necessarily have to possess better heat transfer characteristics than the 304L stainless-steel body material. OFHC copper was desired and a survey, backed with preliminary experimental data, was conducted relative to throat attachment methods. In chronological sequence, the events leading to the successful completion of the solid wall bodies are presented.

(U) A preliminary test program showed a reasonable practicality in arc welding a deposit of OFHC (or deoxidized) copper over a prior deposit of Nickel 61 (to prevent the common CRES/copper cracking). Work continued on this concept using larger samples and deoxidized copper (again, and always, over Nickel 61). It was determined that deoxidized copper would not meet the desired conductivity, 30 percent International Annealed Copper Standard (IACS) being the value obtained. Tests with OFHC copper showed 80 percent IACS which was considered acceptable.

(U) The inner body was the first unit to be welded using the following practice:

1. Apply Nickel 61 to the 304L using the gas metal arc welding process (GMAW).
2. Apply 70 percent copper-30 percent nickel (70Cu-30Ni) to the Ni 61 deposit using GMAW.
3. Apply several layers of OFHC copper to the 70Cu-30Ni deposit using GMAW; then finish the OFHC deposit using the gas tungsten arc welding process (GTAW).

(U) The underlying deposits were such that defect propagation could not be stopped in the upper deposits, and the inner body throat deposit was declared unacceptable.

(U) The outer body was welded in accordance with improved techniques. Although this total deposit contained some known quantities of lack-of-fusion and porosity, it was a significant improvement over the prior effort. The outer body was accepted and finish machined.

(U) Another consideration affected the difference between the two deposits. The inner body was an OD overlay, the outer body was an ID overlay. Thus, shrinkage stresses (tension) in the former would tend to propagate prior flaws and/or generate new flaws in areas weakened by contaminants. The opposite would be true of the outer body.

(U) On the inner body, all but the lower portion of the original deposit to sound metal was removed and rebuilt to contour using the GTA process and Nickel 61 filler (approximately 15 percent IACS conductivity). This was performed successfully. Each pass was mechanically hammer peened to prevent excessive shrinkage, the part being seriously distorted already. Postweld analyses showed the part to be usable. It was finish machined and accepted.

FABRICATION OF 250K INJECTORS

INJECTOR STRIPS, DEBURRING BAFFLES

(U) To furnish design flowrates, the drilled orifices in the injector strips required deburring after drilling. An electrolytic deburring process was developed and used to replace hand deburring. Experience obtained with the process during the program shows that both labor cost and rejection rates were greatly reduced over that for the hand deburring method and that processed injector strips met all engineering requirements.

Electroformed Injector Baffles

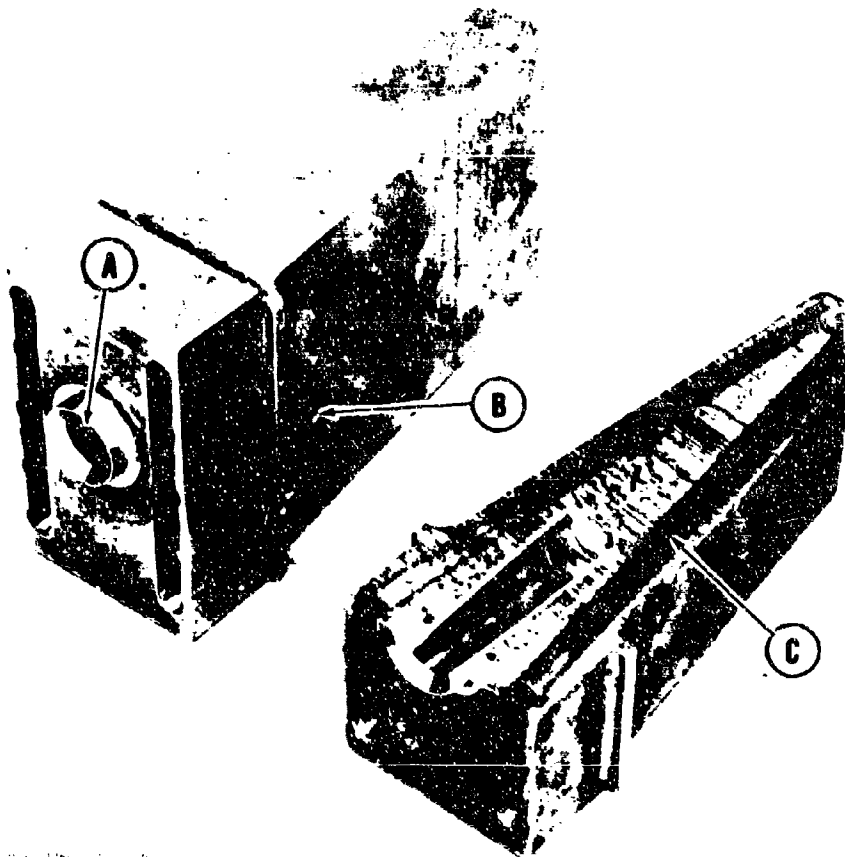
(U) A program was attempted to fabricate the 250K injector baffles by electroforming copper on a stainless-steel core. Six baffles were produced and run through braze cycles simulating the injector assembly brazing process. The baffles blistered during the braze cycles and failed in pressure testing. The program was discontinued.

Baffle Brazing

(U) The component parts of the baffle assembly to be brazed were the stainless-steel liners in the hot-gas passage and a copper closure plug in the manifold at the baffle tip. The stainless-steel liners in the hot-gas passage are shown in Fig. 32. To achieve braze joint reliability consistent with the design, it was necessary to braze and pressure test the baffle units prior to assembly on the injector. The scheduled brazing temperature for the injector was 1900 F, which meant the baffle assembly braze joints had to go through the temperature without loss of joint integrity.

(U) The braze alloy selected for the baffle assembly was 62Cu-35Au-3Ni with a braze temperature of 1920 F maximum. The diffusion rate of this braze alloy into the baffle materials was sufficient to increase the remelt temperature at a safe level for processing through a second braze cycle at 1900 F as a part of the injector assembly.

CONFIDENTIAL



CONFIDENTIAL

- A. Hot-gas passage at base of baffle showing stainless steel liner
- B. Hot-gas passage at side of baffle showing stainless steel liner
- C. Fuel cooling channels

Figure 32. Completed and Sectioned Baffle Assemblies

CONFIDENTIAL

(U) Ten baffle assemblies were brazed during a single furnace cycle. A braze fixture was produced that would accept the 10 units and introduce a purge gas through the cooling channels on each baffle. The purge gas was used to dispel all air that could be trapped in the passage. Figure 33 describes the baffle position and purge gas system on the furnace tooling.

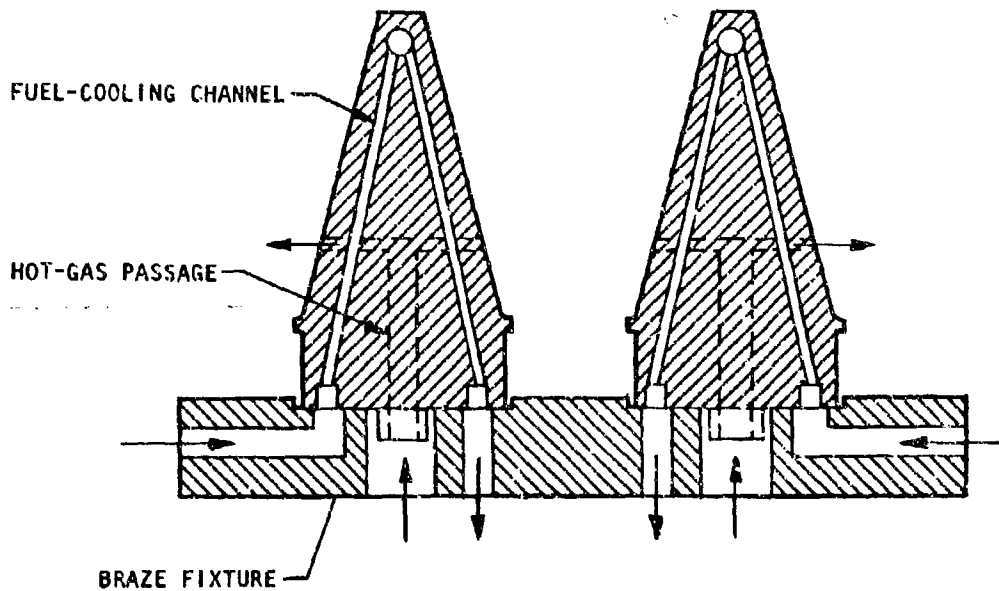


Figure 33. Section Through Braze Fixture and Two Baffles Showing Gas Purge System (Arrows Indicate Direction of Gas Flow)

BRAZING OF INJECTORS

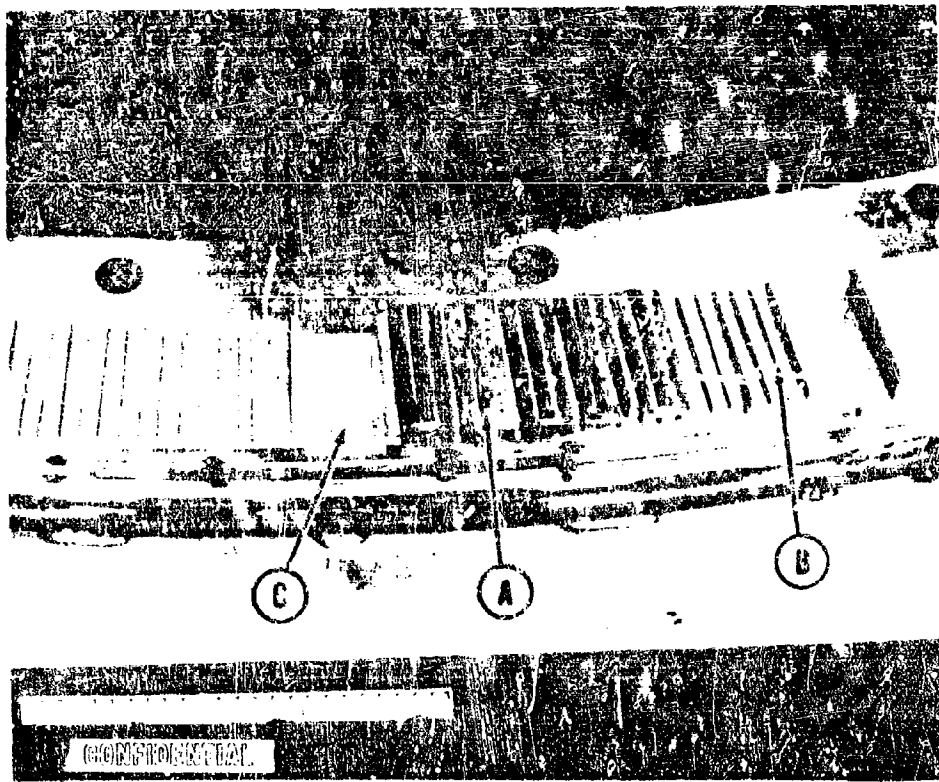
Assembly and Brazing Process

(U) The joint gap tolerances (maximum of 0.004 inch) needed on all the vertical braze joints between the body and the strips and baffles required close control of the machine operations and inspection methods. The machined areas in the body to receive the strips and baffles were broached to achieve repeated close dimensions. An EDM operation followed the broaching to produce a passage from the strips to the oxidizer and fuel manifolds. Figure 34 shows an injector segment with the broaching operation complete prior to the EDM operation. Figure 35 shows an injector segment with the broaching and EDM operation complete. The EDM operation deformed the body lands out of a vertical plane. The lands were straightened and the original dimensions reinstated by the use of a sizing tool.

(U) Laboratory tests were conducted prior to assembly and brazing the injectors. These tests were conducted to establish a method of retaining the strips in position during the braze cycle and the amount and form of braze alloy to be used for each joint. Figure 34 illustrates the first type of braze sample used. The body segment was first used as a test piece to establish dimensional integrity from the broaching operation. The broached strip and baffle sockets are shown in this illustration. Figure 35 illustrates a body segment, used for brazing tests, with both the broaching and EDM operations completed.

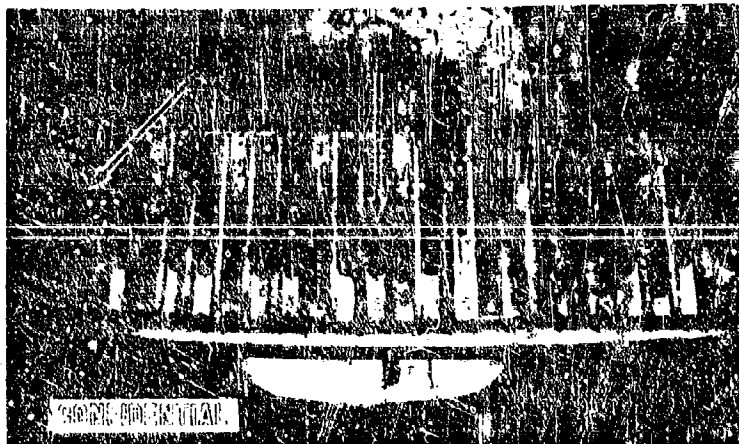
(U) The brazing tests conducted in the laboratory confirmed that the following requirements produced consistent braze joints:

1. The strips and baffles staked in position using two stakes on each land positioned 1/8 inch from each end (Fig. 34)
2. Braze alloy sheet 0.002 inch thick placed in the horizontal joint surfaces of the strips and baffles



- A - Strips
- B - Strip Seat
- C - Baffle Seat

Figure 34. Broached Strip and Baffle Seat on Injector Segment



- A - Passage from strip seat
- B - Passage from baffle seat

Figure 35. Passage From Strip and Baffle Seat to Manifold by the EDM Method

CONFIDENTIAL

3. Braze alloy sheet 0.001 and 0.002 inch thick placed in the vertical joints between the body lands and strips; the two thickness of alloy sheet were necessary to center the strip in the body socket
4. Braze alloy wire placed on top of each body land and at the ends of the strips

(U) Assembly of the component parts prior to furnace brazing was conducted in the white room. Each strip was dimensionally checked prior to assembly, using a precision gage. As the strips were placed in the mating area of the injector body, 0.001 and/or 0.002 inch braze alloy sheet was placed in the vertical joints as needed to equalize the gap widths. The strips were seated firmly and staked in position. Figure 36 shows the preplaced braze alloy rectangular wire and alloy paste used on top of the body lands between strips and baffles. Figure 37 shows the nickel troughs used to hold preplaced braze alloy at the ends of the strips and baffles and the area of preplaced rectangular braze alloy wire in the strip grooves. The braze alloy used was (62Cu-35Au-3Ni) with a solidus temperature of 1832 F and a liquidus temperature of 1886 F. Total quantity of braze alloy used averaged 61 troy ounces.

(U) The furnace braze operation was conducted in the same furnace as the thrust chambers. Fifteen thermocouples were used on each injector assembly. The thermocouples were located at 120 degree intervals around the injector diameter and at thick and thin sections to maintain predetermined temperature gradients to minimize thermal stresses in the body section that could initiate dimensional deformation or possible fractures. Thermocouples were also adjacent to the braze joint to confirm the temperature range in this area for required braze alloy flow.

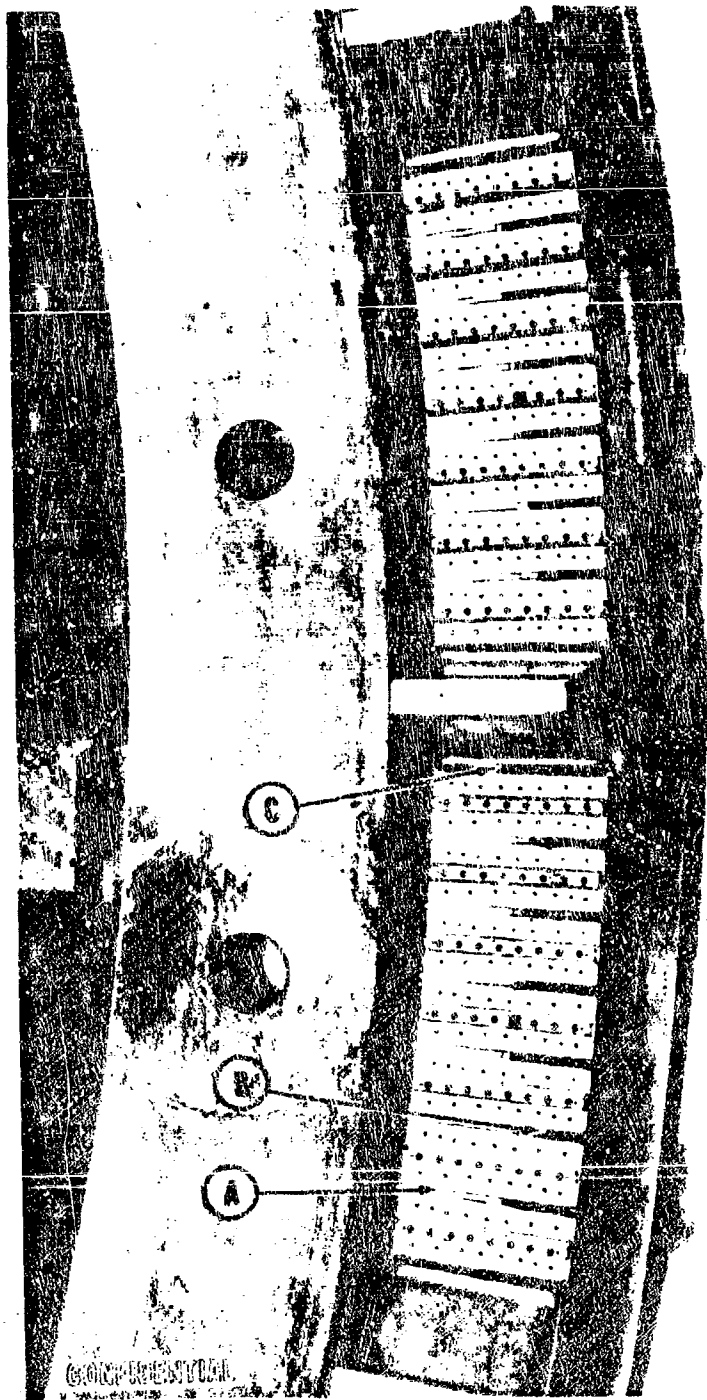
(U) Figure 38 shows an injector assembly with some of the thermocouples attached. Figure 39 shows the injector retort on the furnace hearth with the purge gas lines, thermocouple duct, and vacuum duct attached.

103

CONFIDENTIAL

This page is Unclassified

CONFIDENTIAL



- A - Preplaced braze alloy rectangular wire
- B - Preplaced braze alloy paste between strips
- C - Preplaced braze alloy paste at baffle

Figure 36. Braze Alloy Placement Between Strips

CONFIDENTIAL



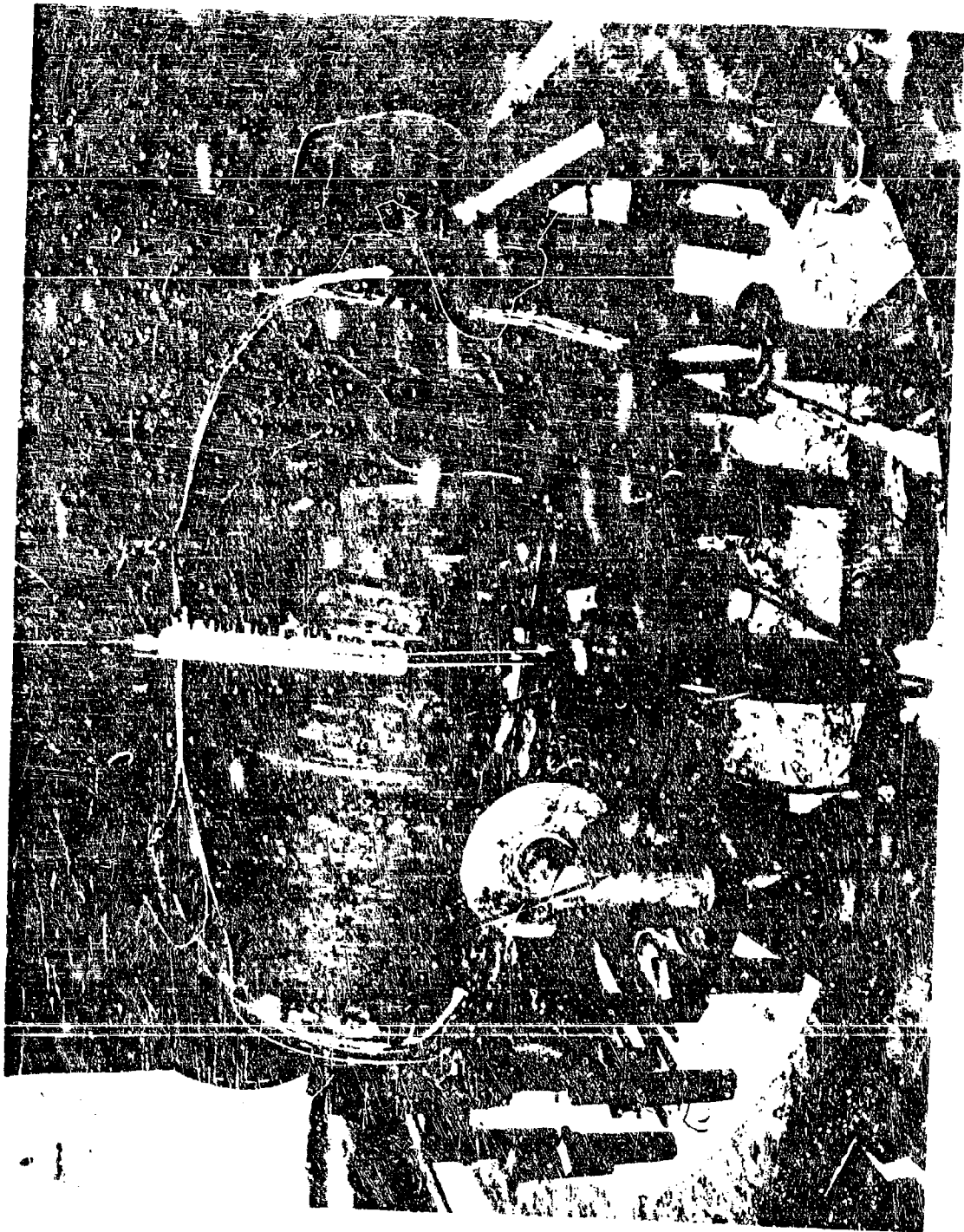
- A - Nickel trough at baffle end to retain braze alloy
- B - Nickel trough at strip end to retain braze alloy
- C - Preplace braze alloy rectangular wire in strip grooves

Figure 37. Braze Alloy and Nickel Trough Placement



A - No. 8 thermocouple attached
B - No. 9 thermocouple attached
C - Position of thermocouples for retort outlet

Figure 38. Partial Thermocouple Attachment



A - Gas exhaust line
B - Gas inlet line

C - Thermocouple duct
D - Vacuum duct

Figure 39. Furnace Retort for Brazing 250K Injector

(U) The injector assembly was supported on the retort base by two deep I-beam section rings sufficient to support and maintain the injector assembly in a level flat plane during the heat cycle.

(U) The average furnace braze heat cycle was extended through 38 hours from the first vacuum evacuation of the retort of 300-microns Hg until the part temperature cooled to 300 F. An average vacuum pressure of 195 to 250-microns Hg was maintained in the retort from ambient temperature until the part reached 300 F. The retort was evacuated when the part temperature had cooled below 300 F. This action was taken to gain information on the magnitude of leak that might be initiated in the retort as a result of the heat cycle. Twenty-eight inches of Hg was the lowest pressure level in the retort that could be achieved. This indicated some leaks had been developed in the retort.

(U) Argon and hydrogen gas were used to purge the oxidizer manifold, fuel manifold, and the retort above a part temperature of 300 F. Argon gas was used below 1400 F on the heating and cooling cycle with hydrogen used from 1400 F through the braze temperature of 1900 to 1920 F and cooling to 1400 F. The average volume of purge gases used was 35,00 cu ft hydrogen and 90,000 cu ft argon.

Injector Pressure Testing Method

(U) A method was developed to seal the propellant orifices so that the braze joints of the injector strips could be leak tested at pressures up to 600 psi. A styrene mineral wax blend material (Plasti-wax 8969) with a 350 F melting point was proved satisfactory for sealing the propellant orifices in injectors when applied to clean injector surfaces preheated to a minimum of 225 F. After leak testing the fuel and oxidizer sides of the injectors, the resin-wax material was dissolved by repeated flushings with hot trichloroethylene.

CONFIDENTIAL

FABRICATION OF 2.5K SEGMENTS

(C) NICKEL 200 TUBE-WALL FABRICATION

(C) Nickel 200 Tube Processing

(C) Raw Material. Raw tubing to be used in the fabrication of the Nickel 200 tubes for the 2.5K segment was purchased. The small 0.156-inch OD by 0.016-inch wall, seamless tubes, were procured. Routine metallurgical examination performed during the receiving inspection of the material showed that it met all specification requirements.

(C) Tapering. It is a well known fact that Nickel 200 has a high affinity for sulfur when exposed to elevated temperatures while in the presence of compounds and materials containing the element. The resultant intergranular attack renders the material unfit for use in thrust chamber tube applications. Therefore, prior to the beginning of tapering, all materials which were scheduled to be used in the tapering, preforming, final forming, and packaging of the tubes were screened for compatibility with Nickel 200. Such materials as tapering lubricant, oil used to fill the tubes during final forming, marking materials, EDM dielectric oil, and packaging materials were checked. The test consisted of heating Nickel 200 tube specimens to 1300 F \pm 25 F for 10 minutes in air, while in contact with the materials being checked for compatibility. Metallographic examination was then performed on the tube specimens to determine the presence of intergranular attack. Only materials that passed the test were allowed to be used.

(C) Prior to beginning the production tapering of the Nickel 200 tubes, a pilot run was made to establish optimum tapering parameters. Results

of these tests (Table 11) determined by metallurgical evaluation showed that the tubes could be tapered in one pass. The production tapering was accomplished without incident. The excellent taperability of Nickel 200 allowed for the manufacture of two straight tapered tubes from one blank. Tapering parameter measuring devices installed on the machine afforded excellent reproducibility.

(U) Metallurgical evaluations were conducted on tapered tubes subsequent to annealing. Results are shown in Table 11. It should be noted that the tapered tubes produced were of excellent quality.

(C) Outside diameter surface laps were found on a number of the tapered tubes evaluated. This discrepancy is one which is quite commonly found on tapered tubes with the working characteristics of Nickel 200. In no case did the laps exceed 0.001 inch.

(U) Preanneal cleaning of the tapered tubes was accomplished by vapor-degreasing including flushing of the tube ID with hot trichloro ethylene followed by ultrasonic cleaning. The latter cleaning operation was performed with the tubes immersed in a Freon TF bath and cleaned at a frequency of 20 to 25 Kc for 5 minutes at room temperature. The tubes were then rinsed in hot (120 F) deionized water with the ID of the tubes being flushed during this operation.

(U) Annealing was carried out at 1500 F \pm 25 F in a continuous tube annealing furnace in a dry hydrogen atmosphere.

(U) Preforming and Final Forming. Preforming of the annealed straight tapered tubes was accomplished without difficulty. The final forming of the tubes was accomplished in a contour cavity book die. Because no internal pressure was used to assist in forming the tube to final configuration, annealing of the preformed tubes was required. Cleaning of the preformed tubes was done in the same manner as the straight tapered tubes.

(C) TABLE II
 RESULTS OF METALLURGICAL EVALUATIONS CONDUCTED
 ON TAPERED NICKEL 200 TUBES (RL000044X)

Specification No.	Lot Designation	Wall Thickness, inches						Metallographic Observations
		0.023 OD		0.075 OD		0.0135 to 0.015 Required		
		Maximum	Minimum	Maximum	Minimum	Maximum	Minimum	
1	Parameter Development	0.0156	0.0151	0.0132	0.0127	0.0127	0.0127	OD lap on 0.075-inch OD, 0.00094 inch deep; no intergranular attack observed
2	Parameter Development	0.0156	0.0151	0.0127	0.0127	0.0127	0.0127	OD lap on 0.075-inch OD, 0.00094 inch deep; no intergranular attack observed
3	Parameter Development	0.0156	0.0151	0.0137	0.0132	0.0132	0.0132	OD lap on 0.075-inch OD, 0.00094 inch deep; ID raw tube drawing scratch 0.0015 inch deep on 0.123-inch OD; no intergranular attack observed
A*	Production	0.0161	0.0152	0.0123	0.0119	0.0119	0.0119	OD lap on 0.075-inch OD, 0.0007 inch deep; no intergranular attack observed
B	Production	0.0156	0.0156	0.0133	0.0128	0.0128	0.0128	OD lap on 0.075-inch OD, 0.0007 inch deep; ID raw tube drawing scratch 0.0009-inch deep on 0.123-inch OD; no intergranular attack observed
C	Production	0.0156	0.0152	0.0133	0.0133	0.0133	0.0133	No intergranular attack observed

Some low wall thickness observed on the 0.075-inch-diameter tube was a result of a tapering machine malfunction.

CONFIDENTIAL

(U) Annealing was carried out at an outside heat treating facility using a batch-type furnace and a dry hydrogen atmosphere. The tubes were annealed in the horizontal position at 1500 F \pm 25 for 5 minutes.

(U) After book die forming, a random sample of finish formed tubes were metallurgically evaluated. Some concavity in the straight side walls of the tubes in the untapered portions at the combustion zone and exit end of the tubes was noted. This condition is one which occurs quite frequently in book die forming and it can be alleviated by applying sufficient internal pressure to allow for 1- to 2-percent plastic deformation during forming. To accomplish this, the die cavity also must be changed to allow for the strain, and the tapered tubes designed so that final configuration will meet engineering drawing requirements for stacking height. However, the concavity would not interfere with design parameters or the brazing operation, and the tubes were used without rework.

(U) Figure 40 shows the location of the metallographic specimens removed from the finish formed tubes, and Table 12 shows the results of the evaluations performed. Figure 41 depicts the conditions observed. No evidence of intergranular attack was found during any of the metallurgical evaluations performed.

(C) Subsequent to the book die forming operations, the finish formed tubes were fluorescent penetrant inspected using a penetrant solution, emulsifier, and developer that were compatible with Nickel 200. Final cleaning of the tubes preparatory for shipment to the white room for assembly of the segment was done in the same manner as cleaning prior to annealing.

Assembly and Brazing Fabrication

(U) Assembly and brazing of the nickel tubular thrust chamber segment was accomplished using 50Au-50Cu material at a braze temperature of 1800 F $\begin{matrix} +15 \\ -0 \end{matrix}$. Figure illustrates the assembly, with one copper side plate removed prior to welding the throat support beams in place.

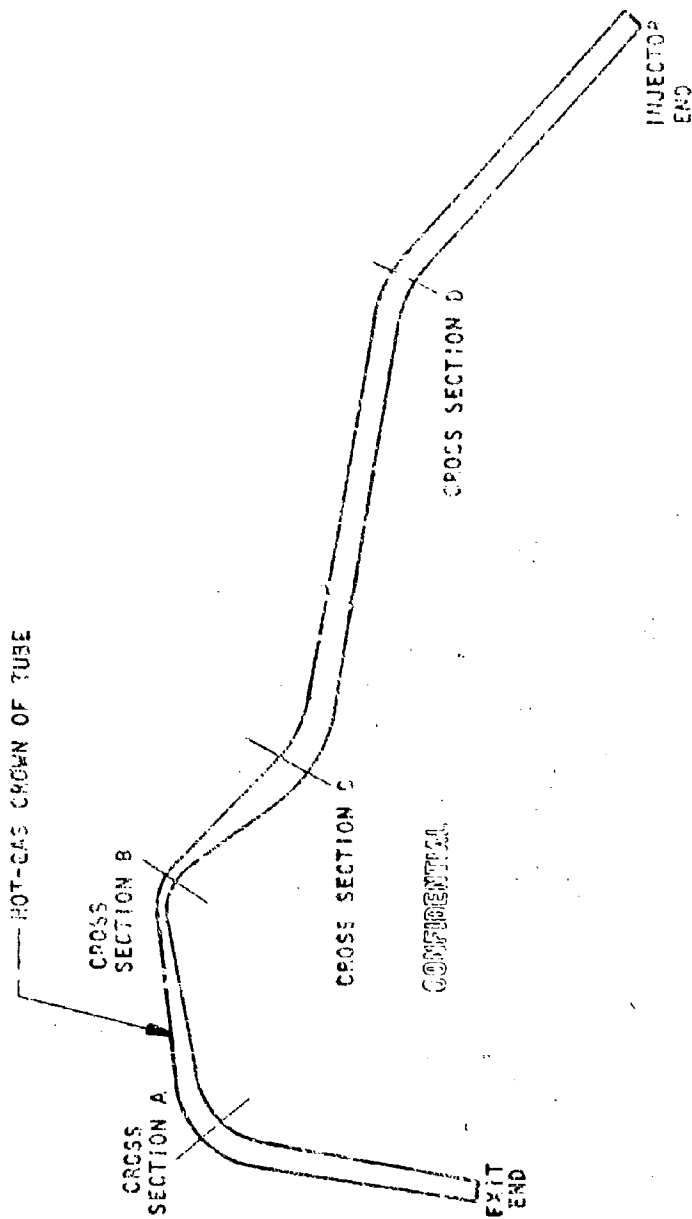


Figure 46. Location of Metallographic Specimens Recovered From Nickel 200 Tubes (RLA/00044X)

(C) TABLE 12

RESULTS OF METALLURGICAL EVALUATION CONDUCTED ON FINISH FORMED NICKEL 200 TUBES
 (LOCATION OF CROSS-SECTION SPECIMENS SHOWN IN FIG. 41)

Specimen No.	*Wall Thickness Hot-Gas Crown, inch				Metallographic Observations
	Gross Section A	Gross Section B	Gross Section C	Gross Section D	
1	0.0142	0.0123	0.0152	0.0142	No intergranular attack observed
2	0.0156	0.0133	0.0152	0.0152	No intergranular attack observed

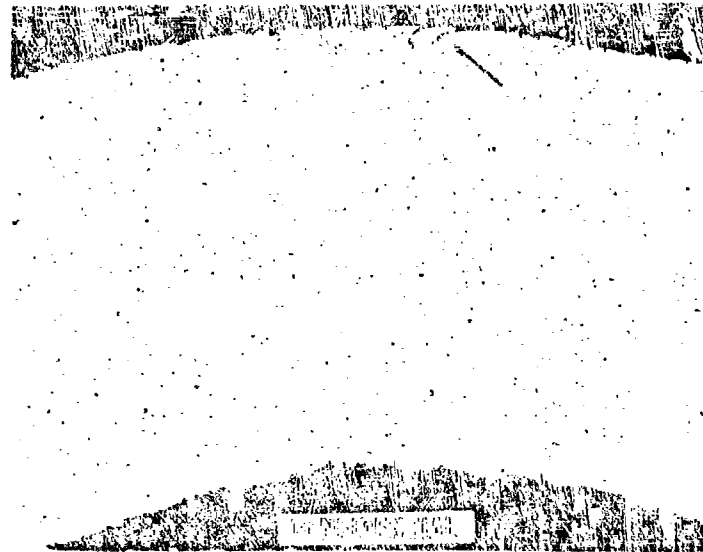
*Wall thickness requirements, inch: Cross Section A: 0.0135 to 0.0125
 Gross Section B: 0.015 to 0.013
 Gross Section C: 0.0155 to 0.0125
 Gross Section D: 0.0135 to 0.0125



a. Photomicrograph showing cross section configuration at cross section B (Fig. 40). Specimen etched with 50-50 nitric-acetic reagent. R - hot gas crown. Mag: 45X



b. Photomicrograph showing cross section configuration at cross section D. Note concavity in side walls and thickening on the crown 180 degrees from hot-gas crown (H). Specimen etched with 50-50 nitric-acetic reagent. Mag. 25X



c. Photomicrograph showing conditions observed on hot-gas crown of cross section D. Arrow points to lap on OD of tube on hot-gas crown.

Figure 41. Typical Conditions Observed on Book 11c Formed Nickel 200, 2.5K Segment Tubes

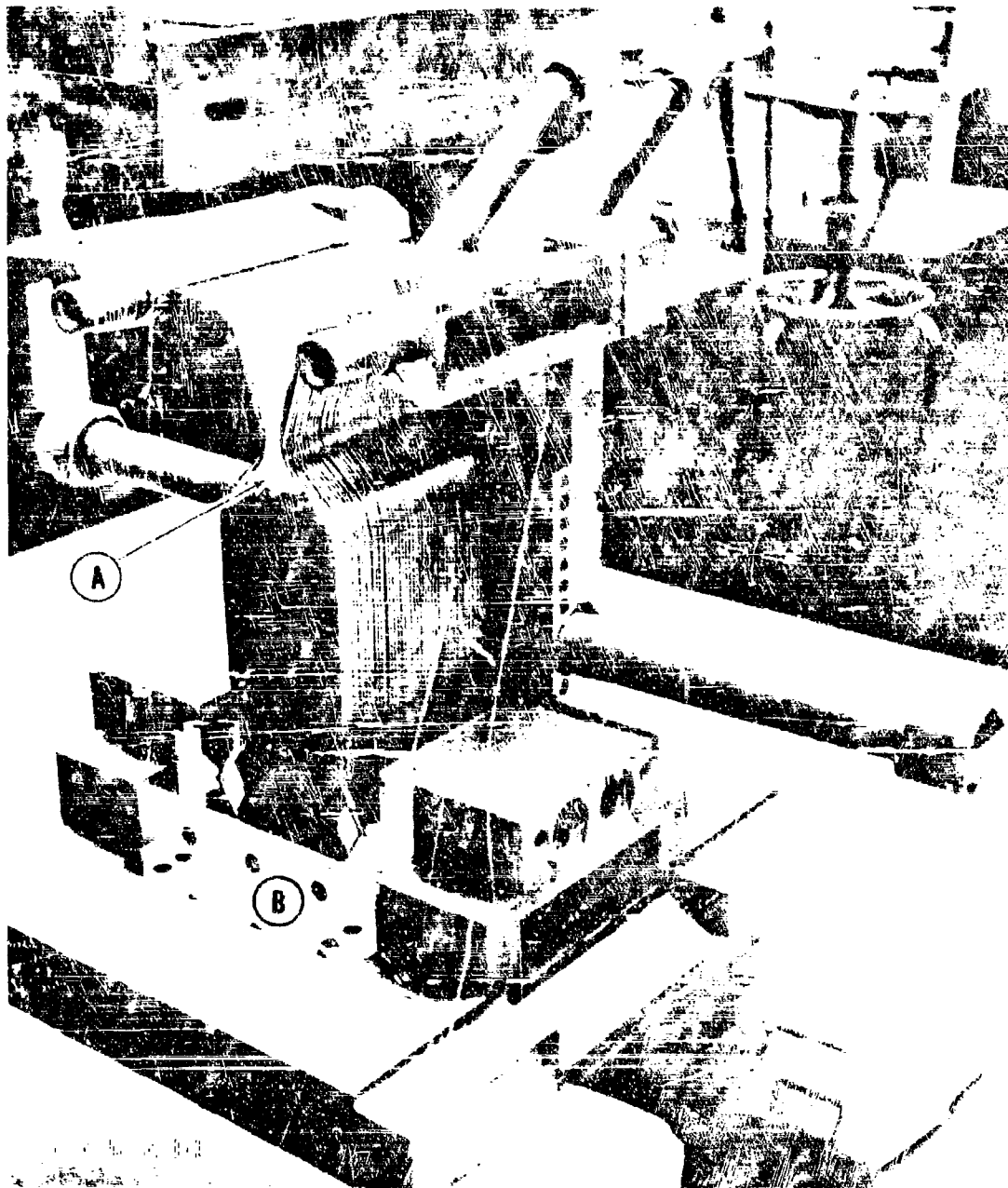


Figure 42. 2.5K Nickel Tubular Thrust Chamber Segment During Assembly. Items noted. (A) refrasil covered throat plug, and (B) 59Au-50Cu braze alloy foil

(C) The assembly was realigned at the leak locations and all other braze joints with the 50Au-50Cu filler material and a second furnace braze cycle was performed at $1790 \text{ F} \pm 15$. The helium leak check following the second furnace braze cycle revealed that all tube-to-manifold leaks had been sealed, while the chamber leaked generally in the throat area. The remaining tube-to-tube leaks in the combustion zone were sealed by stylus silver plating. Water flow testing of each nickel contour tube revealed that none were plugged with braze alloy or other foreign material. Figure 43 illustrates the nickel segment after braze fabrication.

(C) Subsequent to braze fabrication, a tube discrepancy on the 2.5K nickel-tubed segment was investigated. The noted discrepancy was caused by the accidental application of a mini-grinder, which locally removed three tube crowns to varying depths. Repair was accomplished by stylus silver plating followed by soldering (SN60 solder, 60Sn-40Pb) a nickel saddle patch over the plating for repair for reinforcement purposes. Figure 44 illustrates the tube discrepancy repair on the nickel segment. After accomplishing the repair of the tube discrepancy, braze alloy dots were applied to ID tube crowns to function as temperature indicators during hot firing of the thrust chamber segment (Fig. 45).

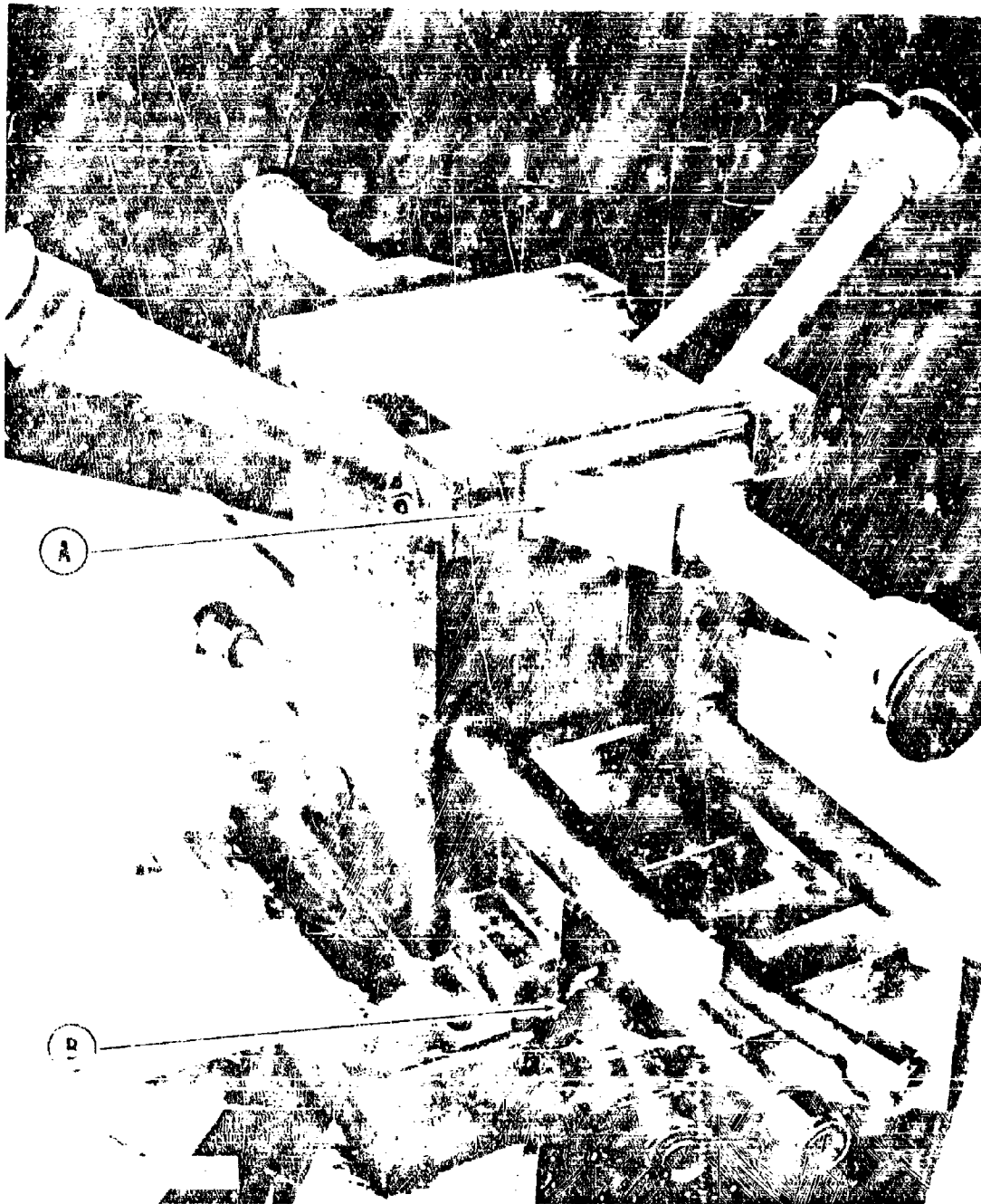


Figure 43. 2.5K Nickel Tubular Thrust Chamber Segment Before Addition of Backup Structure. Items noted: (A) nozzle end manifold assembly welded in after braze fabrication, and (B) injector end manifold assembly welded in after braze fabrication



Figure 44. Repair of 2.5K Nickel Tubular Thrust Chamber Segment.
Area noted: (A) saddle patch



Figure 45. Braze Alloys Dots Applied to the ID Tube Crosses of the 2.7K Nickel Tubular Thrust Chamber Segment. Braze alloys noted: (A) 77Ag-27Zn, (B) 72Ag-28Cu, (C) 80Au-20Cu, and (D) 82Au-18Ni

120
CONFIDENTIAL

CONFIDENTIAL

Electron Beam Welding of Manifold Closures

(C) Both the nickel and copper tube segments incorporated a thrust chamber manifold closure. The opening, sealed by the manifold closure, provided access for braze alloy placement. The type 347 stainless steel closure was rectangular, approximately 1 inch wide by 3 inches long, with a 1/2-inch-deep joint.

(U) The closures were electron beam welded in place after essentially all brazing was complete. The high-voltage equipment was employed in view of "line-of-sight" alignment which was required because of the recessed configuration of the closure joint. Because the four-sided plug dictated that four straight-line welds be made, "masks" were used for weld start and stop points. "Masks" are blocks of the same metal as the part and serve to "lift" the beam from the joint at predetermined locations. The welding of all closures was successful.

Bonding of Backup Structure to Tubes

(C) Procedures were developed for the nonstructural bonding of the backup structure to the Nickel 200 and OFHC copper tube bundles of 2.5K segments. The materials used included glass mat, a standard epoxy resin, and a room temperature curing amine catalyst.

CONFIDENTIAL

(U) After masking of approximate bolt holes, flow passages, etc., a fiber-glass mat was cut to proper size using a card board template shaped to dimensions of the contoured backup. Proper mat thickness was developed during dry fitup operations. A trial assembly was made to determine the quantity of resin required per side. The glass mat, as determined above, was placed against the tube bundle and impregnated using a measured quantity of uncatalyzed epoxy (Epon 828) resin. The backup structure was positioned to the tube bundle and a quantity of resin required to fill all gaps between the backup and thrust chamber assembly was determined. After determining the quantity of material to be used, uncatalyzed resin and mat were removed from all surfaces using methyl ethyl ketone. All surfaces were dried with gaseous nitrogen and a lint-free cloth.

(U) After determining the required quantities for the final assembly, the mat was positioned on the tube contours. The required quantity of resin, as previously determined, was catalyzed using 8 percent by weight tetra-ethyl triamine. The glass mat was then impregnated with catalyzed resin. An additional 25 grams of excess resin were added to ensure an overfill. Contoured backup plates were assembled to the tube bundle with proper attachments. Excess resin was removed and the structure was cured for a minimum of 12 hours at a minimum temperature of 68 F before putting any appreciable stress on the adhesive joint.

(U) All masking tape and other devices used to prevent the resin from getting into surrounding areas was removed after cure of adhesive. Final machining operations required after adhesive bonding were not to be followed by vapor degreasing. Only flushing or wiping with cold solvent were approved as postbonding cleaning methods.

(C) Extensive tube damage was experienced on the nickel-tube segment during hot-firing tests. Unique repair methods were applied successfully to this segment which was subsequently hot fired without incident.

CONFIDENTIAL

OFHC COPPER TUBE-WALL FABRICATION

OFHC Copper Tube Processing

(U) Raw Material. Small diameter, thin wall, seamless OFHC copper tubing (0.169-inch OD by 0.020-inch wall) procured to the requirements of ASTM B75 Type OF was used in the fabrication of the tubes. In addition to the requirements specified in the ASTM specification, an additional test to check for the presence of oxygen in the material was conducted on a sample quantity of raw tubing. This test consisted of heating the tube material in a dry hydrogen atmosphere to 1825 F \pm 25 F and holding at temperature for 4 hours. Upon completion of this thermal treatment, longitudinal and cross section metallographic samples were prepared and the microstructure checked for gassing and open grain boundaries which are indicative of hydrogen embrittlement caused by excessive amounts of oxygen in the raw material.

(U) All raw tubing subjected to this test passed. Metallurgical evaluation of specimens of tubing during routine receiving inspection failed to disclose any injurious defects. The raw tubing was purchased from a vendor.

(U) Tapering. Prior to tapering, the raw material was annealed at 725 F \pm 10 F in a dry nitrogen atmosphere utilizing Rocketdyne's continuous tube annealing furnace.

(U) The tapering of the tubes was carried out entirely with Rocketdyne's manufacturing facility utilizing equipment developed by Rocketdyne specifically for tapering aerospike configuration tubes.

(U) Prior to beginning production runs, development tests were conducted which determined the optimum tapering parameters to be used on production tubes. Metallurgical evaluations were conducted on all sample tubes to determine wall thickness and defect level.

(U) The tapered tubes were produced in one tapering pass. "In-process" metallurgical evaluations were performed on random samples after tapering and again after annealing. Table 13 shows results of these evaluations along with those conducted during tapering parameter development.

(U) Preanneal cleaning operations were performed on raw tubing prior to pretaper anneal and subsequent to tapering utilizing ultrasonic cleaning techniques. The tubes were immersed in a bath of Freon TF and cleaned at a frequency of 20 to 25 kilocycles for 5 minutes at room temperature.

(U) Preforming and Final Forming. Subsequent to the final annealing of the straight tapered tubes, preforming was accomplished. Final forming was accomplished in a contoured cavity book die. Because no internal pressure was exerted on the tube to assist in forming to final configuration, it was found necessary to anneal the preformed tubes. This anneal was accomplished at an outside supplier utilizing a batch-type furnace. The tubes were annealed in the horizontal position in dry hydrogen atmosphere at $925\text{ F} \pm 25\text{ F}$ for 5 minutes. Preanneal cleaning was accomplished using the ultrasonic cleaning technique previously described.

(U) After book die forming, a random sample of finish formed tubes were subjected to metallurgical evaluation. During this evaluation, it was revealed that a number of tubes had a flat spot on the hot-gas crown at the throat region. This flat spot was a result of die mismatch which was corrected early in the forming operation; however, a number of tubes were rejected because of the condition. Figure 46 shows the location of metallographic specimens removed from the finish formed tubes. Figure 47 shows the results of evaluations conducted on finish formed tubes and depicts conditions observed. In addition to the routine metallographic examination conducted on sample tubes after tapering, tapering and annealing, and final forming, the thermal treatment test described previously was also conducted on a section of each tube submitted for metallurgical evaluation. This test was accomplished to increase the assurance that all tube material was OFHC copper. None of the tubes tested in this manner showed any evidence of hydrogen embrittlement.

(C) TABLE 13
 RESULTS OF METALLURGICAL EVALUATIONS CONDUCTED
 ON TAPERED OFHC COPPER TUBES (RL000060X)

Specification No.	Lot Designation	Wall Thickness, inch						Metallographic Observations
		0.0129 OD		0.005 OD		0.019 to 0.021 Required		
		Maximum	Minimum	Maximum	Minimum	Maximum	Minimum	
1	Parameter Development	0.0209	0.0204	0.0204	0.0190	0.0204	0.0190	Taper tear ID, 0.005-inch OD, 0.0009 inch deep
2	Parameter Development	0.0213	0.0199	0.0199	0.0185	0.0194	0.0185	Taper tear ID, 0.005-inch OD, 0.0011 inch deep
3	Parameter Development	0.0199	0.0190	0.0204	0.0190	0.0204	0.0190	No defects
4	Parameter Development	0.0209	0.0204	0.0190	0.0180	0.0190	0.0180	No defects
A	Production	0.0199	0.0199	0.0199	0.0194	0.0199	0.0194	OD laps 0.005-inch OD, 0.00047 inch deep
B	Production	0.0208	0.0203	0.0199	0.0180	0.0199	0.0180	No defects
C	Production	0.0208	0.0203	0.0199	0.0194	0.0199	0.0194	OD laps 0.005-inch OD, 0.00064 inch deep

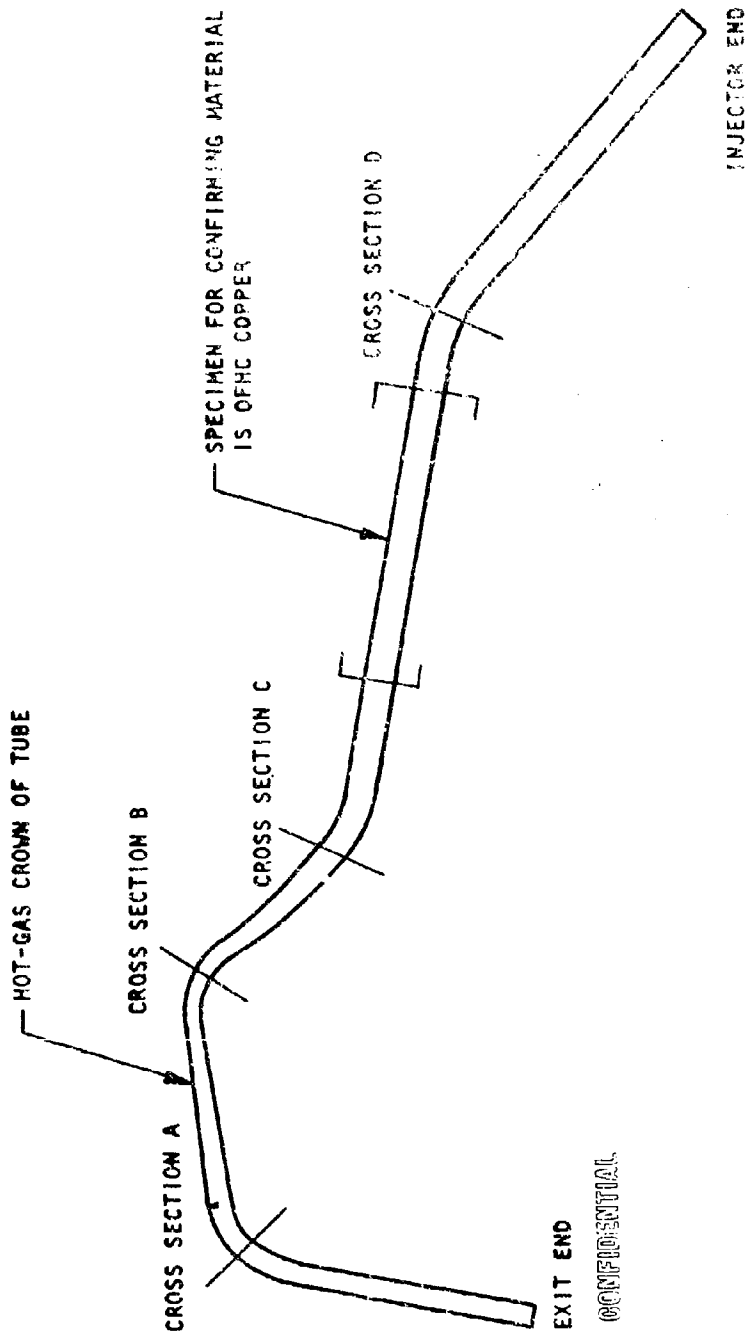


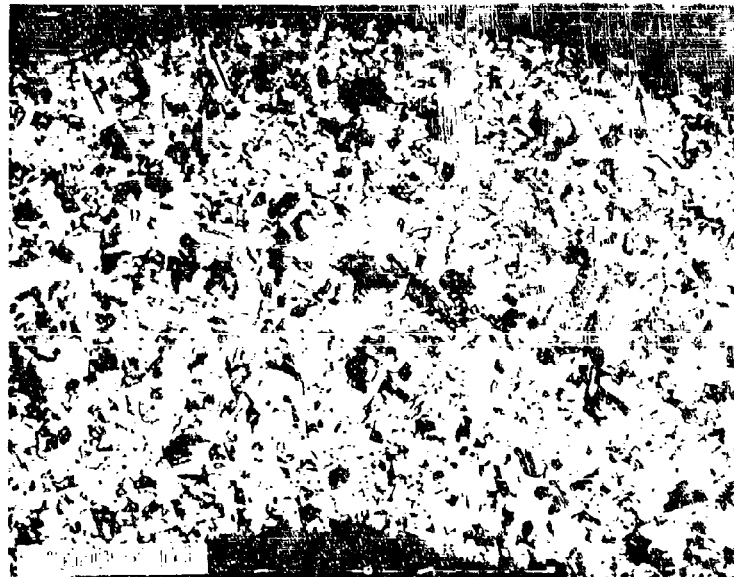
Figure 46. Location of Metallographic Specimens Removed From OFHC Copper Tubes (ALC00060X)



a. Photomicrograph of cross section configuration at cross section B (Fig. 46)
 H - hot-gas crown, specimen etched with Anaconda reagent
 Mag: 25X



b. Photomicrograph of cross section configuration at cross section D (Fig. 46).
 Note concavity in side walls and thickening of wall 180 degrees from hot-gas crown (H). Specimen etched with Anaconda reagent. Mag. 25X



c. Photomicrograph of hot-gas crown at cross section B showing OD surface laps (arrows). Specimen etched with Anaconda reagent. Mag: 150X

Figure 47. Typical Conditions Observed on Book Die Formed OFHC Copper Tubes for 2.5K Segment

CONFIDENTIAL

(H) After final forming, all tubes were subjected to fluorescent penetrant inspection (21-2) before being cleaned and shipped to the assembly white room for stacking.

Assembly and Braze Fabrication

(C) Assembly and brazing of the copper tubular segment was accomplished in accordance with procedures utilized on the nickel segments. Because the copper tubes were also trimmed too short, the same corrective action was performed on the copper segment as was performed on the nickel segment brazed. After the first furnace braze cycle, a 10 psi helium leak check revealed that the segment was not leak tight. The assembly was re-allayed integrating pressure test data and previous repair data obtained from the furnace cycles of the 2.5K nickel tubular segment.

(E) After the second furnace braze cycle, a 10-psi helium leak check revealed the existence of only four leaks; three of these being tube-to-tube leaks and the fourth leak being of the tube-to-manifold variety. During the second furnace braze cycle, a 1/2-inch-square copper strain gage pad, 0.020 inch in thickness, was brazed to the OD side of the copper tube stack aft of the throat support beam. The three tube-to-tube leaks in the combustion zone were sealed by stylus silver plating. The tube-to-manifold leak on the outside of the chamber segment was repaired with SN60 (QQ-S-571) solder. Water flow testing of each copper contour tube revealed that none were plugged with braze alloy or other foreign material.

CONFIDENTIAL

CONFIDENTIAL

FABRICATION OF 20K SEGMENTS

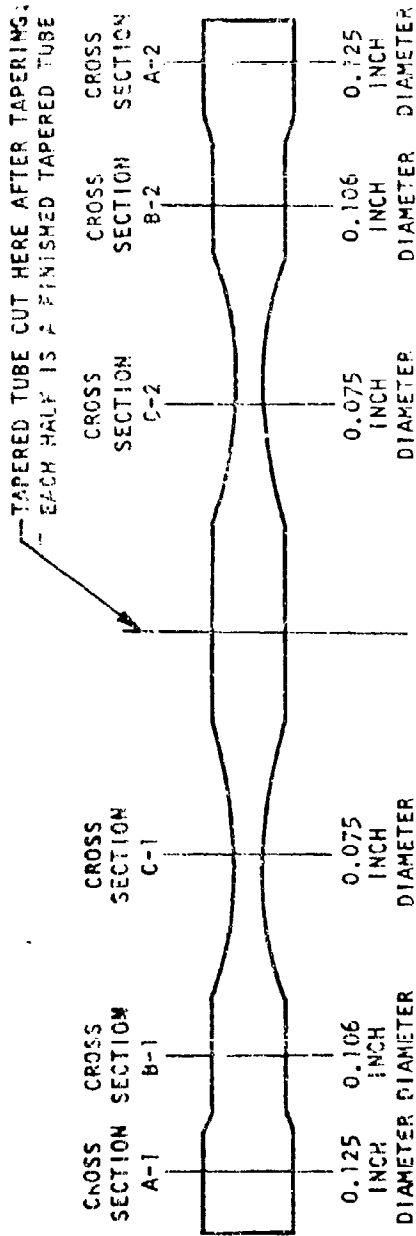
(C) NICKEL 200 TUBE-WALL FABRICATION

(C) Nickel 200 Tube Processing

(C) Raw Material. The raw tubing purchased for use in the fabrication of the Nickel 200, 20K-segment coolant tubes was processed from a vendor. Routine metallurgical evaluation conducted as part of the receiving inspection performed on the raw stock revealed that the wall thickness was slightly higher than the maximum allowable for a 0.014-inch nominal wall. The actual wall thickness of the tubing evaluated ranged from 0.0151 inch minimum to 0.0156 inch maximum. The maximum allowable wall thickness by specification requirement for 0.014-inch wall is 0.0154 inch. No injurious defects were observed and no evidence of intergranular attack was found.

(U) Tapering. Before the development of tapering parameters was started, all materials which were to be used during fabrication and which would contact the tubing were checked for compatibility with Nickel 200. The materials, screened and periodically tested for compatibility, which were used to fabricate the 2.5K Nickel 200 segment tubes were again used. However, to ensure that new lots of material were of the same compatibility level, testing was conducted prior to use. The equipment and basic techniques used in the tapering of 2.5K tubes were utilized in the fabrication of the 20K tubes.

(C) Considerable development work was necessary because the engineering requirement for wall thickness on the 20K tubes was more stringent than those for the 2.5K tubes. The task of developing tapering parameters to achieve final wall thickness profile (Fig. ⁴⁸51) was compounded by the fact that the raw tube-wall thickness was above the 0.014-inch nominal value



CONFIDENTIAL

WALL THICKNESS PROFILE	
CROSS SECTION A - STARTING STOCK	WALL THICKNESS, INCH - 0.0151-0.0156
CROSS SECTION B - 0.156 INCH DIAMETER	WALL THICKNESS, INCH - 0.0125-0.0155
CROSS SECTION C - 0.075 INCH DIAMETER	WALL THICKNESS, INCH - 0.0110-0.0130

Figure 48. Wall Thickness Profile of Tapered RL000109X Nickel 900 Tube. Metallographic Specimens Removed from Tubes During Parameter Development (RL000109X) at Location Shown.

CONFIDENTIAL

by at least 0.001 inch. The successful tapering technique of making two tubes from one blank and thus cutting manufacturing time to a minimum was also employed in the tapering of the 20K tubes.

(U) Tapering parameter development tubes were metallurgically evaluated and found to be of excellent quality. The experience gained during the tapering of the 2.5K tubes helped immeasurably in advancing the state of the art within Rocketdyne. Figure 48 shows tube configuration and location of metallographic specimens. Table 14 shows the results of this evaluation. Once the tapering parameters were established and the results of metallurgical evaluations showed that the process was repeatable in producing high-quality tubes, the planning for production runs was instituted. Table 15 shows the in-process control plan that was instituted. Figure 49 shows the location of specimens removed during metallurgical evaluation.

(U) Results obtained during the tapering of the tubes were excellent. The results produced proved without doubt that with the proper measuring devices and engineering analysis of the tapering process, parameters can be established that will produce tubes of exceptional quality and consistency.

(U) The tapered tubes were made in one pass using improved tapering dies. The use of these dies reduced the incidence of outside-diameter surface laps to an insignificant quantity. The depth of laps that were observed was 0.0005 inch. Table 16 shows the results obtained during in-process control metallurgical evaluations.

(c) TABLE 14

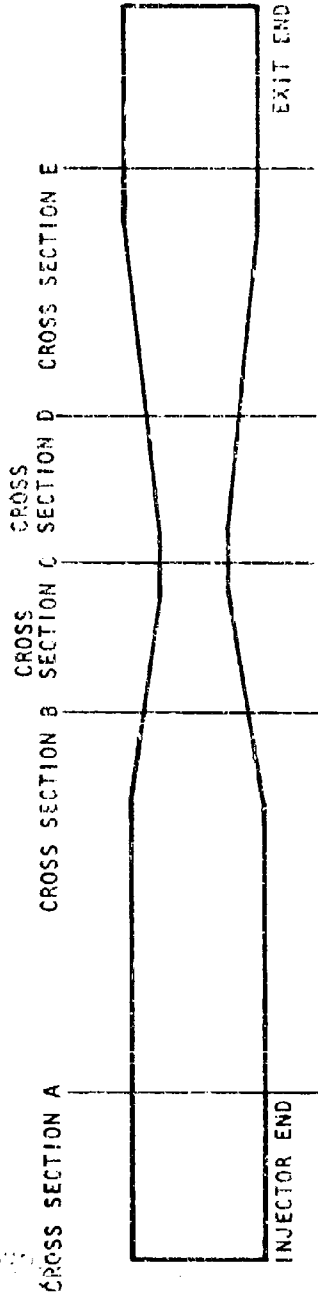
RESULTS OF METALLURGICAL EVALUATIONS CONDUCTED ON TAPERED NICKEL 200 TUBES (R1000109X) DURING TAPERING PARAMETER DEVELOPMENT (Figure 49 Shows Location of Cross-Section Specimen-)

Specimen No.	Tube No.	Wall Thickness, inches		Metallographic Observation
		Required	Results Maximum Minimum	
A-1	1	0.0155 maximum 0.0125 minimum	0.0151 0.0159	No intergranular attack
B-1	1	0.0155 maximum 0.0125 minimum	0.0146 0.0120	No intergranular attack
C-1	1	0.0150 maximum 0.0110 minimum	0.0114 0.0115	No intergranular attack
C-2	1	0.0150 maximum 0.0110 minimum	0.0116 0.0111	No intergranular attack; 0.00047-inch-deep outside diameter lap
B-2	1	0.0155 maximum 0.0125 minimum	0.0157 0.0127	No intergranular attack
A-2	1	0.0155 maximum 0.0125 minimum	0.0151 0.0148	No intergranular attack
A-1	2	0.0155 maximum 0.0125 minimum	0.0142 0.0141	No intergranular attack
B-1	2	0.0155 maximum 0.0125 minimum	0.0147 0.0146	No intergranular attack
C-1	2	0.0150 maximum 0.0110 minimum	0.0117 0.0115	No intergranular attack
C-2	2	0.0150 maximum 0.0110 minimum	0.0116 0.0116	No intergranular attack
B-2	2	0.0155 maximum 0.0125 minimum	0.0151 0.0146	No intergranular attack
A-2	2	0.0155 maximum 0.0125 minimum	0.0142 0.0137	No intergranular attack

(c) TABLE 15

METALLURGICAL SAMPLE REQUIREMENTS ESTABLISHED FOR IN-PROCESS CONTROL AND FINAL ACCEPTANCE OF NICKEL 200 TUBES (RL090109X)

Tube Configuration	Sample Plan	Metallurgical Evaluation	Disposition
Straight Tapered Tubes	Random sample of tubes from each manufacturing lot subsequent to tapering (minimum of three tubes per lot will be evaluated)	<ol style="list-style-type: none"> 1. Measure wall thickness four places 90 degrees apart at critical stations 2. Measure and record all inside- and outside-diameter defects 3. Check microstructure for intergranular attack 	Releases tubes to perform operation
Preformed Tubes Prior to Anneal	First lot only; random sample of tubes prior to sending to vendor for anneal	<ol style="list-style-type: none"> 1. Measure wall thickness on hot-gas crown at throat and other critical stations 2. Measure and record all inside- and outside-diameter defects 3. Check microstructure for intergranular attack 	First article evaluation only; approves preforming tubes without post-taper anneal
Preformed Tubes Subsequent to Anneal	First lot and then as requested by Materials and Processes	<ol style="list-style-type: none"> 1. Measure wall thickness on hot-gas crown at throat and other critical stations 2. Measure and record all inside- and outside-diameter defects 3. Check microstructure for intergranular attack 	First article evaluation for approval of annealing and pre-cleaning operations; spot check subsequent to first-lot processes
Finish Formed Tubes	Random sample of tubes from each manufacturing lot subsequent to hook die forming	<ol style="list-style-type: none"> 1. Measure wall thickness on hot-gas crown at throat and other critical stations 2. Measure and record all inside- and outside-diameter defects 3. Check microstructure for intergranular attack 	Final metallurgical acceptance of tubes



CONFIDENTIAL

WALL THICKNESS PROFILE

- CROSS SECTION A AND CROSS SECTION E - 0.0125-0.0155 INCH
- CROSS SECTION B AND CROSS SECTION D - 0.0125-0.0155 INCH
- CROSS SECTION C - 0.0110-0.0130 INCH

Figure 49. Location of Metallographic Specimens Removed From Straight Tapered Tubes During "In-Process" Control Evaluations (RLM09109X)

(C) TABLE 16
 RESULTS OF METALLURGICAL EVALUATIONS PERFORMED ON STRAIGHT TAPERED
 NICKEL 200 TUBES DURING IN-PROCESS CONTROL CHECKS OF PRODUCTION RUNS
 (FIGURE 52 SHOWS LOCATIONS OF METALLOGRAPHIC SPECIMENS)

Manufacturing Lot No.	Specimen No.	Wall Thickness*, inches												Metallographic Observations
		Cross Section A		Cross Section B		Cross Section C		Cross Section D		Cross Section E		Metallographic Observations		
		Maximum	Minimum	Maximum	Minimum	Maximum	Minimum	Maximum	Minimum	Maximum	Minimum			
9759	1	0.0146	0.0142	0.0157	0.012	0.0118	0.0113	0.0136	0.0133	0.0146	0.0137	No intergranular attack		
	2	---	---	---	---	0.0123	0.0116	0.0136	0.0133	0.0146	0.0137	No intergranular attack		
	3	---	---	---	---	0.0118	0.0118	---	---	0.0151	0.0142	No intergranular attack		
	4	---	---	---	---	0.0127	0.0116	---	---	---	---	No intergranular attack; 0.0002-inch-deep outside- diameter lap on cross section C		
9708	1	0.0151	0.0145	0.0142	0.0157	0.0123	0.0118	---	---	---	---	No intergranular attack		
	2	---	---	---	---	0.0123	0.0118	---	---	0.0151	0.0147	No intergranular attack; 0.0003-inch-deep outside- diameter lap on cross section C		
8062	3	---	---	---	---	0.0123	0.0114	0.0132	0.0127	---	---	No intergranular attack		
	4	0.0151	0.0157	---	---	0.0127	0.0118	---	---	---	---	No intergranular attack		
	5	---	---	---	---	0.0125	0.0118	---	---	---	---	No intergranular attack		
	6	---	---	---	---	0.0123	0.0118	---	---	---	---	No intergranular attack		
	1	0.0148	0.0157	0.0142	0.0152	0.0123	0.0120	0.0128	0.0125	0.0147	0.0142	No intergranular attack		
	2	---	---	---	---	0.0123	0.0118	---	---	---	---	No intergranular attack		
3	---	---	---	---	0.0123	0.0117	---	---	---	---	No intergranular attack			
4	---	---	---	---	0.0127	0.0123	---	---	---	---	No intergranular attack			

*Cross-section requirements are 0.0125 inch minimum, 0.0155 inch maximum for A, B, D and E;
 0.0110 inch minimum, 0.0140 inch maximum for C.

(C) Preforming. Previous experience during the processing of the 2.5k segment, Nickel 200 tubes showed that a considerable number of hours were expended in the cleaning and handling of tubes between the tapering operation and preforming. To reduce production flow time and the chances of tapered-tube damage resulting from handling, development work was accomplished to determine whether or not "as-tapered" tubes could be preformed without the benefit of a posttaper annealing operation. Tooling was developed which made the preforming possible. Metallurgical evaluations conducted on preformed tubes during the development phase of the program showed that the tubes met engineering drawing requirements. Table 17 shows results of this evaluation.

(C) Final Forming. Subsequent to preforming the as-tapered tubes, cleaning was accomplished in preparation for annealing by vapor degreasing and ultrasonic cleaning using the same techniques that were used to clean the 2.5F segment tubes. The post-preform anneal was done in a manner identical with that performed on the 2.5K segment Nickel 200 tubes utilizing the same heat-treating source. Metallurgical evaluation conducted on a number of tubes after anneal and prior to final forming showed them to be free from intergranular attack. Table 18 shows the results of the evaluation performed.

(C) The final forming operation was done utilizing a contour cavity block die. Some concavity existed in the side walls of the tubes in the combustion zone and exit ends of many of the tubes. This condition was experienced during final forming of the 2.5K Nickel 200 tubes also. The depth of the concave depressions was 0.0008 to 0.001 inch.

(E) Results of metallurgical evaluations performed on finished formed tubes are tabulated in Table 19. Figure 50 shows the areas on the formed tube from where metallographic specimens were removed for evaluation, and Figure 51 shows typical observed conditions.

(C) TABLE 17

METALLURGICAL EVALUATION CONDUCTED ON HEAT-TREATED NICKEL 200
TUBES (RL000109X) FROM MANUFACTURING LOT 8062
(FIGURE 50 SHOWS LOCATIONS OF SPECIMENS)

Tube No.	Cross Section Thickness (Required* and Results), inches					Metallographic Observations
	A	B	C	D	E	
1	0.0137	0.0118	0.0142	0.0146	0.0142	No intergranular attack
2	0.0132	0.0113	0.0132	0.0142	0.0137	No intergranular attack
3	0.0142	0.0123	0.0142	0.0146	0.0137	No intergranular attack
4	0.0142	0.0120	0.0137	0.0146	0.0142	No intergranular attack

*Requirements are as follows:

- Column A 0.0125 to 0.0155
- B 0.0110 to 0.0130
- C 0.0125 to 0.0155
- D 0.0125 to 0.0155
- E 0.0125 to 0.0155

(c) TABLE 18


RESULTS OF METALLURGICAL EVALUATION CONDUCTED ON PREFORMED NICKEL 200 TUBES
(SL666109X) SUBSEQUENT TO ANNEALING

Manufacturing Lot No.	Tube No.	Hot-Gas Crown Wall Thickness (Required* and Results), inches					Metallographic Observations
		A	B	C	D	E	
8061 (Initial Lot)	1	0.0135	0.0113	0.0132	0.0137	0.0132	No intergranular attack
	2	0.0137	0.0115	0.0132	0.0144	0.0135	
	3	0.0142	0.0120	0.0132	0.0146	0.0146	
	4	0.0132	0.0113	0.0132	0.0137	0.0132	
8062	1	0.0142	0.0118	0.0142	0.0135	0.0132	
	2	0.0133	0.0114	0.0137	0.0142	0.0135	
	3	0.0140	0.0118	0.0137	0.0142	0.0137	
	4	0.0142	0.0113	0.0137	0.0142	0.0137	
	5	0.0130	0.0110	0.0128	0.0137	0.0133	

*Requirements are as follows:

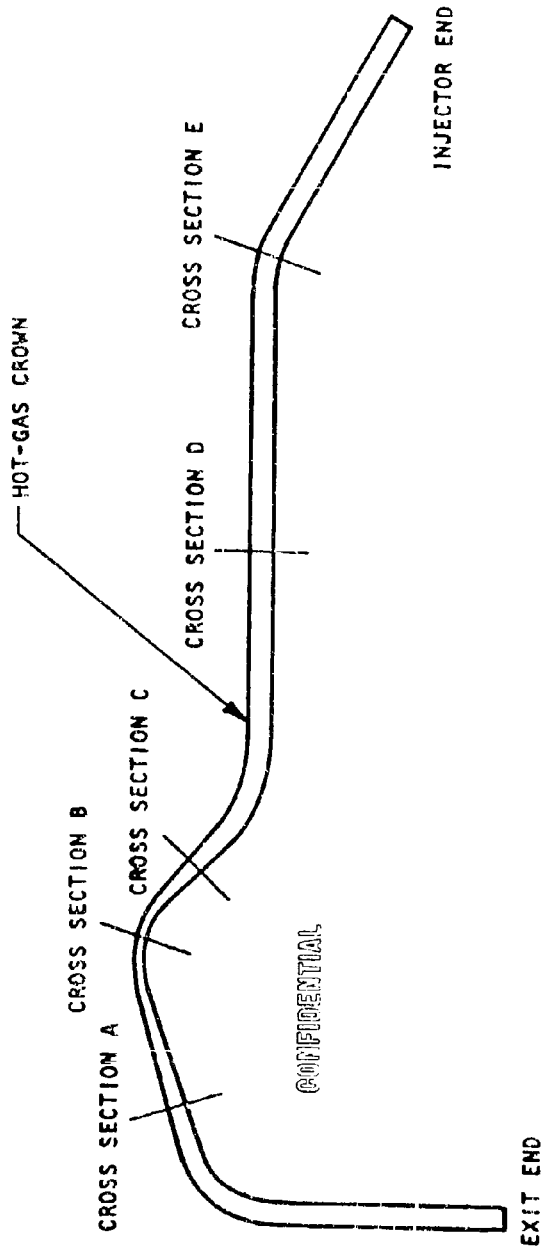
- Column A 0.0125 to 0.0155
- B 0.0110 to 0.0130
- C 0.0125 to 0.0155
- D 0.0125 to 0.0155
- E 0.0125 to 0.0155

(C) TABLE 19
 RESULTS OF METALLURGICAL EVALUATION CONDUCTED ON
 FINISH FORMED NICKEL 200 TUBES (RL000109X)

Manufacturing Lot No.	Tube No.	Hot-Gas Crown Wall Thickness for Cross Section (Required* and Results), inches					Metallurgical Observations
		A	B	C	D	E	
9758	1	0.0137	0.0119	0.0137	0.0142	0.0133	No intergranular attack 
9798	1	0.0137	0.0114	0.0133	0.0142	0.0132	
8061	1	0.0137	0.0118	0.0137	0.0142	0.0132	
8062	1	0.0137	0.0113	0.0137	0.0142	0.0135	
8063	1	0.0137	0.0118	0.0137	0.0137	0.0132	

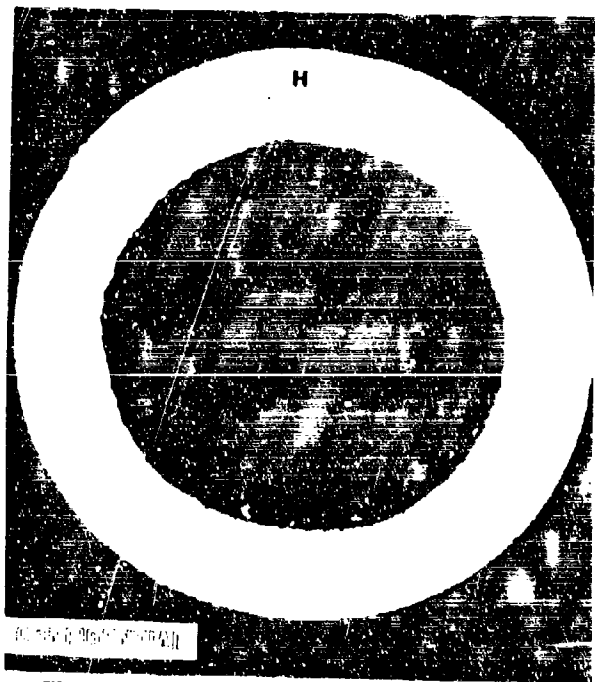
*Requirements are as follows:

- Column A 0.0125 to 0.0155
- B 0.0110 to 0.0130
- C 0.0125 to 0.0155
- D 0.0125 to 0.0155
- E 0.0125 to 0.0155

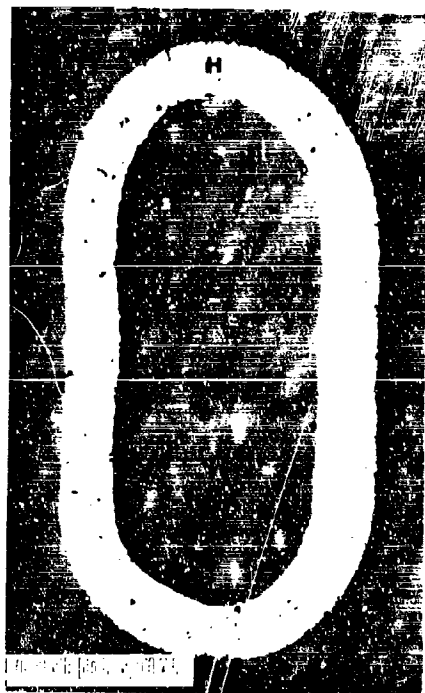


NOTE: LONGITUDINAL SPECIMENS WERE ALSO REMOVED FROM TUBES BETWEEN THE ENDS AND CROSS SECTION A AND CROSS SECTION E AND BETWEEN ALL OTHER CROSS SECTION LOCATIONS TO CHECK FOR EVIDENCE OF INTERGRANULAR ATTACK.

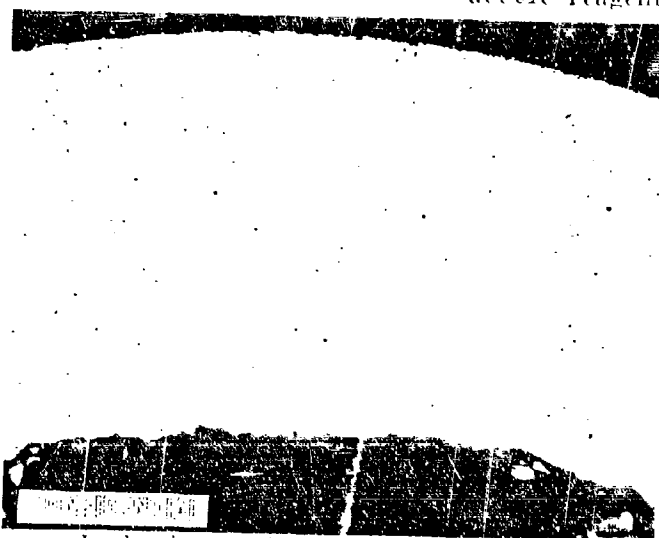
Figure 50. Location of Metallographic Specimens Removed From Preformed and Finish Formed Tubes (RL000199X)



a. Photomicrograph showing cross-section configuration at throat (cross section B, Fig. 50). H = hot-gas crown specimen etched with 50-50 nitric-acetic reagent.



b. Photomicrograph showing cross-section configuration in combustion zone (cross section D, Fig. 50). Note slight concavity on left-side wall. H = hot-gas crown. Specimen etched with 50-50 nitric-acetic reagent.



c. Photomicrograph showing typical microstructure and surface conditions observed on all Nickel 200 tubes metallurgically evaluated.

Figure 51. Typical Conditions Observed on Book-Die-Formed, Nickel 200, 20K Segment Tubes

CONFIDENTIAL

(C) Fluorescent-penetrant inspection was performed on all finished formed tubes using penetrant solutions, emulsifiers, and developer which were compatible with Nickel 200 material.

(U) Final cleaning of the tubes prior to shipping to the assembly white room was done by vapor-degreasing including flushing of the inside diameter with hot trichloroethelene followed by an ultrasonic cleaning at 20 to 25Kc for 5 minutes at room temperature in a bath of Freon TF.

Baffle Seat Assembly and Brazing

(C) Furnace brazing of the subject assembly was accomplished with a 50Au-25Pd-25Ni braze alloy at a brazing temperature of 2070 ±10 F. Selection of this brazing alloy was based upon the need for a material that would not remelt during subsequent brazing of the Inconel 718-Nickel 200 baffle seats into the tube-wall assemblies. The furnace braze tooling concept selected for use on the baffle seat was originally utilized in furnace brazing advanced-design thrust chamber segment hardware. This tooling was designed to apply a uniformly distributed deadweight load of approximately 3 psi on the baffle seat components during the brazing cycle.

(U) Discrepancies in the furnace braze tooling were partially responsible for rejection of the first two units brazed. A dimensional error in the body locating surface on the fixture base resulted in misalignment of tube-to-body and tube-to-closure plate braze joints, which contributed to leakage in these joints. The excessive height of the baffle seat bolt hole locator fixture pin prevented the fixture weight from fully contacting the surface of the closure plate, which contributed to leakage in the braze joint between the closure plate and body. In addition, the fixturing of tubes at the exit end of the assembly proved to be inadequate, and allowed lateral misalignment of tubes during brazing.

(U) The brazing fixture was reworked to correct the dimensional discrepancies noted and to provide better access for alloying the tube-to-body

142
CONFIDENTIAL

joints shown in Fig. 52. Provision was also made on the fixture for applying a constant 5-psi loading on the tubes at the exit end of the assembly in an attempt to maintain lateral tube alignment. Details of the brazing fabrication of the 12 assemblies required for the program are presented in Table 20.

(U) The first two units brazed were used subsequent to rejection for evaluation methods for repair of post-furnace braze leakage, exit end tube misalignment, and tube deformation. Tests were conducted to determine if localized repair of leakage could be accomplished utilizing the plasma arc and tungsten/inert gas processes with 50Au-25Pd-25Ni braze alloy. The large mass difference between the nickel tubes and Inconel 718 body components was found to be a significant restriction upon the ability to achieve satisfactory repairs without subjecting the tubes to damage from overheating. As a result, refurnace brazing was selected as the method for repairing braze joint leakage.

(U) Cold straightening was applied successfully to the correction of exit end tube misalignment. The use of a hydraulic press and suitable tooling resulted in satisfactory realignment of tubes with no effect on tube flow characteristics or tube-to-tube braze joints.

(U) A freeze-expansion forming technique was developed to repair deformed tubes on finished baffle seat assemblies (Fig. 53). Water was placed inside the deformed tube and frozen by immersing the assembly in liquid nitrogen. Expansion of the water upon freezing produced sufficient force to expand the tube and remove the concavity. A final forming operation was used to correct the overexpansion of the tube and restore the original configuration.

End Plate Assembly and Brazing

(U) The four OFHC copper-type 347 stainless-steel end plate assemblies required for the 20K program were furnace brazed with 60Cu-35Au-3Ni braze

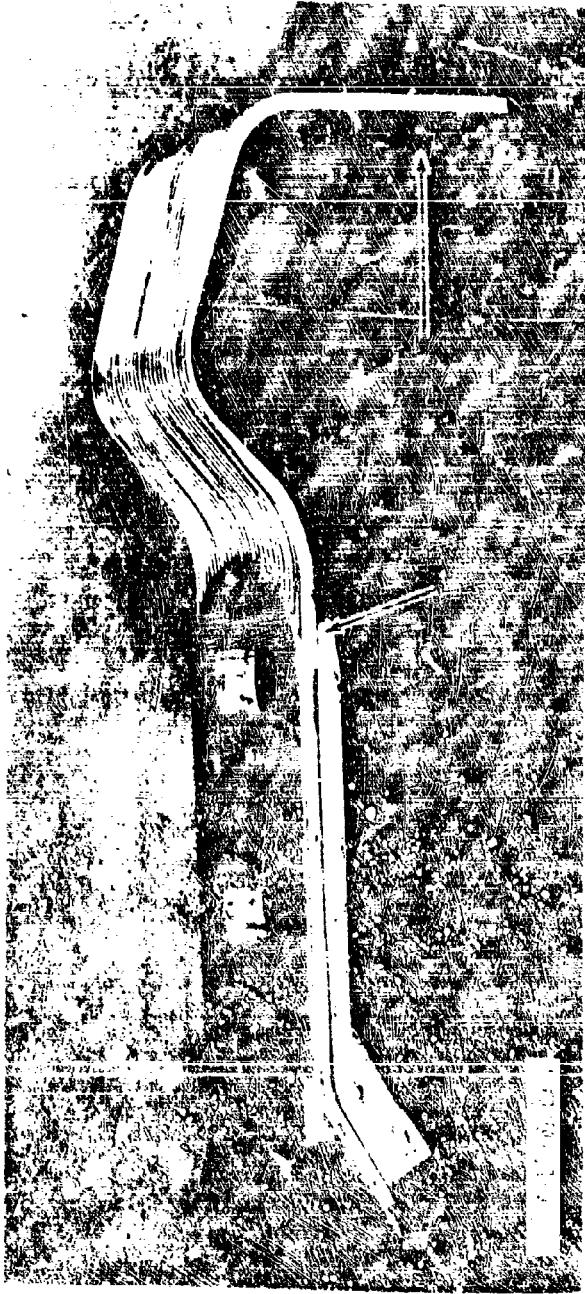


Figure 52. Baffle Seat Assembly RL000113X After Furnace Brazing and Final Machining.
(Areas indicated by arrows: (A) areas where tube misalignment was a problem on initial units; (B) tube-to-body braze joints where fixture was modified for improved braze alloy placement.)

TABLE 20
 BAPPLE SEAT ASSEMBLY (RL000108X) FABRICATION HISTORY

Unit No.	Number of Furnace Braze Cycles	Post-Furnace Braze Repairs	Remarks
1	1	Special furnace cycles for re-alignment of tubes at exit end (not successful)	Unit rejected for braze joint leakage, tube misalignment at exit end and tube end damage at injector end; unit used to evaluate cold forming of tubes for realignment.
2	1	None	Unit rejected for excess braze alloy buildup on tube crowns and side walls of outer tubes and for exit end tube misalignment.
3	2	None	Three leaks repaired in second furnace cycle, unit assembled in RL000108X assembly, unit No. 1
4	2	None	Two leaks repaired in second furnace cycle; unit assembled in RL000108X assembly, unit No. 1
5	1	Torch repaired two tubes damaged in handling using 50/50-25/75 Ni braze alloy	Unit status; backup hardware.
6	2	Straightened tubes deformed during machining, using freeze-expansion technique	One leak repaired in second furnace cycle; unit status; backup hardware
7	1	Straightened tubes deformed during machining, using freeze-expansion technique	Unit assembled in RL000108X assembly, unit No. 2.
8	2	Mechanically straightened tubes deformed during machining	No leakage following first furnace cycle. Second furnace cycle used for braze buildup of tube crowns damaged in machining. Unit assembled in RL000108X assembly, unit No. 3.
9	1	None	Unit assembled in RL000108X assembly, unit No. 2
10	1	None	Unit assembled in RL000108X assembly, unit No. 7
11	1	None	Unit assembled in RL000108X assembly, unit No. 4
12	1	None	Unit assembled in RL000108X assembly, unit No. 4

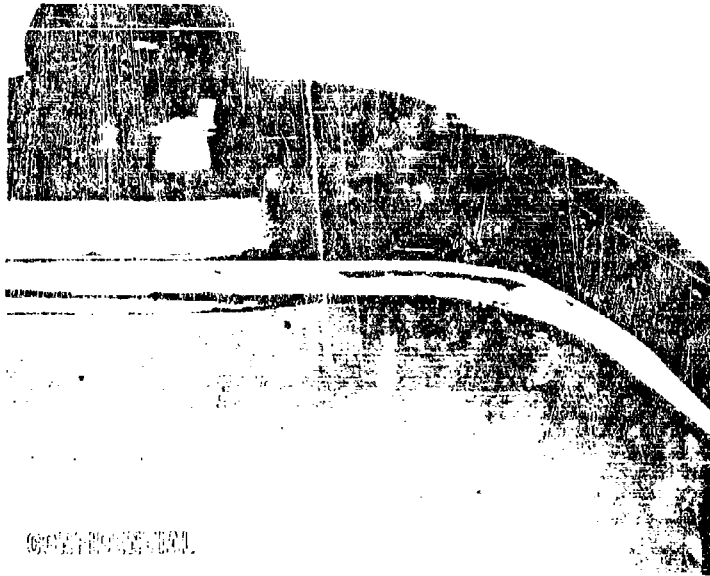


Figure 53. View of Brazed Baffle Seat Assembly
Showing Outer Tube Deformation

plate are shown in Fig. 55 and machining for braze alloy preplacing is indicated. Hydrostatic pressure testing of all four units after first-cycle brazing showed no leakage. The hot-gas-side surface of the last two units brazed were bulged as a result of inadequate restraint of this surface during pressure testing. The bulged areas were satisfactorily reworked by hand forming to ensure proper fit-up with mating components in the chamber braze assembly.

Tube-Wall Assembly and Brazing

(U) The four required tube-wall assemblies were furnace brazed utilizing the same fixturing concept that was applied to brazing the baffle seat assemblies. Some details of this type of fixturing are shown in Fig. 55. Two furnace brazing cycles were performed on each tube wall in an attempt to obtain a leaktight structure prior to brazing the tube walls in the final chamber segment assembly. The first cycle required brazing with 90Ag-10Pd alloy at 1975 ± 10 F, followed by a second cycle at 1805 ± 10 F using 82Au-18Ni alloy. A 0.010-inch-thick nickel backup sheet included in the original tube-wall design was to have been furnace brazed to the injector and exit end manifolds and to the cold-wall side of tubes in the tube-wall assemblies. Difficulties were encountered in forming this sheet to the tube-wall outer-mold line with sufficient accuracy to meet required tube-to-backup sheet braze joint tolerances. As a result, the backup sheet was eliminated from the tube-wall assembly, and appropriate changes in fabrication procedures were established.

(U) The extent of leakage experienced and the repair methods applied following furnace brazing of the tube-wall assemblies is shown in Table 21. A significant decrease in leakage at tube-to-injector end manifold joints resulted from changes in assembly and alloying procedures which were initiated on unit No. 3 tube wall. These included the following:

1. Application of nickel paste filler in addition to the triangular nickel filler wires at tube-to-manifold joints prior to preplacing the first cycle braze alloy paste

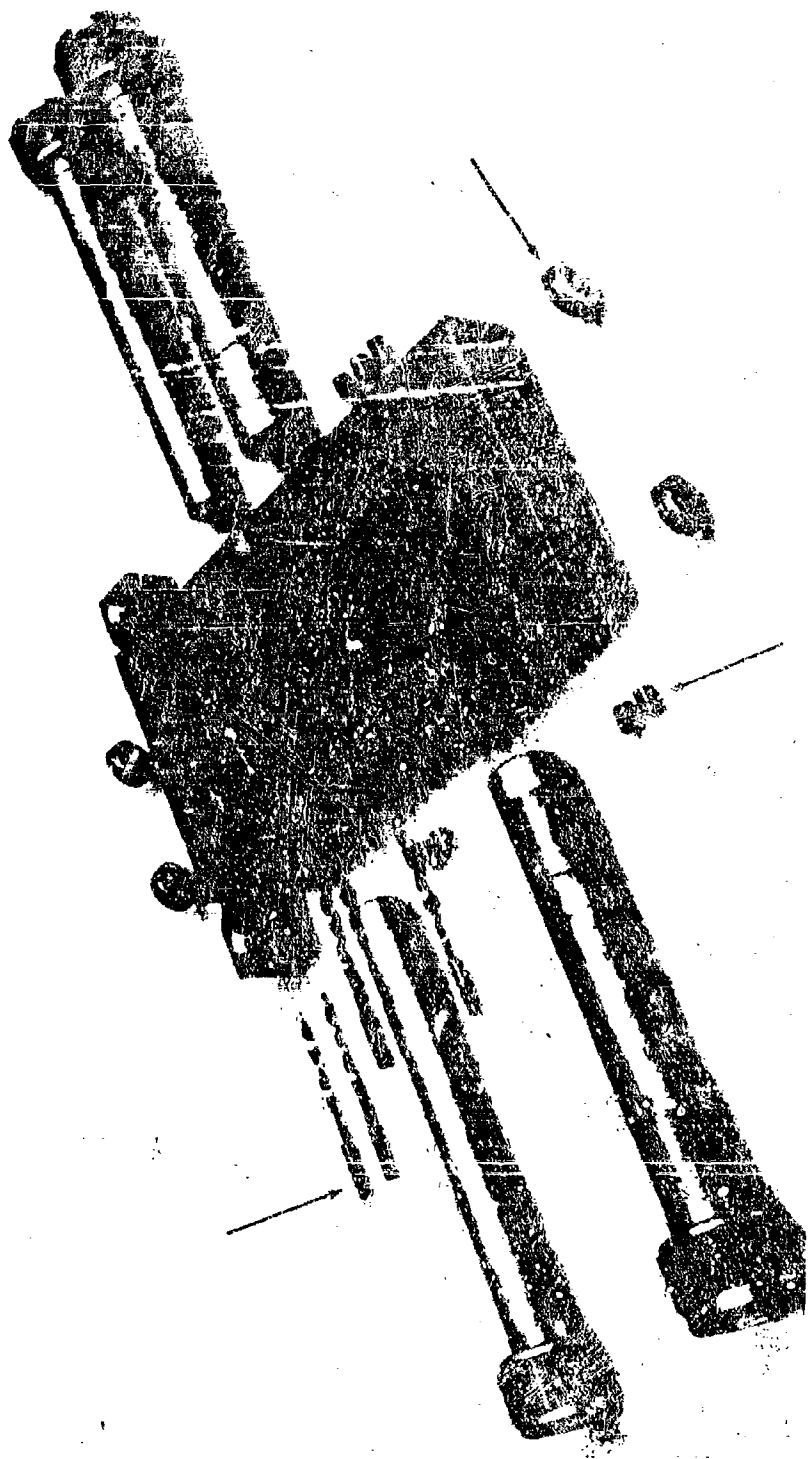


Figure 54. Typical Components of RL00107X End Plate Assembly Before Assembly for Braziag
(Arrows indicate grooves machined in components for preplacing braze alloy wire
preformed rings.)

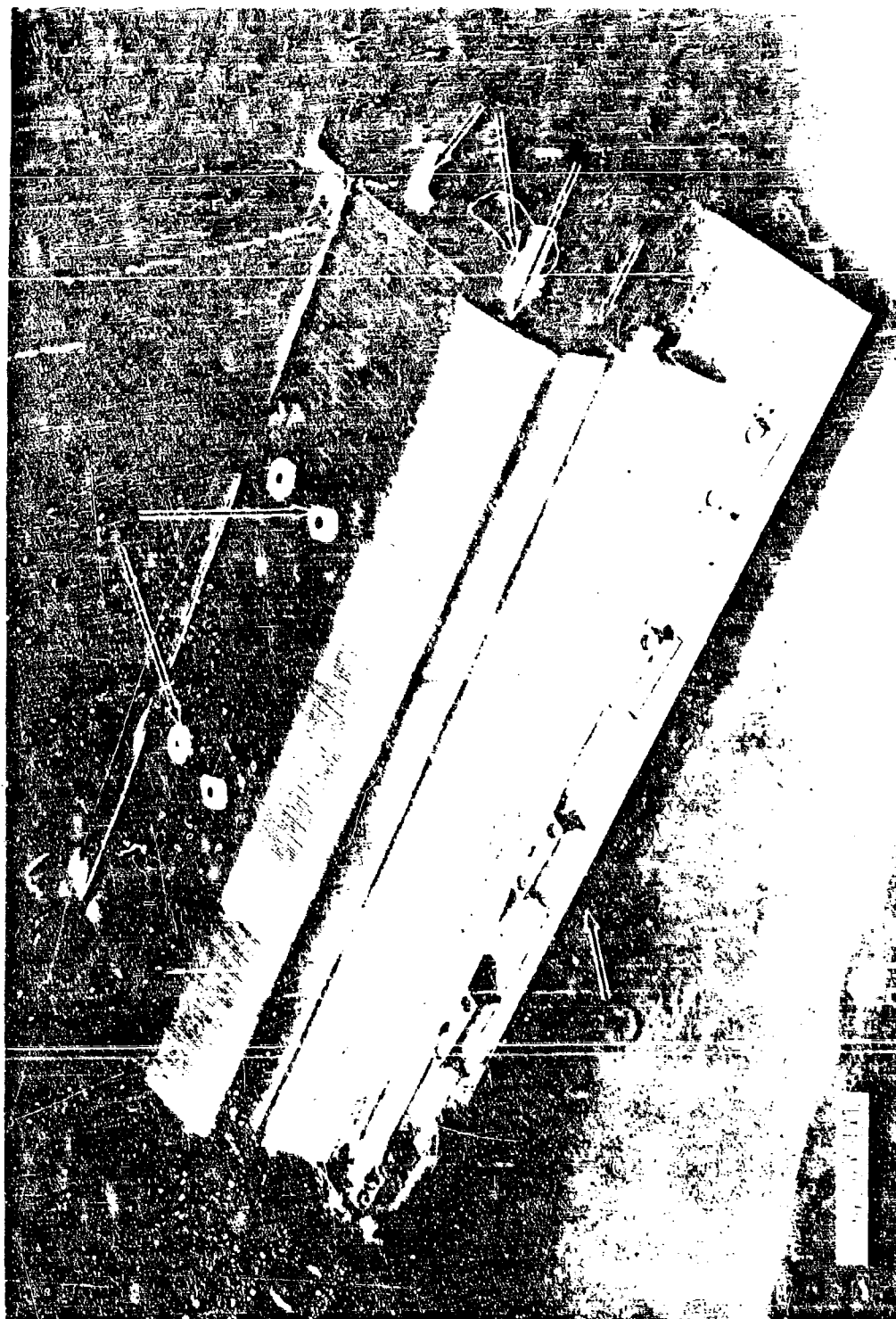


Figure 55. Tube-Wall Assembly Brazing Fixture (Fixture weights and end plates for locating tubes are not shown. Areas indicated by arrows: (A) fixture base plate, (B) fixture contoured plate, (C) fixture end plate retaining pins (end plate removed), (D) ceramic locators pinned to contoured plate for maintaining baffle seat location, (E) Refrasil cloth used to prevent bonding of tubes to fixture.)

TABLE 21

TUBE-WALL ASSEMBLY RL000108X LEAKAGE AND REPAIR HISTORY

Unit No.	Leakage After First Furnace Cycle	Leakage After Second Furnace Cycle	Remarks
1	Several leaks in tube-to-injector end manifold joints at hot-gas side and cold-wall side of tubes; one tube-to-tube leak in throat area at one end of assembly	Seven leaks in tube-to-injector end manifold joints at cold-wall side of tubes	Seven leaks repaired by tungsten/inert gas brazing with RB0170-064 alloy
2	Several leaks in tube-to-injector end manifold joints at cold-wall side of tubes; one hole in tube crown adjacent to injector end manifold at hot-gas side of tubes; gap at outer baffle seat tube and adjacent tube, at both baffle seats, inner compartment side	One tube-to-injector end manifold leak; one tube-to-tube leak at baffle seat	Tube-to-manifold leak repaired by tungsten/inert gas brazing with RB0170-064 alloy. Hole in tube (not repaired in second furnace cycle intentionally) repaired by plasma arc brazing with RB0170-062 alloy; tube-to-tube leak repair made during furnace brazing RL000110X chamber assembly
3	Baffle seat-to-RL000121X manifold joint leak, both baffle seats	None	Tubes plugged at exit manifold end with first-cycle braze alloy; repaired by abrasive blasting
4	Baffle seat-to-RL000121X manifold joint	None	Tubes plugged at exit manifold end with first-cycle braze alloy; repaired by abrasive blasting

CONFIDENTIAL

2. Assembly of tube-wall components on the braze fixture, tack welding of the injector end manifold components, and removal of the assembly from the fixture in preparation for braze alloy preplacement
3. Application of a braze alloy paste fillet at the tube-to-manifold joints and all other braze joints, excluding tube-to-tube type, prior to replacing the assembly on the braze fixture (Fig. 56 and 57).

(U) Prior to these changes, all filler material and braze alloy paste applications were made with the tube wall assembled on the braze fixture, which permitted no access to the tube-to-manifold joint area noted in Fig. 56.

(U) Visual examination of unit No. 1 tube wall following the first furnace brazing operation showed that both outboard tubes had been displaced toward the brazing fixture in the throat area, resulting in their lateral misalignment with adjacent tubes. It was concluded that this condition was caused by the inability of Refrasil cloth placed between the tube wall and brazing fixture to follow the growth of the fixture during furnace brazing. This would result in the Refrasil cloth being shorter than the braze fixture and tube wall at or near the brazing temperature, thus eliminating the support of the Refrasil under the outboard tubes and allowing them to move down toward the fixture (Fig. 58). Prior to performing furnace brazing operations on unit No. 2, the brazing fixture was modified as shown in Fig. 59, which eliminated any further occurrence of the problem experienced with unit No. 1 tube wall.

(U) A hole through the crown of one tube was discovered during the pressure testing of unit No. 2 tube wall subsequent to completion of the first furnace brazing cycle. Examination of the hole at magnification revealed no characteristics to indicate what may have created the discontinuity. Laboratory brazing tests were conducted on the lot of braze alloy paste that was used on this unit in an attempt to determine if some contaminant in the paste had caused the discontinuity. Test results were negative.

151
CONFIDENTIAL

This page is Unclassified

CONFIDENTIAL

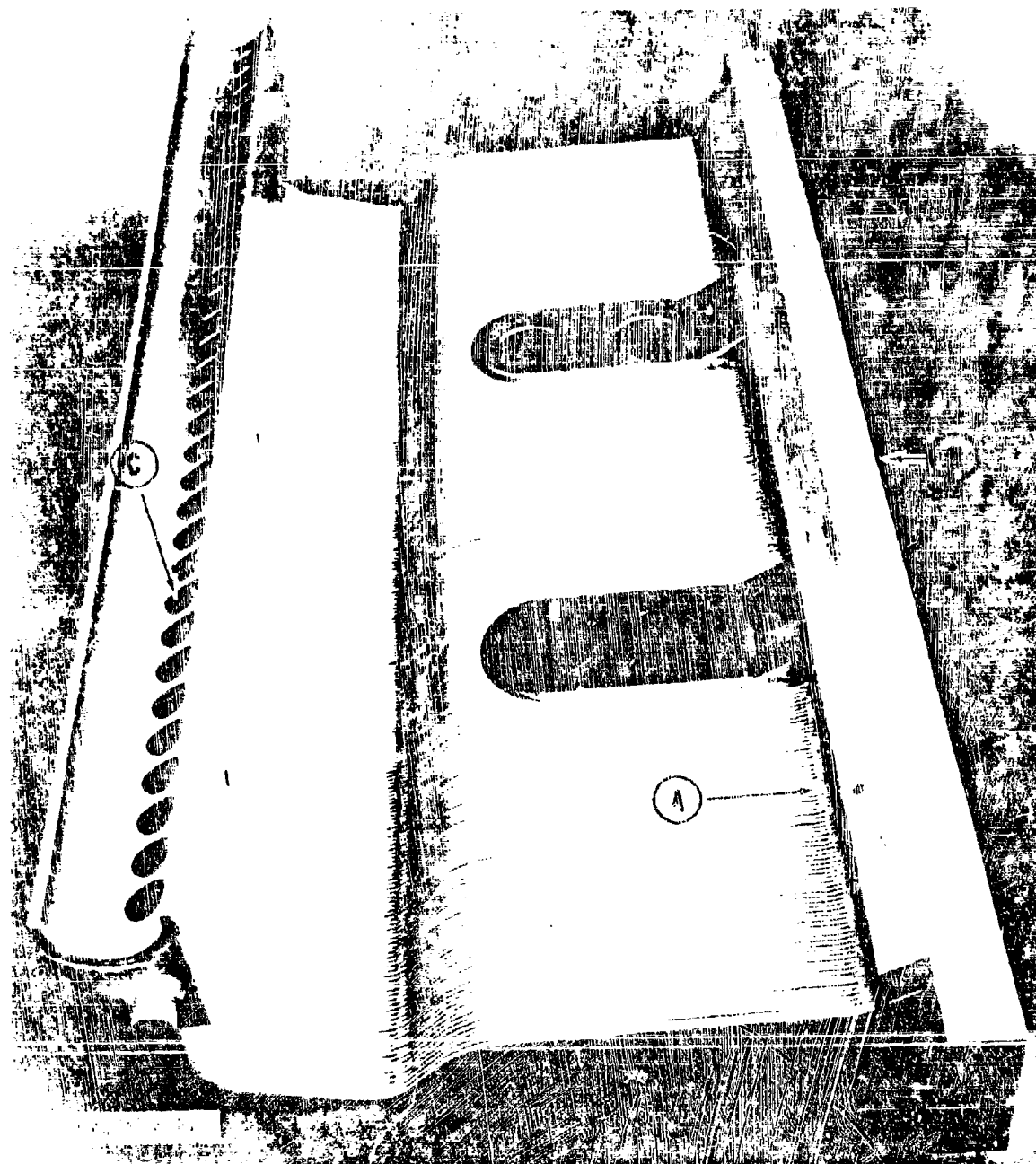


Figure 50. Tube-Wall Assembly RL000108X Following Assembly on the Brazing Fixture Cold Side Up (Areas indicated by arrows: (A) braze alloy paste fillet applied to tube-to-RL000121X manifold joints, commencing with unit No. 2; (B) injector end manifold cavity (not shown in this view) through which internal braze joints were alloyed; (C) ports in exit end manifold through which internal braze joints were alloyed.)

152

CONFIDENTIAL

CONFIDENTIAL

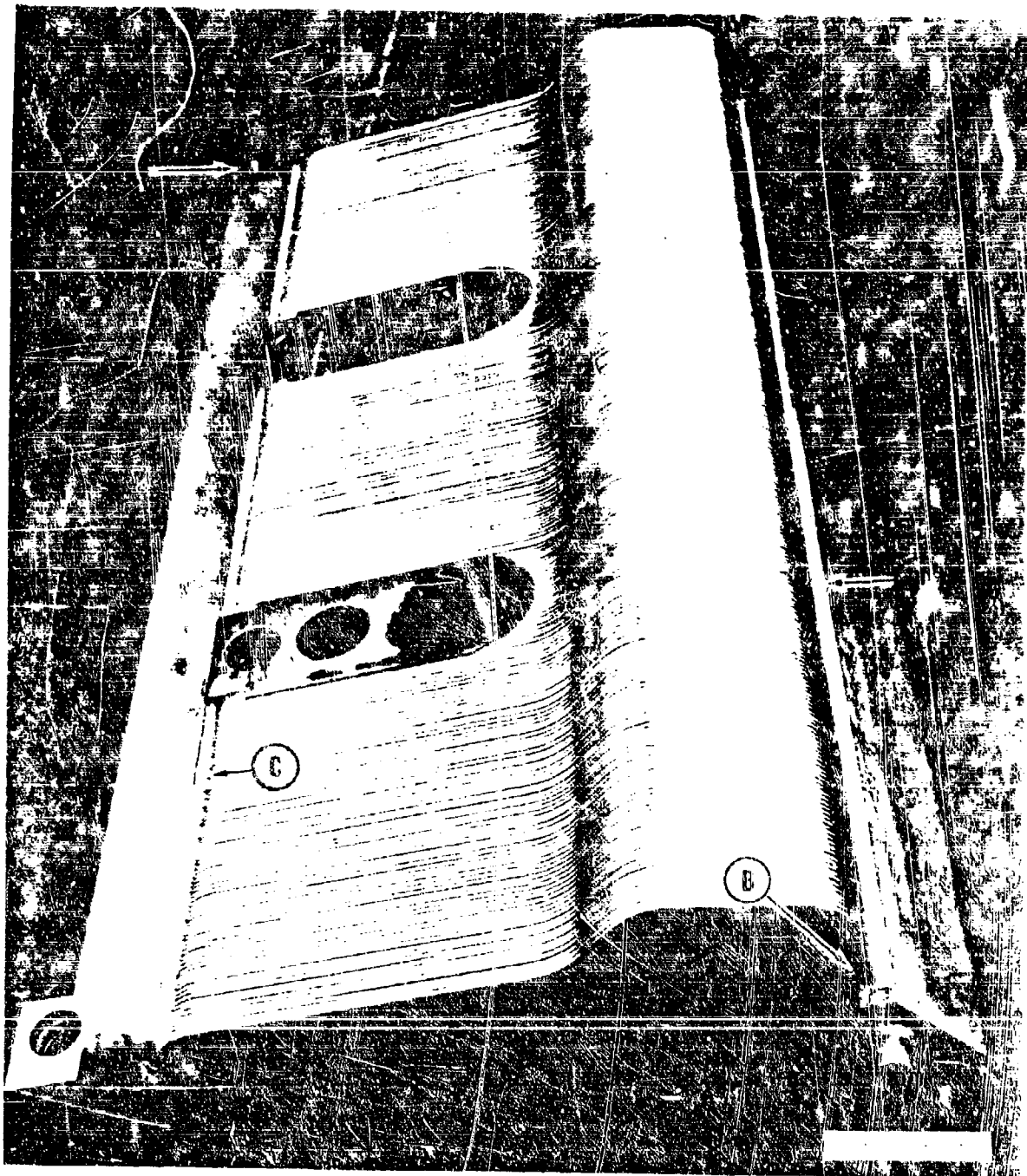


Figure 57. Hot-Gas Side of RL000108X Tube Wall Assembly Shown in Fig. 56 (Areas indicated by arrows: (A) braze alloy paste fillet applied at tube-to-exit end manifold joints, hot-gas side; (B) braze alloy paste fillet applied at tube-to-exit end manifold joints, cold-wall side; (C) braze alloy paste fillet applied at tube-to-RL000120X manifold joints; (D) fusion tack weld between RL000120X and RL000121X manifold for fixturing purposes.) 153

CONFIDENTIAL

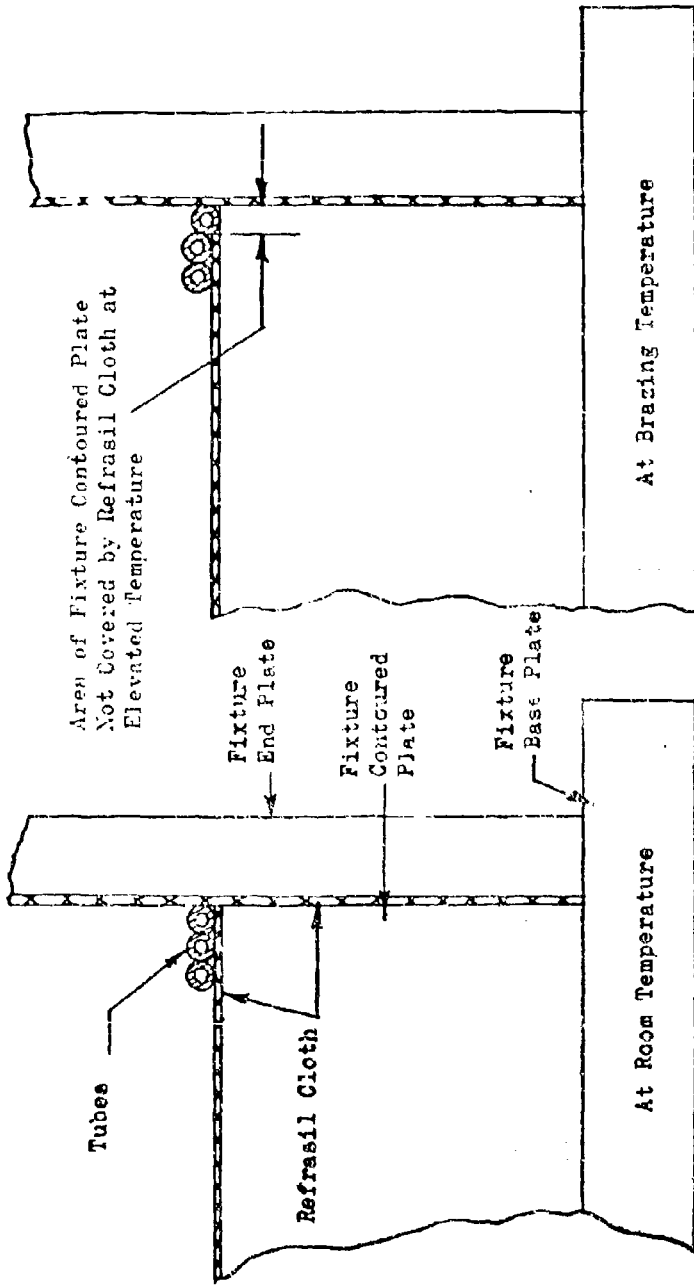


Figure 58. Cross-Sectional Views of Tube Wall and Braze Fixture Taken at Throat Area, Showing Probable Cause of Outboard Tube Lateral Misalignment on Unit No. 1

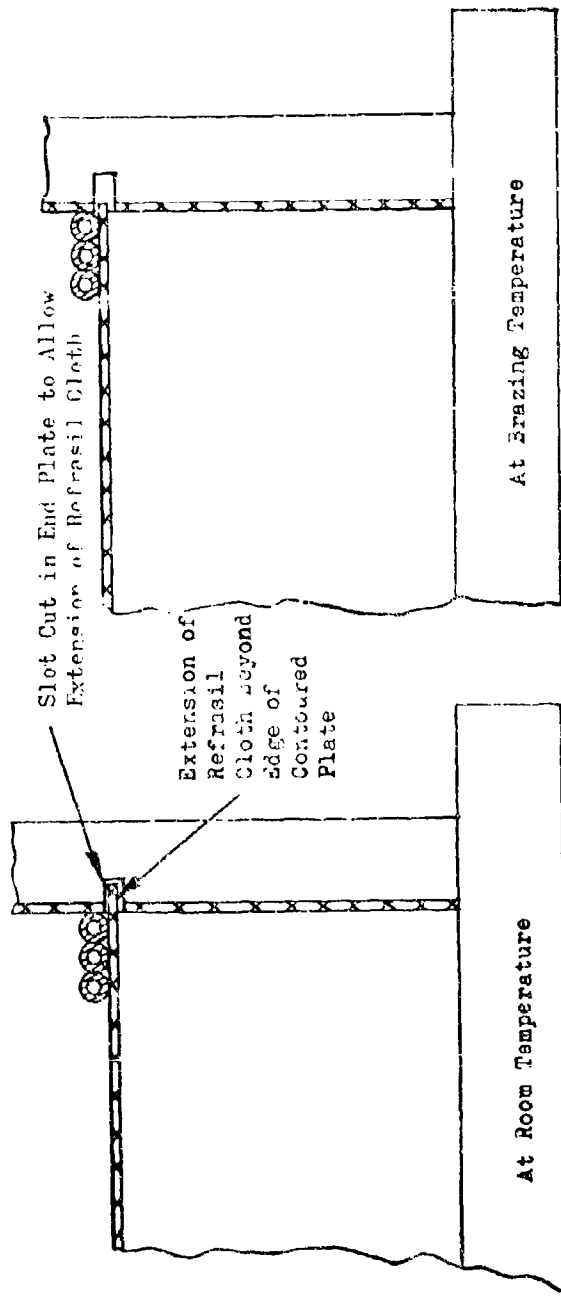


Figure 59. Cross-Sectional Views of Tube Wall and Braze Fixture Taken at Throat Area Showing Fixture Change That Was a Solution to The Outboard Tube Lateral Misalignment Problem

Braze joint leaks that existed in the tube-wall assemblies following second-cycle brazing (Table 21) were manually repaired to ensure maximum integrity of each tube wall prior to assembly and brazing of chamber assemblies. Laboratory tests showed that the 82Au-18Ni braze alloy applied to tube-to-manifold leaks would not be affected by the subsequent chamber assembly furnace brazing cycle. The same braze alloy was not to be used for repairing the hole in the tube on unit No. 2 because of the potential for remelting the alloy during subsequent furnace brazing of the chamber assembly, and therefore, the higher-temperature 90Ag-10Pd alloy was selected for this application. An exception to the procedure for manual repair of leaks following second cycle brazing was established with unit No. 2 tube wall. A tube-to-tube leak adjacent to the baffle seat was repaired as a part of the subsequent chamber assembly furnace brazing operation to avoid possible stress cracking of the Inconel 718 baffle seat components associated with manual brazing.

(U) Plugged tubes were evident on unit No. 3 and 4 following first-cycle brazing. The plugging was located at the exit end of both units, and was a result of the braze alloy flowing into the tube ends or the inadvertent application of braze alloy paste in the tubes during preparations for brazing. The absence of tube plugging on the preceding tube walls indicated possible omission of the required braze stopoff application in the ends of tubes that were plugged on unit No. 3 and 4. This condition was corrected by abrasive blasting the braze alloy plugs from inside the tubes. This operation was accomplished with no evidence of tube damage, and subsequent testing verified acceptable flow characteristics of these tubes.

Thrust Chamber Assembly, Brazing and Repairs

(U) A 50Au-50Cu braze alloy was selected for furnace brazing the thrust chamber assembly based on laboratory evaluation tests conducted in conjunction with the fabrication of 2.5K thrust chamber segment hardware. Braze fixturing consisted of a flat plate with means for locating and fixing one end of the chamber assembly and applying a constant load

CONFIDENTIAL

(approximately 5 psi) normal to the copper end plate at the opposite end of the assembly.

(C) Various braze joint gaps were observed during assembly of the first unit, the locations of which are noted in Table 22. Shims that were inserted at end plate-to-tube wall outer-tube joints moved out of position during the furnace brazing cycle, causing leakage at these joints. Figure 60 shows this assembly following the furnace brazing cycle; shimmed areas are indicated. The gaps that were evident in the shimmed braze joints depicted in Fig. 61 after furnace brazing were attributed to the following factors:

1. The thermal expansion difference between the type 347 stainless-steel manifolds and the Nickel 200 tubes in the tube-wall assemblies caused an increase in the tube-to-end plate braze joint gap during the furnace cycle.
2. Seizure during the furnace cycle of the pins in the mating holes in the end plate (Fig. 60) at the end of the chamber on which a constant fixture load was applied resulted in additional gapping at tube-to-end plate joints. This condition also caused the formation of gaps in the exit end beam-to-end plate joints as shown in Fig. 61.

(U) The tube-to-end plate braze joint gaps observed during the assembly of the first chamber were a result of the tube-wall width being undersize, predominantly in the throat area. This condition was evident to the greatest extent in tube-wall unit No. 2 and 3, which were assembled with one less than the nominal number of tubes. In addition, measurement of the width of tubes assembled in tube-wall unit No. 4 showed the tubes to be approximately 0.0005 inch narrower in the throat area than the balance of the tube length. These two factors and possible restraint imposed on the tubes by the fixture during tube-wall brazing appear to have contributed to the undersize throat condition in the tube walls. Efforts to develop

CONFIDENTIAL

TABLE 22

CHAMBER BRAZE ASSEMBLY RL000110X FURNACE BRAZING HISTORY

Unit No.	Discrepancies Noted During Assembly	Corrective Action	Post-Furnace Braze Visual Results
1	<p>Gaps up to 0.040 inch in RL000107X End Plate-to-RL000107X End Plate-to-RL000108X Tube-Wall Outer Tube Joints (all corners of chamber)</p> <p>Gap in RL000107X End Plate-to-RL000121X Injector End Manifold Joint (one end of chamber)</p> <p>Void in Tube-to-Tube Joint Adjacent to Baffled Seat on RL000108X Tube Wall, Unit No. 2</p>	<p>Gaps reduced to 0.002 inch maximum by shimming</p> <p>Gap reduced to 0.002 inch maximum by shimming</p> <p>Nickel paste filler applied prior to braze alloy preplacement</p> <p>Shimming to reduce gaps; deferred until torch braze operation</p>	<p>Some shims moved out of position; intermittent voids, all four joints; new gaps in RL000119X exit end beam-to-RL000107X end plate joints, One End of Chamber</p> <p>Recessed braze fillets at shim one half of joint length</p> <p>Continuous braze filled in previous void area</p>
2	<p>Gaps Up to 0.070 Inch in RL000107X End Plate-to-RL000108X Tube-Wall Outer Tube Joints (all corners of chamber)</p> <p>Gap in RL000107X End Plate-to-RL000121X injector End Manifold Joint (both ends of chamber)</p>	<p>RL000107X end plates remachined; RL000121X manifold joint forging surface hand reworked; remaining gap reduced to 0.002 inch maximum by shimming</p>	<p>Continuous braze filletting; no evidence of voids</p>

CONFIDENTIAL

This page is Unclassified

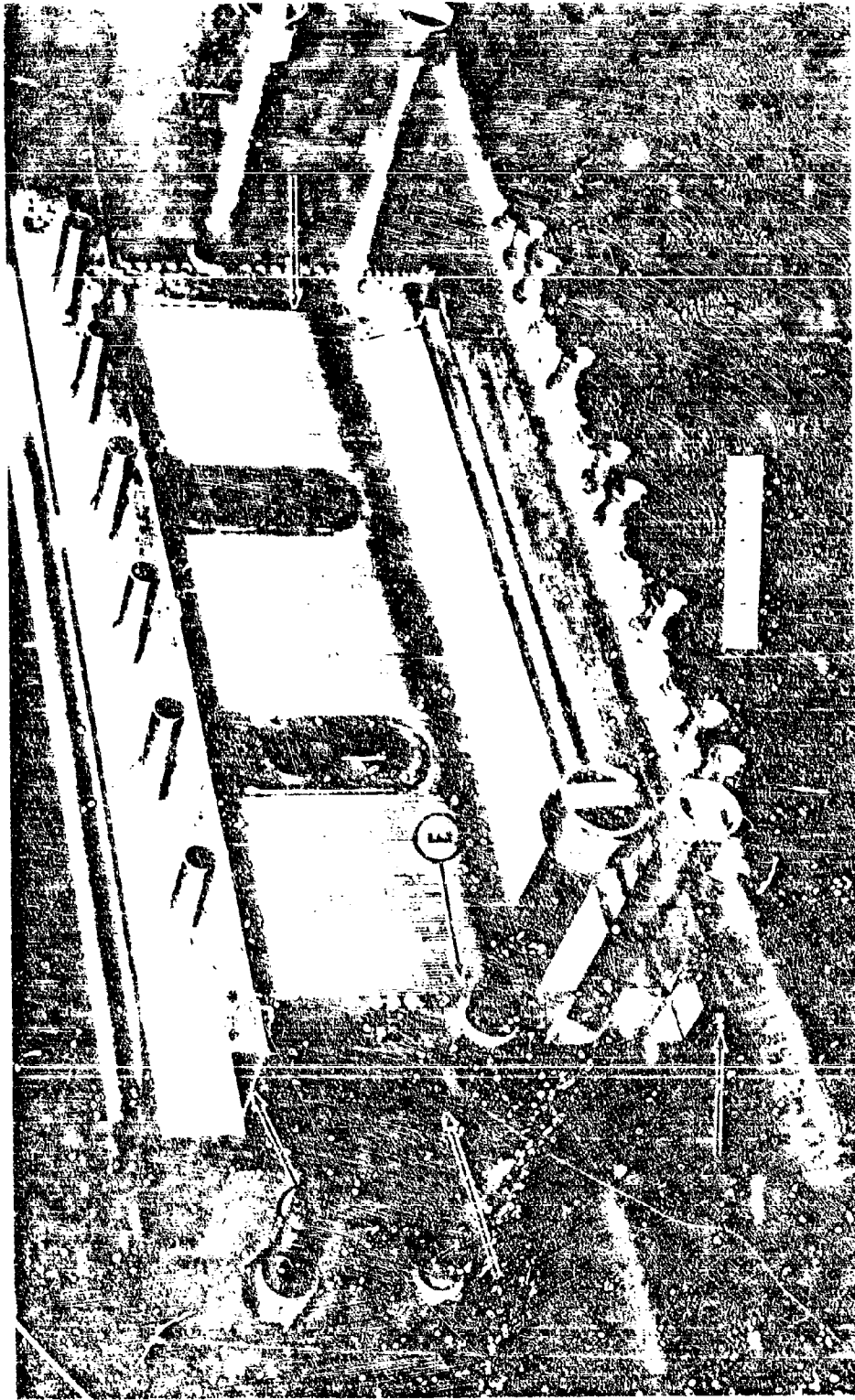


Figure 60. Unit No. 1 RL000110X Chamber Braze Assembly. After Furnace Brazing (Chamber is shown inverted with respect to brazing position. Areas indicated by arrows: (A) constant fixturing load applied to RL000107X end plate and opposite end of chamber held in fixed position during brazing; (B) tube-to-end plate joint shimmed prior to brazing; (C) plate-to-manifold joint shimmed prior to brazing; (D) holes in end plate in which 005-40 pins, not visible, apparently seized during brazing; (E) area of chamber shown in Fig. 61.)

CONFIDENTIAL

two modifications resulted in a significant improvement in the brazing of the second chamber, as indicated by the absence of gaps at the exit end beam-to-end plate joints.

(E) Both chambers exhibited leakage following torch brazing of tube-to-end plate joints which was repaired as described in Table 23. The internal tube-to-injector end manifold leakage (leakage from manifold cavity to vent ports in the manifold) experienced on unit No. 1 was avoided on unit No. 2 by modifying the pressure test procedures applied to the tube-wall assemblies. This permitted detection and correction of leakage in this area prior to assembly and brazing of the chamber.

Electron Beam Welding of Manifold Cover Plates

(U) The design of the 20K thrust chamber incorporated a rectangular plate (304L stainless steel) electron beam welded into a matching recess in the upper opening above the tubes on the thrust chamber body (347 stainless steel). The primary purpose of this cover was to provide a dam to prevent brazing alloy from running into and plugging the thrust chamber tubes during attachment of the upper thrust chamber flange. The only problem encountered was distortion caused by unequal mass on the sides of the joint. The configuration was such that the cover provided firm lateral restraint, causing the smaller outer edge to bow inward. Although this effect was small, less than that which would have occurred with other welding processes, it was still excessive. The bowing was discerned during welding of samples to establish the welding schedule, using low-voltage equipment. By this time the actual parts had been machined beyond the point where extra mass could have been left on to compensate for the undesirable differential.

(U) In an effort to reduce the distortion, the joint thickness was reduced, restraining tooling was applied, and a "back-step" weld pass sequence was employed. Even with these precautions, distortion was considered excessive. A postweld, prebraze, stress-relieving operation was required to bring the parts back into proper dimensional conditions.

160
CONFIDENTIAL
This page is Unclassified

CONFIDENTIAL

TABLE 23
CHAMBER BRAZE ASSEMBLY RL000110X POST-TORCH BRAZE LEAKAGE AND REPAIRS

Unit No.	Location of Leaks	Repair Methods
1	<p>RL000114X Injector Seal Ring to-RL000108X Tube Walls--Both Ends, Outside of Chamber; One End, Inside of Chamber</p> <p>Tube-to-Injector End Manifold--Both Center Compartments, Outside of Chamber.</p> <p>RL000108X Tube Wall Outer Tube-to-RL000107X End Plate-One joint</p> <p>FL000107X End Plate-to-RL000108X Tube Wall Injector End Manifolds--One end of chamber</p> <p>Previous Repair of Hole in Tube on RL000108X Tube Wall, Unit No. 2</p> <p>Tube-to-Injector End Manifold--Internal (Leakage through manifold vent port), two areas</p>	<p>Tungsten/inert gas brazed with RE0170-064 (82Au-18Ni) alloy</p> <p>Tungsten/inert gas brazed with RE0170-064 alloy</p> <p>Styius-type silver plating</p> <p>Tungsten/inert gas brazed with RE0170-064 alloy</p> <p>Torch brazed with RB0170-105 (90Ag-5Pd-4Cu-1Ni) alloy</p> <p>Slot milled in RL000121X manifold, torch brazed leaks with RB0170-089 (50Au-25Ag-22Cu-3Zr) alloy; tungsten/inert gas brazed closure in manifold with RB0170-064 alloy</p>
2	<p>Tube-to-Injector End Manifold--Outside of Chamber</p> <p>RL000114X Injector Seal Ring-to-RL000108X Tube Walls--Both ends, Outside of Chamber.</p> <p>Tube-to-Joint at Baffle Seat--RL00108X Wall, Unit No. 3</p>	<p>Tungsten/inert gas brazed with RE0170-064 alloy</p> <p>Tungsten/inert gas brazed with RB0170-064 alloy</p> <p>Tungsten/inert gas brazed with RB0170-064</p>

161
CONFIDENTIAL
This page is Unclassified

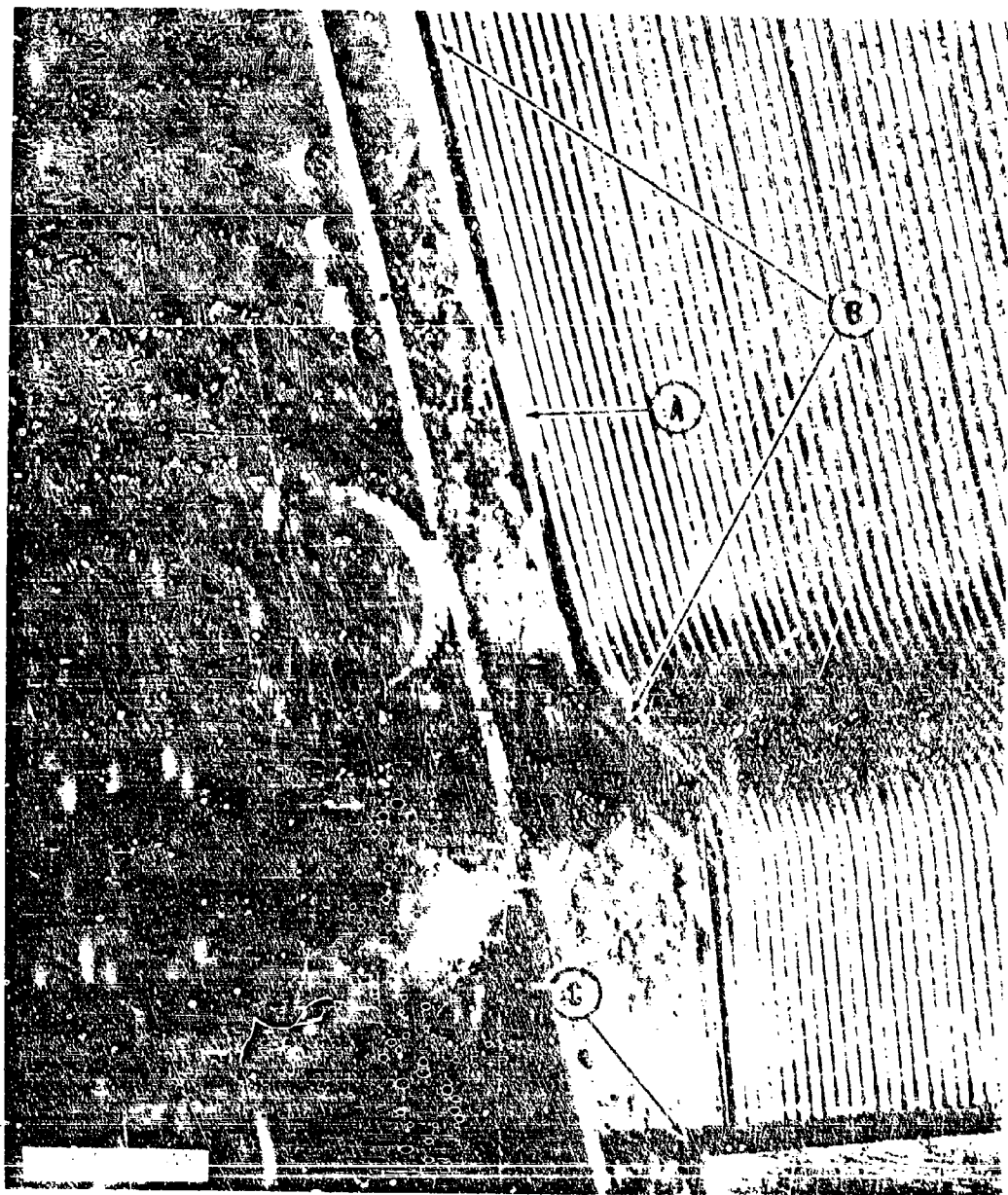


Figure 61. View of Area of Thrust Chamber Indicated by Arrow (E) in Fig. 60, Showing Gap Condition After Furnace Brazing. (Areas indicated by arrows: (A) OFHC copper shim inserted prior to brazing; (B) braze joint voids typical of all four corners of chamber; (C) RL000119X exit end beam-to-end plate joint gap, this end of chamber only.)

CONFIDENTIAL

a suitable method for restoring the required throat dimension on brazed tube walls were not successful. The procedures for assembling unit No. 4 tube wall, which was being assembled when the tube-wall dimensional problem was discovered, were modified as follows:

1. Refrasil cloth was applied to the fixture tube contact surface with the weave of the cloth oriented at a 45-degree angle with respect to the ends of the fixture to achieve greater stretching of the cloth during brazing, thus minimizing tube restraint.
2. After assembly and before furnace brazing, the tubes were mechanically worked in the throat area in an effort to increase tube width. These modifications resulted in a significant improvement in the throat dimension of unit No. 4 tube wall;

(C) A torch-brazing procedure was established and applied to the first chamber for sealing tube-to-end plate braze joint voids. Four Nickel 200 tubes were brazed into the corners of the chamber as a part of this procedure to provide film cooling of the throat area adjacent to the end plates. OFHC copper shims were fitted, where possible, into the tube-to-end plates joints; the joints and adjacent areas were preheated to approximately 400 F using quartz infrared lamp heaters prior to torch brazing. The 45Ag-15Cu-16Zn-24Cd (MIL-S15395, type 7) braze alloy was used for this application, and subsequent visual examination indicated satisfactory braze flow and joint filleting.

(D) The assembly and brazing procedures for the second chamber were subsequently modified as follows:

1. Shimming of tube-to-end plate braze joint gaps was eliminated prior to furnace brazing.
2. The pins on the tube-wall exit end manifolds were covered with Refrasil cloth, and the mating holes in the end plates were bored 0.060 inch oversize to minimize possible pin seizure.
3. The braze fixture constant load applied to one end plate of the assembly was increased from 5 to approximately 10 psi. The latter

CONFIDENTIAL

Bonding of Titanium Backup Structure to Tubes

(C) Evaluation tests were performed to develop the technique necessary for the successful use of adhesives for the structural bonding of titanium structure to the nickel tube bundle of the 20K segments. These test series included the development of optimum:

1. Metal cleaning and surface preparation procedures for nickel and titanium
2. Primer systems for each adhesive-metal combination
3. Adhesives with best combinations of mechanical properties over the operating temperature range
4. Applications and cure systems for use with the best adhesive
5. Preparation of specifications for the use of the most promising adhesive system

As a result of these evaluation tests, the adhesive bonding technique, including determination of the thickness of adhesive required, metal preparation, and priming processes, selection of an adhesive, assembly procedures, and curing schedules, was developed for bonding the titanium backup structure to the 20K toroidal segment tube bundle.

(U) The thickness of the required adhesive was determined using Verifilm 643 strips in a trial assembly. Figure 62 shows strips of Verifilm applied on the tube bundle.

(U) The adhesive used for the bonding operation was an epoxy-nitrile daeron mat-supported film. Figure 63 shows the adhesive film applied to a titanium backup structure. This adhesive was used in conjunction with BR-38 primer. A standard epoxy resin (Epon 828) was used to fill the gap between the backup structure and the end plates. In addition, an RTV silicon rubber (RTV 560) was used as a vibration dampening agent in the cavity between the bottom of the backup structure and the outer portion of the exit manifold.

CONFIDENTIAL

(U) The hot firing tests were successfully completed even though subsequent analysis revealed minimal bond between the adhesive and tubes, and good bond between the adhesive and titanium backup structure.

(C) The lack of bond between the nickel tubes and the adhesive was a primer failure caused by improper cleaning of the nickel tubes. In addition:

1. Backup plates were not completely bottomed during assembly, resulting in reduced pressure on adhesive during cure.
2. The location of backup structure and baffle seats was not positive enough to assure that loads were applied to the adhesive film during through bolt torquing operations.
3. Because of the absence or loss of pressure on the adhesive during cure, there was essentially zero bond strength in these areas.

CONFIDENTIAL

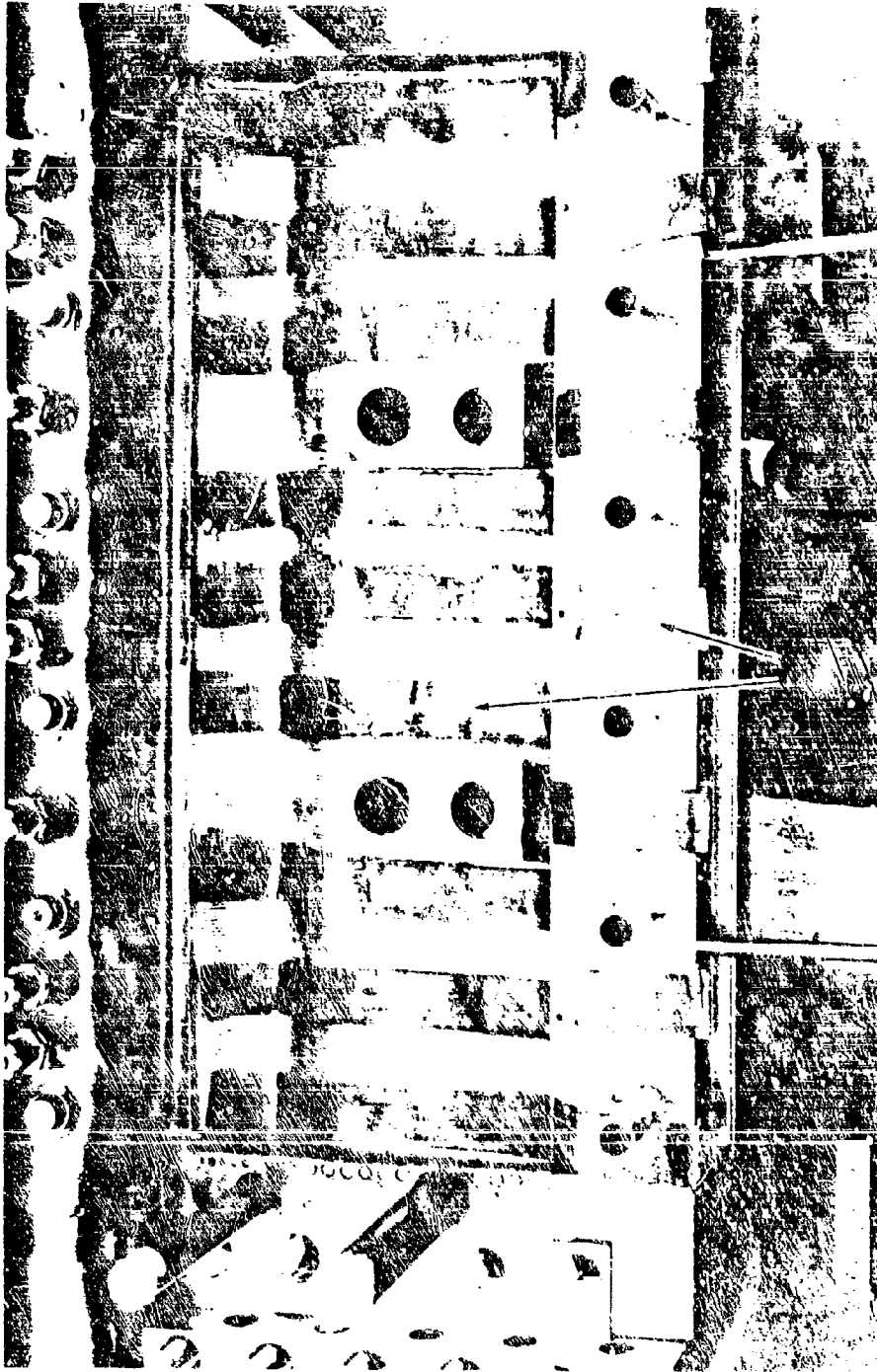


Figure 62. Uncured Strips of VeriFilm 645 Applied to the Tube Bundle Prior to Trial Assembly to Determine Thickness of Required Adhesive (Strips (arrows) were distributed to provide a thorough thickness measurement between surfaces to be bonded.)

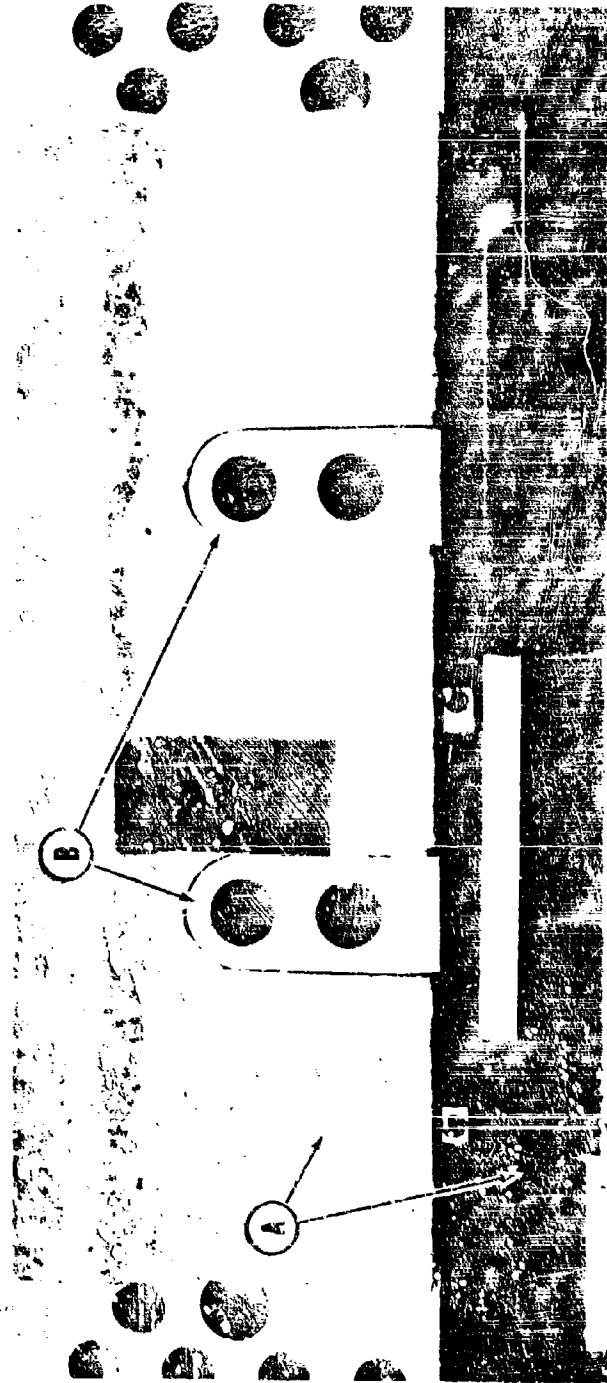


Figure 63. Uncured Adhesive Film Pattern Applied to a Titanium Backup Structure Prior to Assembly to a Tube Bundle (Arrows show: (A) adhesive film and (B) baffle seat cutouts in film.)

CONFIDENTIAL

INJECTOR FABRICATION

Baffle Assembly and Brazing

(U) Four of the subject assemblies were furnace brazed using 62Cu-35Au-3Ni braze alloy. The braze fabrication history for these units is presented in Table 24. The first two assemblies exhibited leakage at the type 347 stainless-steel sleeve-to-OFHC copper shell braze joints (Fig. 64), which was sealed after subjecting these units to a second furnace cycle using the 62Cu-35Au-3Ni braze alloy. Leakage in these joints were attributed to excessive gap in the adjacent copper shell-to-Inconel 718 body joint (Fig. 64), which resulted in braze alloy starvation of the sleeve-to-shell joints. Preparation of the third and fourth units was modified to include the preplacement of 0.002-inch-thick braze alloy sheet in the sleeve-to-shell joints, which eliminated the starvation and subsequent leakage in these joints.

Injector Assembly and Brazing

(U) The braze joint configuration between the injector strips and body on the 20K was similar to the configurations used on the 2.5K and 250K injectors. The body material was type 347 stainless steel and the strip material was OFHC copper. The braze joint area on the strips were gold plated, and nickel plate was applied to the body. The plating thickness on both parts was 0.0002 to 0.0004 inch. The braze alloy used was 62Cu-35Au-3Ni for the first braze cycle and 82Au-18Ni for the second braze cycle with a braze temperature of 1900 to 1920 F and 1800 to 1825 F, respectively. No laboratory tests were conducted before brazing this unit because data had been accumulated from previous experience in brazing the 2.5K injectors.

TABLE 24

BAFFLE ASSEMBLY 81000104X FABRICATION HISTORY

Unit No.	Number of Brazing Cycles	Repair Procedure	Remarks
1	2	Reallayed all shell-to-body and sleeve-to-body joints with 62Cu-35Au-2Ni alloy and rebrazed	No leakage after rebrazing.
-	2	Reallayed all shell-to-body and sleeve-to-body joints with 62Cu-35Au-2Ni alloy and rebrazed	No leakage after rebrazing.
3	1	None required	Commencing with this unit, 0.002-inch braze sheet was placed in sleeve-to-shell joints. No leakage.
4	1	None required	No leakage.

CONFIDENTIAL

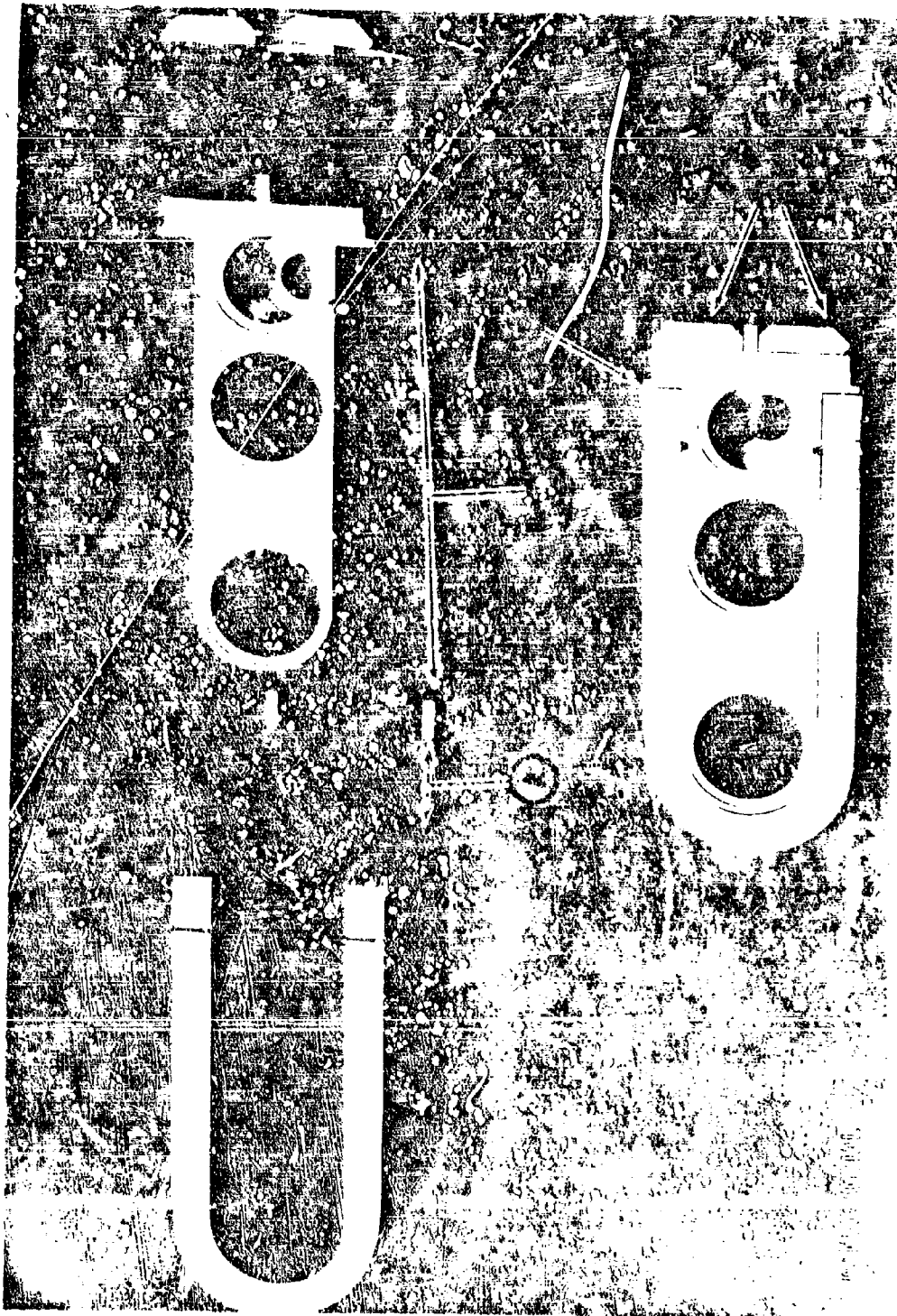


Figure 64. Baffle Assembly RLO00104X Showing Components Before and After Assembly (Areas indicated by arrows: (A) sleeve-to-shell joint where braze alloy sheet was inserted on third and fourth unit; (B) sleeve-to-body joint; (C) shell-to-body joint where excessive gap caused starvation of sleeve-to-shell joints on first and second unit; (D) coolant circuit closures fusion welded to body after brazing.)

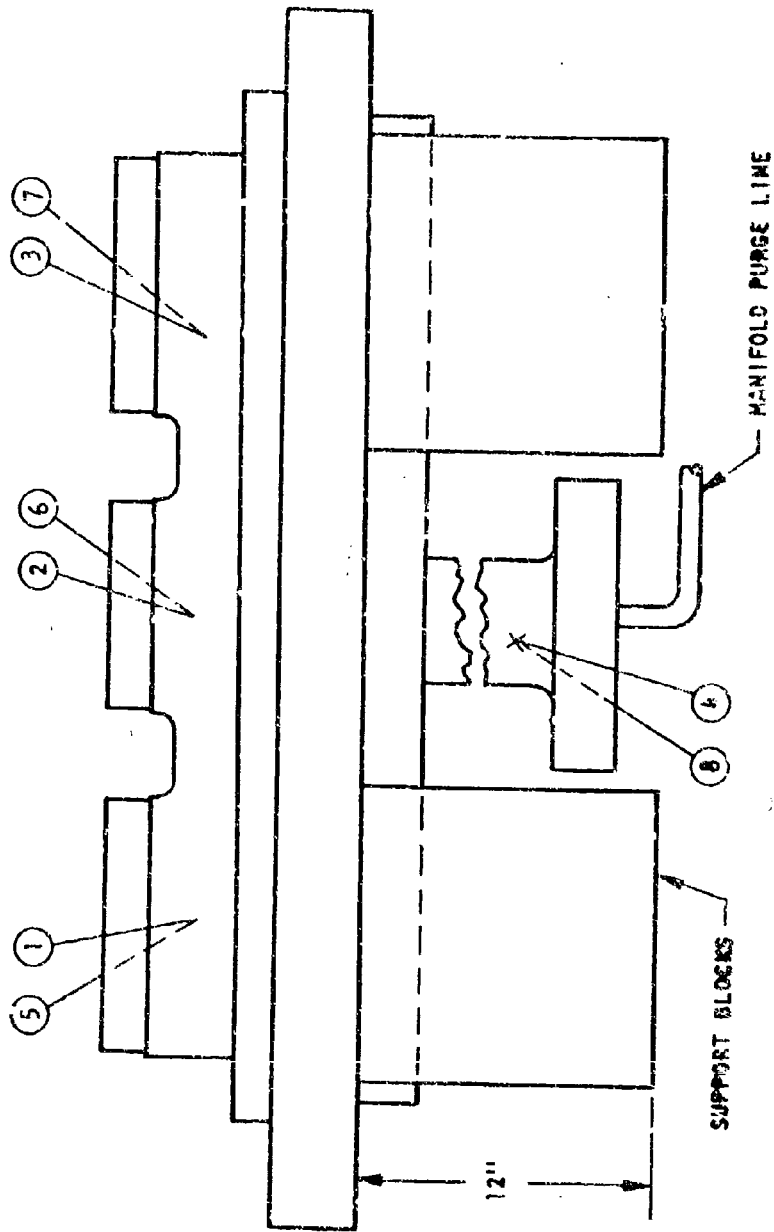
170
CONFIDENTIAL

CONFIDENTIAL

(U) The retort used for the No. 1 unit in this operation had been contaminated on the inside diameter surface from a previous heat cycle. This condition contaminated the atmosphere during the first braze cycle, resulting in some void areas in the braze joints. The unit received a second braze operation at another NAR facility. Braze alloy for the second cycle was 82Au-18Ni with a furnace temperature of 1800 to 1825 F in dry-hydrogen atmosphere. A leak test with helium gas at 60 psi disclosed no leakage.

(U) The first braze cycle on unit No. 2 was performed at the same NAR facility. Prior to pressure testing, Plasti-wax was used to seal propellant orifices (described previously for 250K injector processing). Pressure testing with helium gas at 60 psi revealed one pinhole leak at the strip end. This leak was repaired by cutting a small depression at the leak area and filling the depression by tungsten/inert gas brazing with 82Au-18Ni alloy. This unit did not require a second furnace braze operation.

(U) The thermocouple location during the braze cycle and the assembly position in the furnace is shown in Fig. 65.



○ = THERMOCOUPLES NO. 5, 6, 7, AND 8 ON OPPOSITE SIDE

Figure 65. Thermocouple Location, Purge Line Position, and Position in Furnace

CONFIDENTIAL

Security Classification

DOCUMENT CONTROL DATA - R & D		
<i>(Security classification of title, body of abstract and indexing annotation must be entered when the overall report is classified)</i>		
1. ORIGINATING ACTIVITY (Corporate author) Rocketdyne, a Division of North American Rockwell Corporation, 6633 Canoga Avenue, Canoga Park, California 91304		2a. REPORT SECURITY CLASSIFICATION CONFIDENTIAL
		2b. GROUP 4
3. REPORT TITLE ADVANCED CRYOGENIC ROCKET ENGINE PROGRAM AEROSPIKE NOZZLE CONCEPT—MATERIALS AND PROCESSES RESEARCH AND DEVELOPMENT REPORT (U)		
4. DESCRIPTIVE NOTES (Type of report and inclusive dates) Final Report, November 1967		
5. AUTHOR(S) (First name, middle initial, last name) Rocketdyne Engineering		
6. REPORT DATE 30 January 1968	7a. TOTAL NO. OF PAGES 184	7b. NO. OF REFS 0
8a. CONTRACT OR GRANT NO. AF04(611)-11399 b. PROJECT NO.	9a. ORIGINATOR'S REPORT NUMBER(S) R-7251	
c. d.	9b. OTHER REPORT NO(S) (Any other numbers that may be assigned this report) AFRPL-TR-67-278	
10. DISTRIBUTION STATEMENT "In addition to security requirements which must be met, this document is subject to special export controls and each transmittal to foreign governments or foreign nationals may be made only with prior approval of AFRPL (RPPR/STINFO), Edwards, California 93523."		
11. SUPPLEMENTARY NOTES		12. SPONSORING MILITARY ACTIVITY AFRPL, Edwards, California
13. ABSTRACT (U) Reported herein are the results of Materials and Processes effort related to development and fabrication of experimental Aerospike thrust chamber hardware. This report includes information relative to the selection of materials and information concerning the fabrication of the 250K combustor bodies and injectors, the development of the small tapered thrust chamber tubes, and the development of tooling and successful brazing of the small tubes to backup structure, and the injectors. Fabrication details of the 2.5 and 20K segment hardware is also included. Highlighted are: (1) Data for prediction of tube life, based on elevated temperature cycle strain tests, analytical calculations, and life cycle tests, (2) the development of small-diameter, tapered, variable wall thickness, formed tubes with an internal surface roughness requirement, (3) the brazing of the small tapered tubes to the backup structure utilizing the pressure bag concept, and (4) the thermographic method of braze bond inspection.		

DD FORM 1473
1 NOV 65

CONFIDENTIAL

Security Classification

14 KEY WORDS	LINK A		LINK B		LINK C	
	ROLE	WT	ROLE	WT	ROLE	WT
Aerospike Annular Configuration Thrust Chamber Injector Tubes, Type 347 Stainless Tubes, Nickel 200 Brazing, Furnace Tubes, Small Diameter, Thin Wall Tube Forming Tubes, Repair of Brazing Development						